NATURAL RESOURCES

# GEOLOGIC MAP OF THE ADAMS MOUNTAIN AND HUNTERS 7.5-MINUTE QUADRANGLES, STEVENS COUNTY, WASHINGTON

by Alexander N. Steely

WASHINGTON GEOLOGICAL SURVEY
Map Series 2023-06
December 2023

**INTERNALLY REVIEWED**

WASHINGTON STATE DEPARTMENT OF NATURAL RESOURCES
WASHINGTON GEOLOGICAL SURVEY

# GEOLOGIC MAP OF THE ADAMS MOUNTAIN AND HUNTERS 7.5-MINUTE QUADRANGLES, STEVENS COUNTY, WASHINGTON

by Alexander N. Steely

WASHINGTON
GEOLOGICAL SURVEY
Map Series 2023-06
December 2023

*This geologic map was funded in part by the USGS National Cooperative Geologic Mapping Program, award no. G21AC10361*

***This publication has been subject to an iterative technical review process by at least one Survey geologist who is not an author. This publication has also been subject to an iterative review process with Survey editors and cartographers.***

WASHINGTON STATE DEPARTMENT OF
NATURAL RESOURCES
WASHINGTON GEOLOGICAL SURVEY

## INDEMNIFICATION

Research supported by the U.S. Geological Survey, National Cooperative Geologic Mapping Program, under USGS award number G21AC10361. The views and conclusions contained in this document are those of the authors and should not be interpreted as necessarily representing the official policies, either expressed or implied, of the U.S. Government.

## WASHINGTON STATE DEPARTMENT OF NATURAL RESOURCES

Hilary S. Franz—*Commissioner of Public Lands*

## WASHINGTON GEOLOGICAL SURVEY

Casey R. Hanell—*State Geologist*
Jessica L. Czajkowski—*Assistant State Geologist*
Ana Shafer—*Assistant State Geologist*

**Washington State Department of Natural Resources**
**Washington Geological Survey**

*Mailing Address:*
1111 Washington St. SE
MS 47007
Olympia, WA 98504-7007

*Street Address:*
Natural Resources Bldg, Rm 148
1111 Washington St SE
Olympia, WA 98504

*Phone:* 360-902-1450
*Fax:* 360-902-1785
*Email:* geology@dnr.wa.gov
*Website:* http://www.dnr.wa.gov/geology

*Publications and Maps:*
www.dnr.wa.gov/programs-and-services/geology/publications-and-data/publications-and-maps

*Washington Geology Library Searchable Catalog:*
www.dnr.wa.gov/programs-and-services/geology/washington-geology-library

*Suggested Citation:* Steely, A. N., 2023, Geologic map of the Adams Mountain and Hunters 7.5-minute quadrangles, Stevens County, Washington: Washington Geological Survey Map Series 2023-06, 1 sheet, scale 1:24,000, with 56 p. text. [https://www.dnr.wa.gov/publications/ger_ms2023-06_geol_map_adams_mountain_hunters_24k.zip]

*Cover photo:* View of Lake Roosevelt from near Fruitland, Washington. Photo by A. Steely.

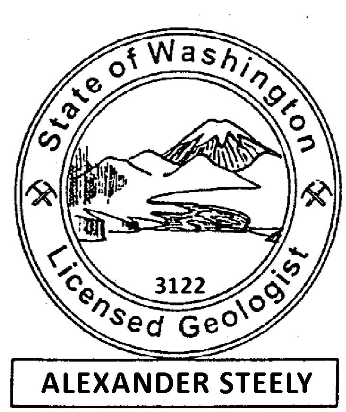


ALEXANDER STEELY

December 2023

# Contents



### FIGURES



### TABLES



### MAP SHEET

# Geologic Map of the Adams Mountain and Hunters 7.5-minute Quadrangles, Stevens County, Washington

by Alexander N. Steely[1]

[1] Washington Geological Survey
1111 Washington St SE
MS 47007
Olympia, WA 98504-7007

## ABSTRACT

New geologic mapping, geochemistry, and geochronology, as well as compilation of existing geologic maps, improve our understanding of the >1.3 billion-year geologic history in the Adams Mountain and Hunters 7.5-minute quadrangles.

Metasedimentary and metavolcanic rocks of the Deer Trail Group and Windermere Group are the oldest in the area (~1.3–0.7 Ga). These rocks are typically foliated or cleaved, and contain evidence for the rifting of Rodinia. The Addy Quartzite straddles the Precambrian–Paleozoic boundary and underlies a thick sequence of metacarbonate and shale, which are exposed in a now-vertical sequence of thrust sheets. Paleozoic metasedimentary and metavolcanic rocks of the Roberts Mountains allochthon are found in the northern part of the map area.

Two voluminous granitic plutons intrude the Paleozoic and older rocks: a 100–105 Ma zoned pluton near the Germania mine, which hosts tungsten and molybdenum mineralization (in addition to other critical and commodity elements), and a 71–74 Ma pluton near Fruitland, which is locally associated with mineralized skarn.

Eocene andesitic to rhyolitic flows and tuffs were rapidly emplaced 51.5–52.2 Ma on the exhumed 71–74 Ma pluton and are found in fault-bounded half grabens that presumably developed above the Kettle detachment fault. The volcanic rocks are similar to the Sanpoil Volcanics farther west; both are adakites and likely formed by partial melting of continental crust and not from subduction.

Much of the map area was repeatedly covered by continental glaciers during the Pleistocene, the most recent of which left a variety of deposits from lacustrine beds of Glacial Lake Columbia, to ice-marginal kame terraces and deeply incised bedrock gorges that record glacial retreat.

## INTRODUCTION

The adjacent Adams Mountain and Hunters 7.5-minute quadrangles are located in Stevens County, about 80 km northwest of Spokane (Fig. 1). Lake Roosevelt and the Columbia River form the western edge of the Hunters quadrangle, and the land rises gently eastward toward the crest of the Huckleberry Mountains in the Adams Mountain quadrangle. The area contains many hard-rock mines and mining districts, and was a major producer of tungsten and magnesium during the First and Second World Wars. The Cedar Canyon mining district is located in the southern part of the map area and includes the Germania Mine, which was one of the largest single producers of tungsten in the U.S. at the time (Wolff and others, 2014). Production and exploration largely ended in the mid-1950s as tungsten demand dropped, with 1955 being the last year of active mining at Germania. Other mining in the area also stopped in the mid to early 20th century due to a combination of mostly economic factors. Renewed interest in critical minerals has focused attention on this previously productive area, which hosts known deposits of the critical minerals tungsten, magnesium, zinc, and barite and occurrences of the critical minerals fluorite, manganese, gallium, nickel, tin, and antimony. Other possible commodities include molybdenum, gold, silver, and lead (Culver and Broughton, 1945; Huntting, 1956; Derkey and others, 1990).

The intention of this mapping is to provide the geologic framework necessary to aid critical mineral inventory efforts and to understand the critical mineral endowment of the nation. This is accomplished by refining the previously published mapping and adding detailed geochemistry and geochronology. The data in this report will help form the basis of an ore-genesis model for the Huckleberry Mountains and other similar tectonic settings in northeastern Washington.

This publication builds upon a multitude of previous studies, notably the geologic maps of Becraft and Weis (1963), Campbell and Raup (1964), Du (1979), Evans (1987), Lindsey (1988), Smith

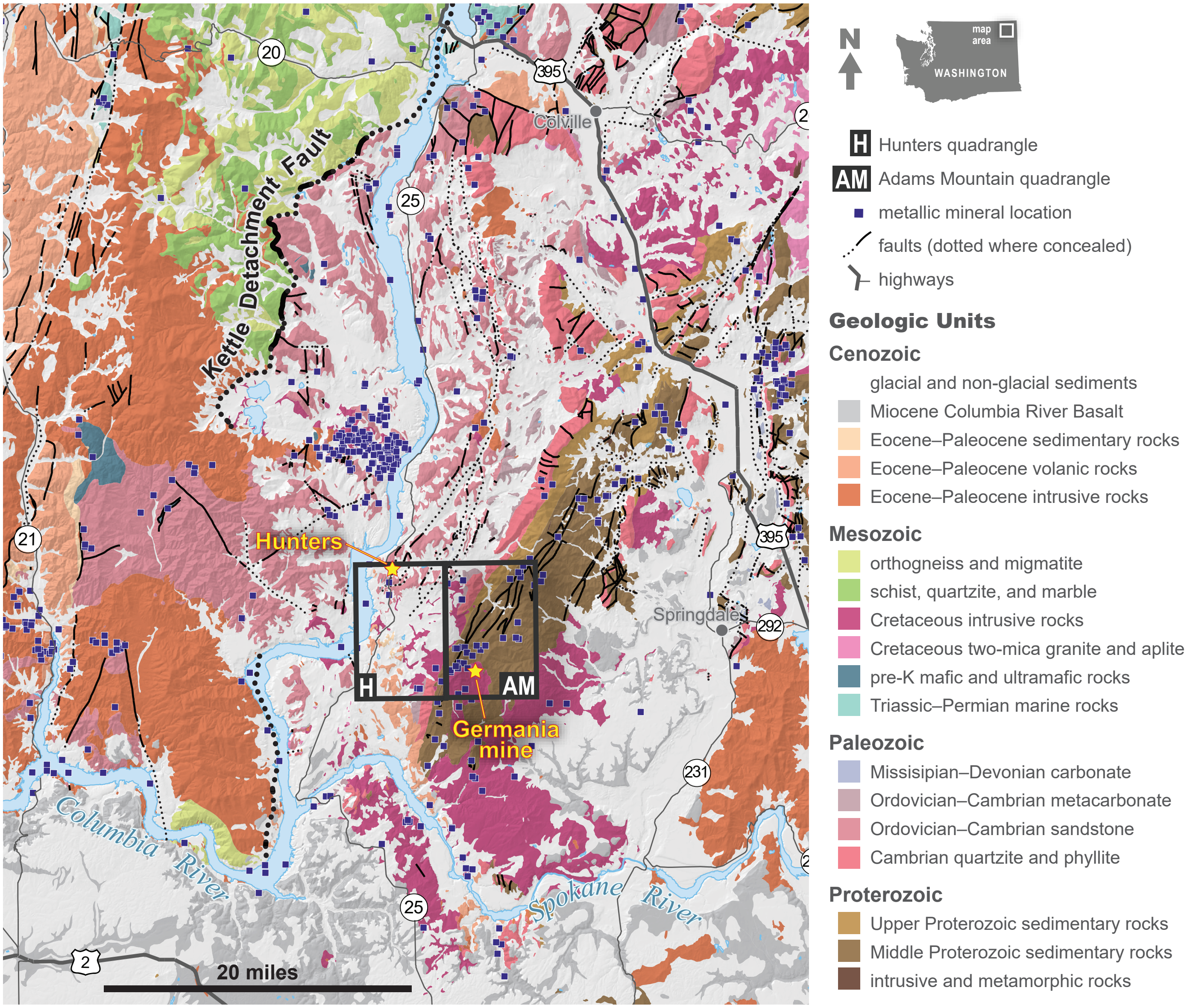


**Figure 1**. Regional geology and tectonic setting near the Hunters and Adams Mountain 7.5-minute quadrangles. Geology is simplified from Joseph (1990a,b) and Waggoner (1990a,b). Mineral occurrence data are from the Washington Geological Survey (WGS) (2023).

(1991a), and Miller (1996). Additionally, the mineral resources of the region have been the focus of many studies since the first publications by Bancroft and Lindgren (1914) and Weaver (1920) documented their existence. Several publications in the late 1940s and 1950s inventoried mineral occurrences and mine activities (Culver and Broughton, 1945; Purdy, 1954; Huntting, 1956; Anderson and Puffett, 1954). Two topical studies have sought to understand the geology and geochemistry of tungsten deposits in the Cedar Canyon area (Du, 1979; Bunning, 1985) and two others are focused on zinc-lead deposits (Fluet, 1986; Fluet and others, 1987). The most-recent mining-related publications in the map area are a series of reports on inactive and abandoned mine lands, which detail the known geology, history of mining and production, and current state (including estimates of tailing volume) for the Germania, Deer Trail, Queen Seal, and Cleveland mines (Wolff and others, 2006a,b, 2007, 2014).

Access to the map area is generally good. Most of the Hunters quadrangle consists of private land parcels, whereas the Adams Mountain quadrangle contains a mixture of public and private land; access to private land, where needed, was generally quite good. An established network of paved and gravel or dirt roads coupled with hiking provided sufficient access to most areas. A large wildfire burned much of the Huckleberry Mountains in 2015 and thick regrowth made access impossible in some areas but this was a minor portion of the entire map area.

## GEOLOGIC OVERVIEW

The oldest rocks in the study area are Mesoproterozoic and Neoproterozoic metasedimentary and metavolcanic rocks of the Deer Trail and Windermere Groups exposed in the northern and eastern part of the map area (Fig. 1). These rocks consist of fine-grained siliciclastic units (phyllite, slate, and argillite), quartzite, and carbonate (predominantly dolomite) that are capped by Neoproterozoic greenstone, conglomerate, and diamicton. The Cambrian to Neoproterozoic Addy Quartzite overlies these older rocks with a pronounced angular unconformity, and underlies Paleozoic metacarbonate, slate, and chert (Lindsey, 1988). A fault-bound belt of largely Ordovician metasandstone and greenstone is found in the northwest portion of the map area and is considered part of the Roberts Mountains allochthon, which was accreted during the Mesozoic (Smith and Gehrels, 1992b). Jurassic and Late Cretaceous compression associated with terrane accretion was responsible for crustal thickening along numerous north–northeast-striking thrust-fault systems both regionally and within the map area (Armstrong, 1982; Monger and others, 1982). Throughout much of north and northeastern Washington, numerous Late Cretaceous plutons were also emplaced at this time (Fox and others, 1977; Miller and others, 2009) including some peraluminous plutons farther to the northeast.

A major crustal reorganization occurred after the Late Cretaceous, when subduction of buoyant crust (the Siletzia terrane) substantially altered subduction dynamics (Breitsprecher and others, 2003). The result in much of north–central and northeast Washington and southern British Columbia was a period of rapid extension and tectonic denudation along low-angle normal faults that brought mid-crustal rocks to the surface (Armstrong, 1982; Kruckenberg and others, 2008). This process created the metamorphic core complexes of the nearby Kettle and Okanogan gneiss domes and was responsible for voluminous Eocene plutons, dikes, and extrusive volcanic rocks in much of northeast Washington (Fox and others, 1977; Hansen and Goodge, 1988). This map area is in the hanging wall of the Kettle detachment fault (Fig. 1) which accommodated several tens of kilometers of east–west oriented extension in the mid Eocene (Kruckenberg and others, 2008). The result of this is a thick sequence of Eocene volcanic flows and tuffs deposited in north-trending grabens that developed on exhumed Late Cretaceous plutons.

Continental glaciers advanced southward down the Columbia River valley many times over the late Pleistocene, completely covering the lower elevations of the map area (Flint and Irwin, 1939; Waitt and Thorson, 1983) and depositing a sequence of glacial deposits and landforms. Kiver and Stradling (1995) suggest that much of this glacial ice, from about the town of Hunters south, may not have been grounded and instead terminated in Glacial Lake Columbia. Outburst floods from Glacial Lake Missoula farther east provided some thin beds of coarse sediment to the area that are interbedded with otherwise fine-grained glaciolacustrine deposits.

## METHODS

The geologic map is based on field observations collected during the summer and fall of 2022 using standard geologic field techniques and a compilation of previous mapping in the area. During field work, rocks and deposits were described, attitudes of bedding, faults, fractures, and folds were measured, and samples were collected for analytical work or later characterization. All data were recorded on a tablet using Esri FieldMaps software. Hillshades from lidar (Washington Geological Survey, 2017) and red-relief maps—following the approach of Yokoyama and others (2002), implemented in the Topographic Openness module from the SAGA toolbox in QGIS 3.28—were used as basemaps in the field. After field work, a 1:24,000-scale geologic map was developed in the GeMS schema (USGS, 2020) using Esri ArcGIS Pro software. Three cross sections were developed using the new and compiled map data to illustrate subsurface relationships. Detailed unit descriptions were written from a combination of field observations, analytical data collected and discussed below, and a compilation of previous work in the area. This effort relied heavily on the existing 1:48,000-scale mapping of Campbell and Raup (1964), and the 1:24,000-scale mapping of Lindsey (1988) and Smith (1991a). Many lines on our map are compiled directly from these sources and our GIS data provide feature-level attribution of data sources to show this.

During mapping ~590 new observations were collected, including 126 new attitude measurements of bedding, flow foliation in volcanic units, faults and slickenlines, joints, dikes, and minor fold axes. The map also includes 638 orientations compiled from Campbell and Raup (1964), Du (1979), Lindsey (1988), and Smith (1991a). Compiled data are attributed to their original data source in the GIS data and are placed according to the original author and thus may appear to be located in a geologic unit different than that in which they were originally mapped. In volcanic units the ‘bedding’ symbol is used to show a measured orientation between two different lithologies (for example, between a flow and a tuff) and the ‘flow foliation’ symbol is used where a measured orientation lacks a change in lithology and there is evidence of compaction or flow foliation. Due to scale, not all attitudes are shown on the map plate, but all are included in the GIS data.

To determine the crystalization age of volcanic tuffs and flows, seven samples were analyzed using the $^{40}Ar/^{39}Ar$ method; four additional samples were analyzed with this method to understand the intrusive age of dikes and muscovite-bearing granitic rock near the Germania Mine. Zircons from 13 samples were analyzed using the U-Pb method to determine crystalization ages for the broad array of intrusive rocks present in the map area. For all 24 geochronology samples, both thin sections and major- and trace-element geochemical results were obtained. An additional 67 rock samples and 9 mine-tailing samples were also analyzed for geochemistry, and most of these samples were also thin-sectioned. The geochemical results from Bunning (1985)—mostly tin, tungsten, and molybdenum values—are also included in this publication.

Summary results of geochronology are in Table 1; analytical methods and sample information are in Appendix A and Appendix B; detailed tabular and analytical data are in the Data Supplement. Sample sites, known as stations, are labeled on the map plate and show locations where there is at least one type of analysis. The stations are numbered from north to south by 7.5-minute quadrangle. Measurements and data are reported using the metric system except for elevation, which is reported in feet-above-mean-sea-level (ft) to aid in comparison with topographic maps.

## DESCRIPTION OF MAP UNITS

### Holocene and Late Pleistocene Nonglacial Deposits

ml **Modified land and artificial fill (Holocene)**—Mixed earth materials of varied grain size and sorting placed to

**Table 1**. Summary of new ages for the Hunters and Adams Mountain 7.5-minute quadrangles. All stations also have a thin section and geochemical analysis (see Table 2) except for station 92, which lacks a thin section. Uncertainties are provided at 2-sigma (95%) confidence. Analytical data and petrographic analyses of some thin sections are in the Data Supplement.

| Station ID | Interpreted geologic unit | Dating method | Age (Ma) | Age type | Material | Geochemical classification** |
|---|---|---|---|---|---|---|
| 15 | Ki | U–Pb | 104.28 ±0.64 | Crystalization | zircon | granite / rhyolite |
| 18 | $Kig_f$ | U–Pb | 74.17 ±0.34 | Crystalization | zircon | granite |
| 19 | $Kigd_f$ | U–Pb | 73.35 ±0.28 | Crystalization | zircon | gabbroic diorite |
| 21 | $Kigd_g$ | U–Pb | 100.46 ±0.44 | Crystalization | zircon | monzonite |
| 23 | Ki | U–Pb | 104.38 ±0.20 | Crystalization | zircon | granodiorite / dacite |
| 28 | $Kigd_f$ | U–Pb | 71.44 ±0.35 | Crystalization | zircon | granodiorite |
| 33 | Ki | $^{40}Ar/^{39}Ar$ | 95.07 ±0.18 | Eruption | biotite | granodiorite / dacite-trachyte |
| 38 | Ki | $^{40}Ar/^{39}Ar$ | 71.64 ±0.13 | Metamorphism | muscovite | granite / rhyolite |
| 41 | $Kigd_g$ | U–Pb | 103.45 ±0.23 | Crystalization | zircon | granodiorite |
| 42 | $Kig_g$ | U–Pb | 103.96 ±0.45 | Crystalization | zircon | granite |
| 43 | $Kigd_g$ | U–Pb | 100.12 ±0.40 | Crystalization | zircon | granite |
| 45 | $Kig_g$ (vein) | $^{40}Ar/^{39}Ar$ | 88.08 ±0.15 | Metamorphism | muscovite | granite |
| 49 | $Kig_g$ | U–Pb | 101.82 ±0.47 | Crystalization | zircon | granite |
| 50 | $Kig_g$ (vein) | $^{40}Ar/^{39}Ar$ | 99.02 ±0.21 | Metamorphism | muscovite | monzonite |
| 62 | Eva | $^{40}Ar/^{39}Ar$ | 51.55 ±0.10 | Crystalization | hornblende | dacite-trachyte |
| 63 | $Kigd_f$ | U–Pb | 74.04 ±0.24 | Crystalization | zircon | granodiorite |
| 64 | $Kig_f$ | U–Pb | 73.34 ±0.34 | Crystalization | zircon | granite |
| 66 | Evt | $^{40}Ar/^{39}Ar$ | 52.12 ±0.14 | Crystalization | plagioclase | rhyolite |
| 73 | Eva | $^{40}Ar/^{39}Ar$ | a. 51.89 ±0.10<br>b. 51.61 ±0.11<br>c. 52.06 ±0.10 | Crystalization | a. hornblende<br>b. groundmass<br>c. biotite | trachy-andesite |
| 74 | Evt | $^{40}Ar/^{39}Ar$ | a. 51.94 ±0.09<br>b. 50.10 ±0.10 | Crystalization | a. hornblende<br>b. groundmass | andesite |
| 77 | Eva | $^{40}Ar/^{39}Ar$ | 51.50 ±0.10 | Crystalization | hornblende | trachy-andesite |
| 88 | Evt | $^{40}Ar/^{39}Ar$ | a. 52.01 ±0.11<br>b. 51.63 ±0.10 | Crystalization | a. plagioclase<br>b. biotite | dacite |
| 90 | Eva | $^{40}Ar/^{39}Ar$ | 52.19 ±0.11 | Crystalization | groundmass | andesite |
| 92 | $Kigd_f$ | U–Pb | 73.69 ±0.33 | Crystalization | zircon | diorite |

* Associated petrographic analysis available in the Data Supplement

** Using the Total-Alkali-Silica diagram of Le Maitre and others (2002)

elevate the land or to modify topography; may contain organic material, concrete, or debris; where mapped adjacent to historic mine sites, likely contains waste rock or spoils; may be engineered; loose to compact; typically shown where thick and (or) extensive or where modification has sufficiently altered the original characteristics of a deposit such that it is no longer recognizable. Mapped predominantly along major roads, areas of development, and near mines.

Qa **Alluvium (Holocene)**—Gravel, sand, silt, and clay, in varied abundance; locally contains scattered boulders; well to poorly sorted; may be stratified, unstratified, or contain other sedimentary structures indicative of fluvial transport; generally loose. Unit is mapped where there is at least some evidence of geologically recent fluvial deposition or erosion; as such it is found along the major perennial streams and rivers. Unit thickness is as thin as ~2 m along smaller streams, but is substantially thicker in many locations, especially along Hunter Creek where it may be several tens of meters thick. The unit is considered Holocene. Where unit Qao is present, unit Qa is topographically lower and (or) inset into unit Qao.

Qao **Alluvium, older (Holocene)**—Gravel, sand, silt, and clay, in varied abundance; locally contains scattered boulders; well to poorly sorted; may be stratified, unstratified, or contain other sedimentary structures indicative of fluvial transport; locally contains organic material and (or) soil; generally loose. Unit is mapped adjacent to major perennial streams and rivers where evidence for geologically recent fluvial deposition or reworking is absent; the top of the deposit is typically several meters above the stream channel. Although not present everywhere, there is typically a lower, inset deposit (unit Qa) between the stream or river and deposits of unit Qao. The unit varies from ~2–20 m thick and is considered Holocene, though some deposits in areas above the glacial trim line could be as old as the late Pleistocene.

Qaf **Alluvial fan (Holocene)**—Pebble to boulder gravel and sand in varied abundance; may contain organic material; mapped largely from lidar along and adjacent to streams where they emerge from confined channels into broader and flatter topography. Unit is differentiated from other Holocene units primarily based on the presence of fan-shaped surface morphology.

Qls **Landslide (Holocene to late Pleistocene (?))**—Boulders, cobbles, pebbles, sand, silt, clay, soil, organic material, and blocks of older deposits or bedrock, in varied abundance; typically matrix supported; generally unsorted; clasts angular to rounded, depending on source material; loose to compact. May include deposits from both shallow (depth less than that of tree roots) and deep-seated landslides, debris flows, and rock fall. Thickness is often poorly constrained and varies from a few to several tens of meters, but may locally be much thicker. Unit Qls is interpreted to be Holocene, but some deposits could be older in areas above the glacial trim line. Absence of a mapped landslide does not indicate the absence of landslide hazard.

Qc **Colluvium and talus (Holocene to late Pleistocene (?))**—Boulders, cobbles, pebbles, sand, silt, clay, soil, organic material, and semi-intact blocks of older deposits or bedrock, in varied abundance; clast to matrix supported; clasts range from angular to rounded, depending on source material; loose to compact. Includes talus, scree, and colluvium; may include deposits from small, unmapped shallow landslides. Thickness is poorly constrained but appears to vary from ~1–20 m; some talus slopes have been quarried for local road material and are greater than 10 m thick. Small outcrops of unit Qc are widespread in the map area; large accumulations are generally found on the moderate slopes beneath boldly outcropping units, such as Neo- and Mesoproterozoic quartzite. The unit is interpreted to be largely Holocene but may locally include some deposits from the late Pleistocene. This unit locally contains outcrops of other units too small to be mapped separately.

## Late Pleistocene Glacial Deposits

During the most-recent ice age in the latest Pleistocene, a large continental ice sheet formed in British Columbia, one lobe of which (the Colville lobe) advanced southward down the Columbia River valley (Flint and Irwin, 1939; Weis and Richmond, 1965; Waitt and Thorson, 1983; Atwater, 1986). Within the map area this glacier split, with one part advancing westward down the Columbia River, and another advancing southeast down Enterprise Valley (Kiver and Stradling, 1995). At its maximum, the ice was about 1,000 m thick near the town of Hunters (Atwater, 1986) and tapered to its edge several km south of the map area past McCoy Lake. It appears that ice of the Columbia lobe was likely present in the map area between about 17 ka and 13 ka, and that during recession it stalled for a while just north of Hunters (Atwater, 1986; Kiver and Stradling, 1995). Another glacier some 30–40 km to the west—the Okanogan lobe—impounded the Columbia River near Grand Coulee and created Glacial Lake Columbia, principally at about 1,700 ft elevation (Flint and Irwin, 1939; Waitt and Thorson, 1983; Atwater, 1986). Kiver and Stradling (1995) suggest that much of the Columbia lobe ice, from about Hunters south, may have been ungrounded and terminated in the lake. Also during this time, outburst floods from glacial Lake Missoula to the east flowed into glacial Lake Columbia and are recorded as coarse-grained deposits within the lake sediments (Atwater, 1986). All of the glacial deposits in this map are from the most-recent glaciation and most contain a variety of clast lithologies representative of the diverse geology exposed upriver. Boulders (1–3 m across) are found dispersed on the surfaces of kame terraces, mantling the surface of many ice-contact deposits, and littered across exposures of bedrock below about 2,400 ft; most boulders are granitic.

Qgo **Glacial outwash (Pleistocene)**—Light gray to tan sand and pebble to cobble gravel; minor silt and clay; rare diamicton (till); typically moderately to well sorted and well stratified; weakly developed soil profile and little to no weathering of clasts; locally contains scattered boulders up to 4 m across; contains a wide variety of clast lithologies, including granitic rock, both high- and low-grade metasedimentary rock, gneiss, and volcanic rocks; thickness varies but is probably no more than about 30 m thick. This unit is only mapped near and in Enterprise Valley, where it is found near and slightly above ~1,700 ft and may overlie lacustrine deposits near O-Ra-Pak-En Creek. A subtle north–south-trending elongate hill south of Enterprise reaches a maximum height of 25 m and is 800 m wide and about 2,200 m long; it may be a remnant sand-and-gravel bar deposited during the many outburst floods that Kiver and Stradling (1995) suggest coursed through Enterprise Valley.

Qgod **Glacial outwash, delta facies (Pleistocene)**—Light gray to tan or olive-drab gravel and sand; loose to somewhat consolidated; clasts are typically pebbles and cobbles with some boulders, mostly unweathered, and commonly somewhat less rounded than in other glacial units; matrix is typically coarse sand to granules; sorting varies but is generally poor to moderate; bedding was difficult to observe, but crudely stratiform with locally developed topsets and foresets. This unit is mapped near the mouths of two incised bedrock gorges that empty into Hunters Creek just north of the map area. Here the deposits are fan shaped with flat tops, steep outer edges, and multiple inset flat surfaces; clast lithologies match the bedrock exposed in the gorges just upstream of the deposits; the top elevations of the deltas are ~2,250–2,275 ft for the eastern delta and ~2,150–2,175 ft for the western one; maximum thickness for the deposits is inferred to be 80–100 m based on topography. It is not clear if the deltas were subaerial or subglacial; both deltas are above the elevation for the bedrock gorge that fed the lower kame terrace (unit Qgikl) and could have been the source of water and sediment for that deposit.

Qgl **Glacio-lacustrine deposits (Pleistocene)**—White to gray or buff sand, silt, clay, and gravel, in varied abundance typically found below about 1,700 ft; lenses or beds of glacial diamicton are rare; unit typically consists of consolidated and cohesive laminated fine sand, silt, and clay interbedded with ~1-m-thick poorly sorted to well-graded sand and rounded pebble- to cobble-gravel; some coarse beds are cross bedded and (or) have ripple cross lamination; most are broadly lenticular or wavy over tens to hundreds of meters; rip up clasts (commonly of silt or sand) are locally present near the base of coarser beds; fine-grained intervals are typically a few meters thick and have centimeter-scale light–dark alternation (varves); also contains some deposits of unsorted, angular, locally derived bedrock in a matrix of silt to sand. Beds are typically flat to gently dipping; locally beds are contorted and near the mouth of Hunters Creek beds are nearly vertical, probably as a result of slumping during deposition, as noted elsewhere by Kiver and Stradling (1995). Description compiled from my observations and those of Kiver and Stradling (1995) and Joseph (1990a).

The laminated and varved fine-grained sediments are interpreted as having formed on the lakebed of glacial Lake Columbia (Flint and Irwin, 1939; Joseph, 1990a), the surface of which was at ~1,700 ft elevation for most of its history. Some lacustrine beds along Hunters Creek above 1,700 ft may have been deposited during a brief lake highstand at ~2,400 ft or resulted from local impoundment by glacial ice (Kiver and Stradling, 1995). Within the fine-grained sediment are lenses and wedges of unbedded matrix-supported clasts interpreted as either water-laid till or, where there is nearby steep bedrock, debris flows and colluvium. Bedded coarser-grained deposits are also found within the fine-grained sediment and are interpreted as outburst flood deposits (Atwater, 1986); in the Sanpoil River valley west of the map area, there are as many as 89 such deposits (Atwater, 1986). Near the mouth of O-Ra-Pak-En Creek just west of the map area, Kiver and Stradling (1995) describe interbedded ripple-laminated sand and varved silty clay, which they interpret as at least 10 glacial flood events, with those from glacial Lake Columbia recording southeast flow through Enterprise Valley and those from glacial Lake Missoula recording northwest flow.

Qgikl
Qgikm
Qgiku **Ice-contact kame terraces (Pleistocene)**—Light gray, dark gray, buff, or olive-gray gravel and sand in varied amounts, with minor lenses and beds of pebble to boulder diamicton (till); gravelly beds loose to consolidated; till lenses compact and dense; clasts have little to no weathering; matrix lightly weathered in many locations; unsorted to well sorted, with most gravelly beds moderately to poorly sorted; clasts mostly subangular to subrounded. Well-developed unpaired terrace surfaces are typical and usually have higher topography to their east and ice-contact deposits (including eskers) to their west; these are interpreted as kame terraces deposited between glacial ice on the west and mountainous terrain on the east. Deeply incised bedrock gorges connect these deposits across transverse bedrock ridges. Thickness varies from 10–20 m on the upstream side of bedrock gorges to over 100 m on the downstream side.

Three separate subunits are mapped based mostly on elevation. The upper subunit (unit Qgiku; highest and easternmost) crosses two drainage divides and grades from 2,750–3,050 ft north of Hunters Creek to ~2,300–2,350 ft at the southern map boundary. A middle subunit (unit Qgikm) is less expansive. The subunit emanates from the incised lower portion of the same bedrock gorge used by unit Qgiku between Hunters Creek and Alder Creek at ~2,300 ft and flows through a different bedrock gorge into O-Ra-Pak-En Creek at ~2,100 ft. From there it presumably flowed into glacial Lake Columbia. The lower subunit (unit Qgikl) crosses a series of bedrock gorges south of Hunters and grades from an initial elevation of ~1,950–2,000 ft to ~1,800 ft near O-Ra-Pak-En Creek.

This unit is interpreted as having formed when ice-marginal streams and rivers along the valley's eastern side were blocked and diverted as glacial ice advanced through the Columbia River valley. These streams and rivers coalesced and flowed along the ice edge, forming an integrated and large fluvial system from north of Hunters Creek to Enterprise Valley in the south. During this time the river system carved deep gorges where it was forced across bedrock ridges and deposited one-sided kame terraces along the glacier's edge where the gradient of the river was lower. As the glacier receded and thinned, base-level lowered and successively lower (and farther west) bedrock gorges were carved. Though kame terraces were likely created during older glaciations, the deposits of unit Qgik are all relatively unweathered and were therefore likely deposited during the most-recent glaciation in the late Pleistocene.

Qgic **Ice-contact deposits (Pleistocene)**—Light gray to tan varied assortment of diamicton (till) and structureless to stratified, poorly sorted silty sand to cobble and boulder gravel; clasts have little to no weathering; diamicton ranges from very compact to somewhat compact and typically consists of unsorted lenses of silt and clay matrix with dispersed pebbles to large boulders, locally up to 3 or 4 m across; fine-grained stratified deposits are typically compact, can locally include laminated silt and clay, but more typically are silty sand or pebbly sand. The surface of this unit is locally littered with mostly granitic boulders; in many locations abundant kettles several meters to tens of meters deep are preserved; where the unit lacks kettles, the surface may be somewhat dimpled or preserve elongate drumlins and other glacial-flow features (for example, northwest of Hunters). As mapped, this unit locally includes lodgment till, though this appears to be present only in minor amounts and typically only north of Fruitland. More commonly, the till is somewhat less compact than is typical of lodgment till and is more likely ablation till or water-lain till. As mapped, the unit also contains some moraine deposits, notably along Fruitland Valley Road and near Mudgett Lake, both of which are also noted by Kiver and Stradling (1995); the latter area contains moraines with numerous accumulations of large boulders along and near moraine crests. This unit is similar to unit Qgice, but generally lacks sinuous esker-like features.

Qgice **Ice-contact deposits with eskers (Pleistocene)**—Light gray to tan varied assortment of diamicton (till) and structureless to stratified, poorly to moderately sorted sandy cobble gravel; clasts have little to no weathering; diamicton ranges from very compact to somewhat compact and typically consists of unsorted lenses of silt and clay matrix with dispersed pebbles to large boulders, locally up to 3 or 4 m across; the stratified deposits are typically crudely bedded. This unit is largely similar to unit Qgic, but contains abundant and narrow linear to sinuous ridges several meters tall of somewhat stratified gravel that are interpreted as eskers. Some of these features are relatively flat-lying and found on the up-valley (stoss) side of glaciated bedrock ridges, but most are preserved on the down-valley (lee) side where they dip down slope (and down valley) and are locally very abundant. This asymmetry may be due to the interaction of transverse bedrock ridges with advancing ice, or differences in subglacial hydrostatic pressure on the lee side of the bedrock ridges that favor subglacial deposition.

Qge **Eskers (Pleistocene)**—Light gray to tan generally stratified sand and gravel; typically somewhat consolidated; clasts have little to no weathering and are mostly subrounded; the matrix is usually fine to coarse sand and contains abundant pebbles and cobbles with uncommon boulders; silty layers are locally present, but minor overall; beds are crudely stratiform and locally have lenticular geometries. Deposits of this unit have a characteristic sinuous trace and are usually 5–10 m tall and 10–70 m wide. This unit is generally mapped where the eskers are pronounced and are either partly buried by kame terraces (unit Qgik) or were deposited adjacent to the kame terraces at the glacier's margin; these deposits are most abundant and clearly expressed on the west (valley) side of the upper kame terraces north and south of Alder Creek.

## Undivided Quaternary Glacial and Nonglacial Deposits

Qu **Undivided deposits beneath Lake Roosevelt (Quaternary) (cross section only)**—Inferred fluvial and alluvial deposits of the Columbia River, glacio-lacustrine deposits, and (or) till, outwash, or ice-contact deposits; may contain some landslide deposits; likely covered by a thin veneer of Holocene lacustrine deposits of Lake Roosevelt. Shown on the cross section under Lake Roosevelt where bathymetry and lake-adjacent geology suggests there may be Quaternary-age deposits in the Columbia River valley.

## Tertiary Volcanic Rocks

Interbedded flows and tuffs in the map area were first described by Weaver (1920) and named the Gerome andesite. Becraft and Weis (1963) mapped and described the rocks south of this map, and Campbell and Raup (1964) mapped the rocks (but did not describe them) in the map area. Pearson and Obradovich (1977) obtained an ~50 Ma K-Ar hornblende age south of the map area and correlated the rocks with the Sanpoil Volcanics of Muessig (1962); Waggoner (1990a) retained this correlation and Joseph (1990a)—citing interpretations in Pearson and Obradovich (1977)—correlated the tuffaceous unit of Campbell and Raup (1964) and Becraft and Weis (1963) with the O'Brien Creek Formation. New $^{40}Ar/^{39}Ar$ ages on three tuffs and four flows show that the entire sequence in the map area was erupted from ~51.5–52.2 Ma (Table 1) and geochemistry from 25 samples indicates a high degree of similarity with the Sanpoil Volcanics (see *Geochemistry*).

The volcanic rocks consist of interbedded flows and pyroclastic deposits that are mapped separately where exposure permits. In general, flows form bold ridges whereas pyroclastic units erode more easily and are less commonly exposed. Composition varies from andesite to rhyodacite; euhedral and lustrous hornblende are characteristic of flows. An aggregate thickness of ~457 m was estimated by Becraft and Weis (1963); I estimate 520–620 m from the cross sections and note the unit appears to thin westward. Everywhere in this map the flows appear to be deposited on granodiorite (unit Kigdf); to the south the unit has a pronounced angular unconformity with Cambrian through Mesoproterozoic rocks (Becraft and Weis, 1963), which indicates that the older rocks were generally west dipping instead of vertical to overturned as they are now.

Eva **Intermediate to felsic flows and minor tuff (Eocene)**—Light to dark gray andesite and trachyandesite flows with minor dacite flows and interbedded pale-colored tuff and lapilli tuff; flows weather reddish brown, purple, or greenish-gray and are typically porphyritic, with sparse to abundant phenocrysts of lustrous black 2–10 mm hornblende being distinctive and characteristic; plagioclase and augite phenocrysts are less common than hornblende; biotite and quartz are rare; groundmass is typically dark gray, with plagioclase laths, hornblende, augite, and rare biotite in an aphanitic to glassy matrix; trace minerals include apatite, zircon, titanite, and magnetite. Most rocks are at least somewhat altered, with plagioclase altering to sericite and (or) smectite, hornblende altering to actinolite, chlorite, epidote, and (or) phlogopite, and the groundmass altering toward various clays and zeolites. The degree of alteration increases toward faults. Locally rocks are moderately altered and fractures are filled with calcite and quartz. In general, flows are dense and cut by abundant, closely spaced (5–100 cm) joints, creating a hackly appearance; flows generally range from ~10 to 30 m thick, though flow tops and bottoms are difficult to recognize except where there are intervals of pyroclastic rock between them. Geochemistry and thin sections from 17 samples of unit Eva, four of which are dikes (Table 2; Figs. 2 and 3), show that, with the exception of a few dacite samples, calc-alkaline andesite and trachyandesite are the most common rock type, and that dikes of this unit have higher iron and lower silica values than unit Ki. One sample (station 67) has anomalously low total alkali values but it is also adjacent to a fault and highly altered. Description is primarily from my observations supplemented with some descriptions from Becraft and Weis (1963).

This unit is mapped where flows are thicker and (or) more abundant than tuffs. Also mapped as dikes in a few localities, including within the Cretaceous plutonic rocks and Proterozoic rocks east of the main exposures of flows; these could be feeder dikes for volcanic rocks that project above the modern ground surface but have been eroded. Argon ages are 51.50–52.19 Ma (Table 1; stations 62, 73, 77, and 90).

Evt **Felsic to intermediate pyroclastic rock and minor flows (Eocene)**—Light gray, silver gray, light green, and beige tuff, lapilli tuff, and tuff breccia with minor interbeds of flow rock similar to that from unit Eva; pyroclastic rocks range in composition from andesite to rhyolite and are most commonly dacite; typically crystal vitric, with euhedral to subhedral zoned plagioclase and less abundant hornblende, augite, biotite, and magnetite in a groundmass of devitrified glass and minor glass shards; lithic fragments are uncommon. The tuff and lapilli tuff are typically unwelded and weather easily, though rarely some beds are slightly welded and more resistant; unit appears to be unbedded to poorly bedded, though a lack of good exposure makes this a tentative observation. East of Mudgett Lake (at station 74) there is a thick exposure of monolithologic block-and-ash flow containing clast-supported blocks up to 3 m across of light gray to mauve hornblende-phyric trachyandesite in a lithologically similar matrix; the stratal relationship of this set of outcrops to those around it is not clear. Just to the north, a folded interval of off-white, silvery gray, and beige crystal vitric rhyodacite tuff with sparse rounded clear quartz eyes is found between Highway 22 and Newbill Lake; andesite flows or dikes are present on its western outcrop belt. In general the unit appears to be thickest and most prevalent near the middle of its outcrop belt and thins both north and south. In contrast to south of the map area (Becraft and Weis, 1963), there are no sedimentary rocks within this unit. Seven sites are analyzed using geochemistry (Figs. 2 and 3) and show that most tuffs are calc-alkaline dacite or rhyolite and that the andesite and trachyte samples are from sites with large blocks of flow rock. Argon ages at three sites (stations 66, 74, and 88) are 51.94–52.12 Ma. Alteration is weak to strong, pervasive, and has generally altered the groundmass and smaller lapilli to various clays and zeolites. Adjacent to faults, the rock is bleached white to yellow, chalky, locally silicified, and there are often clasts with slickensided surfaces dispersed in the soil.

**Table 2**. Stations by map unit. Most stations have a co-located geochemical analysis and thin section; some sites also have geochronology. The exceptions are station 91, which lacks geochemistry, stations 92–101, which only have geochemistry and are predominantly from mine tailings, and stations 102–117, which are geochemical sites from Bunning (1985). Analytical data and petrographic analyses of some thin sections are in the Data Supplement. Red color indicates samples from dikes; blue indicates samples of veins or pegmatites.

| Map unit | Station IDs |
|---|---|
| Evt | 55, 66†, 68, 72, 74†, 79, 88† |
| Eva | 8, 20, 48, 62†, 67, 69, 70, 73†, 75, 76, 77†, 78, 80, 82, 83, 84, 90† |
| Ki | 1, 7, 15*, 23*, 26, 30, 33†, 35, 38†, 54 |
| $Kig_f$ | 18*, 64*, 65, 89 |
| $Kigd_f$ | 14, 19*, 28*, 61, 63*, 71, 85, 87, 92* |
| $Kigb_f$ | 31, 40 |
| $Kiqm_g$ | 52, 53 |
| $Kig_g$ | 42*, 44, 45†, 46, 47, 49*, 50†, 51, 111, 112, 115, 116, 117 |
| $Kigd_g$ | 21*, 41*, 43*, 81 |
| $Ocb_c$ | 59, 60 |
| $Omv_b$ | 56, 58 |
| $Oms_d$ | 91, 57 |
| $OCl_m$ | 5, 6, 9, 11, 13, 86, 103, 104 |
| $Cph_a$ | 10, 16 |
| $Zg_h$ | 3, 12, 22, 34 |
| $ZYcg_h$ | 2, 17 |
| $ZYq_b$ | 36 |
| $Ycb_s$ | 4, 24, 25, 109, 110 |
| $Ycb_{wd}$ | 27 |
| $Ycb_{cc}$ | 29, 32, 37, 39, 106 |
| ml (mine tailings) | 93, 94, 95, 96, 97, 98, 99, 100, 101, 102, 105, 108, 113, 114 |

* U–Pb age

† $^{40}Ar/^{39}Ar$ age

Red indicates dikes

Blue indicates veins or pegmatite

## Cretaceous Intrusive Rocks

Plutonic rocks in the map area were originally considered to be part of the Loon Lake granite of Weaver (1920). Campbell and

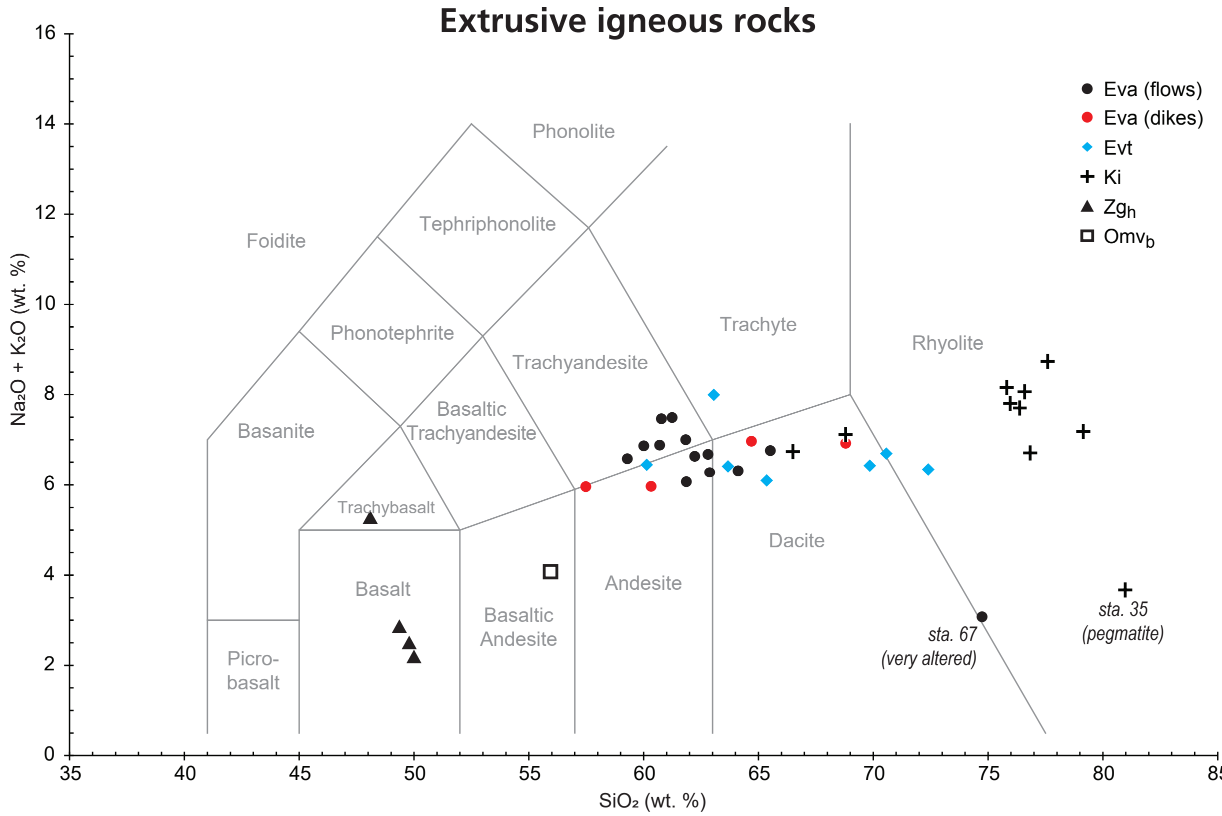


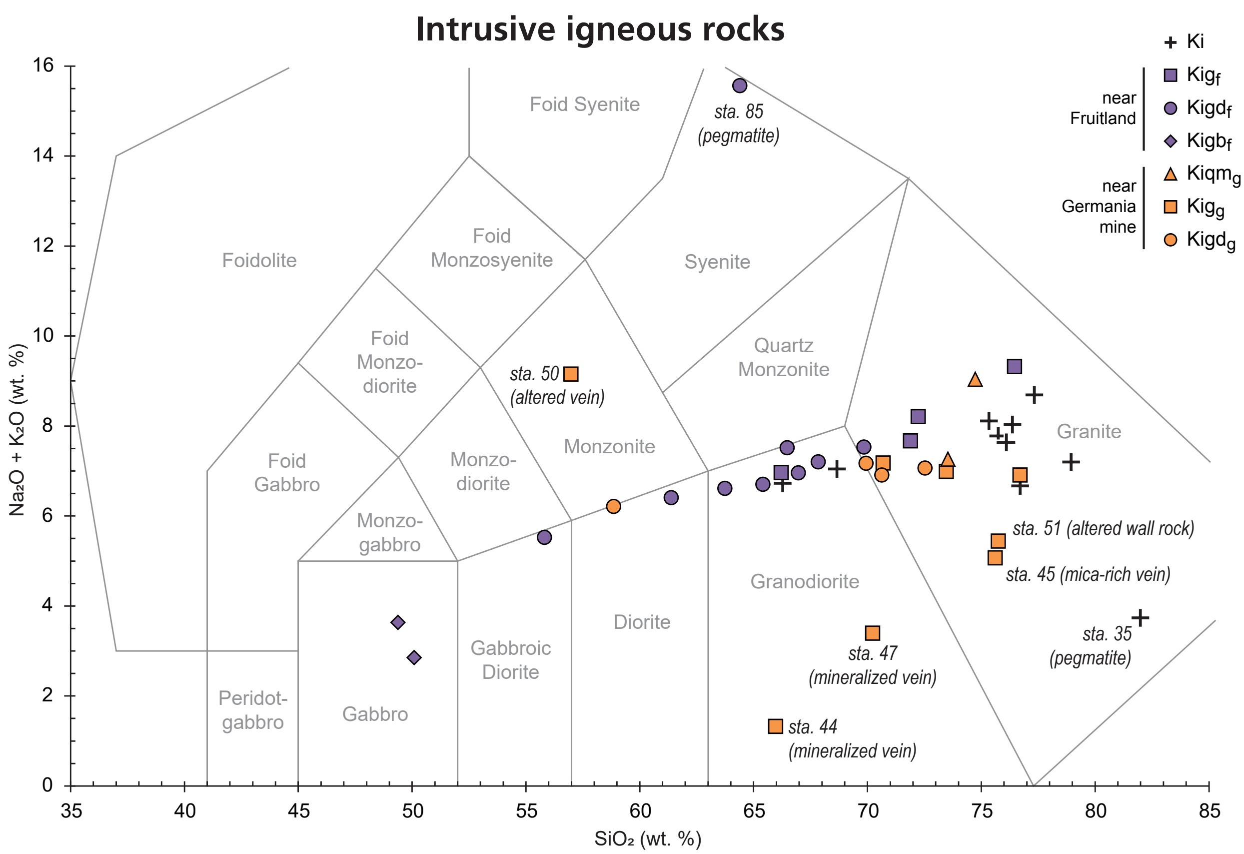


**Figure 2**. Total Alkali-Silica (TAS) diagrams for extrusive igneous rocks (top) and intrusive igneous rocks (bottom). Units Eva and Evt appear to show decreasing alkali content with increasing silica content, like the similarly aged Sanpoil Volcanics in the Republic graben to the northwest (Morris and others, 2000). The Cretaceous suite of intrusive rocks are varied, but appear to show increasing average alkali content with increasing silica content. Unit Ki is provided on both diagrams; outliers are labeled for ease of reference; all data shown on figures are normalized and are from this study; data provided in the Data Supplement are un-normalized values. Classification based on Le Maitre and others (2002) and implemented in the TAS diagram plotter of Stosch (2022).

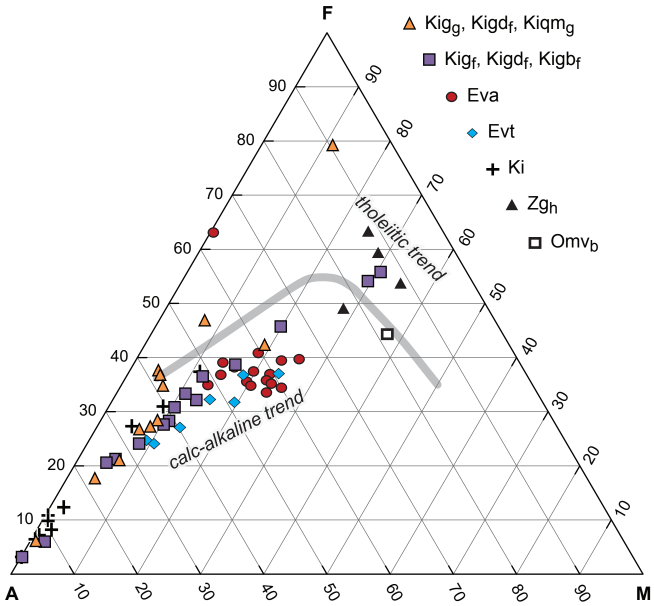


**Figure 3**. Total alkali-iron-magnesium (AFM) plot for igneous rock units showing calc-alkaline trend for most Eocene and Cretaceous rocks and a tholeiitic trend for Neoproterozoic basalt. Implemented in the AFM diagram plotter of Stosch (2022).

Raup (1964) and Becraft and Weis (1963) found that the plutonic rocks near the Germania Mine were zoned. Their mapping reveals a more biotite-rich granodiorite outer zone that grades through a porphyritic granite into a quartz monzonite core. Campbell and Raup (1964) also describe an expansive granodiorite in the western half of their map. Joseph (1990a) and Waggoner (1990a) summarized the body of knowledge on the plutons in this area and the informal names of Joseph (1990a) are generally used. Most of the plutonic rocks have been considered by past workers to be Cretaceous in age like the Loon Lake batholith, a finding that was generally confirmed by various types of dating near the Midnite Mine just south of the map area (Ludwig and others, 1981). This work shows that there are at least two main phases of plutonic activity, a mid-Cretaceous period at about 100–105 Ma corresponding to the plutonic rocks near the Germania Mine and scattered dikes throughout the area, and a late-Cretaceous event between 71 to 74 Ma that created the plutonic rocks near Fruitland and those near the Midnite Mine. Table 3 helps to show similarities and differences between intrusive units because they are broadly similar and Figure 2 highlights major geochemical differences. Mineral abundances are provided as a percent of the entire rock.

Ki **Dikes (Cretaceous)**—White, light to dark gray, yellowish gray, or greenish gray, slightly porphyritic rhyodacite, quartz latite porphyry, quartz porphyry, granophyre; granite, monzogranite, alaskite, aplite, and pegmatite; dikes developed in the plutonic rocks near the Germania Mine are typically aplitic to pegmatitic; dikes are usually poorly exposed, though somewhat more resistant than the rock into which they intrude, and tend to form slight ridges; thickness ranges from about 1 m to more than 30 m; contacts with metasedimentary rocks are commonly sharp and lack evidence of chilling; milky quartz, clear quartz, and K-feldspar are common in coarser-grained leucocratic dikes, as is minor pyrite; phenocrysts of euhedral to anhedral quartz and plagioclase are common in some finer-grained dikes; hornblende, biotite, muscovite, magnetite, and tourmaline are locally present in small quantities. Many dikes are bleached and sericiticly altered with limonite replacement of pyrite and (or) biotite, typically where dikes are found associated with faults; some intrusive rocks near faults have well-developed slickensides indicating at least some amount of movement occurred after intrusion. Ten geochemical analyses (Table 2; Fig. 2) show that most dikes are quite felsic and are easily distinguished from Eocene-age dikes based on this and lower iron content. Description compiled from Becraft and Weis (1963), Campbell and Raup (1964), Miller (1996), and my own observations.

Two U-Pb dates from zircons are mid Cretaceous: a bleached and faulted rhyodacite dike exposed along the Hunters–Springdale Road is 103.4 ±0.2 Ma (station 41), and a grayish green quartz latite porphyry dike exposed along a fault just northeast of the Turk Mine is 104.4 ±0.2 Ma (station 23). Both of these ages confirm the general inference of past workers that the dikes are likely Cretaceous in age and similar in age to the intrusion of the plutonic rocks near the Germania Mine. An argon age on biotite (station 33) is 95.1 ±0.2 Ma and could plausibly be about the same age as the other mid-Cretaceous dikes and plutons. An argon age on muscovite (station 38) is much younger (71.6 ±0.1 Ma) and the same age as the plutonic rocks near Fruitland; it could thus be a dike from the younger plutonic phase, or be an older mid-Cretaceous dike that has been reheated by the younger plutonism.

## PLUTONIC ROCKS NEAR FRUITLAND

Kigf **Granite near Fruitland (Late Cretaceous)**—Light- to medium-gray; medium grained; seriate to equigranular; granite to granodiorite (quartz 30–34%; K-feldspar 29–30%; plagioclase 26–30%); biotite typically present at <6 percent; minor to trace hornblende, titanite, apatite, and zircon; plagioclase weakly altered to clinozoisite and sometimes smectite; biotite moderately altered to chlorite; hornblende, where present, completely altered to carbonate and chlorite. Four geochemical analyses indicate that the unit ranges from granodiorite to granite (Fig. 2).

Two U-Pb zircon ages from rocks of this unit are late Cretaceous: one age (station 64) just south of the Fruitland Valley Road is 73.3 ±0.3 Ma and suggests that the rock there might be a younger phase of the main body of the granodiorite near Fruitland; the other age (station 18) is 74.2 ±0.3 Ma, which is slightly older than all of the ages from the granodiorite near Fruitland and also older than a quartz monzodiorite ~70 m to the south (station 19). Where this unit crops out south of Fruitland Valley Road, it was described by Campbell and Raup (1964) as quartz monzonite and later described as monzogranite by Joseph (1990a) who included it with somewhat similar rocks near the Germania Mine. Based

**Table 3**. Selected characteristics for plutonic rocks in the map area. All ages are from this publication except for those noted with an asterisk (*), which are from Ludwig and others (1981) and Asmerom and others (1988). Abbreviations: Q = quartz, A = alkali feldspar, P = plagioclase.

| Map unit | Main lithology | Color | Grain size | Grain distribution | QAP abundances (% of total minerals) | Other minerals (% of total minerals) | Accessory minerals | Age(s) (Ma) | Other major characteristics |
|---|---|---|---|---|---|---|---|---|---|
| $Kig_f$ | granite | light to medium gray | medium | equigranular to seriate | Q 30–34<br>A 29–30<br>P 26–30 | biotite <6%<br>hornblende <1% | titanite, apatite, zircon | 73.34 ±0.34<br>74.17 ±0.34 | dikes are rare |
| $Kigd_f$ | granodiorite | light gray to yellowish gray | medium to coarse | equigranular to slightly porphyritic | Q 13–22<br>A 7–21<br>P 50–75 | biotite ~5%<br>hornblende 1–3% | titanite, apatite, zircon, magnetite | 71.44 ±0.35<br>73.35 ±0.28<br>73.69 ±0.33 | dikes are rare |
| $Kigb_f$ | gabbro | dark gray | fine | equigranular to slightly porphyritic | Q 0<br>A 5<br>P 30 | actinolite (secondary) 59% | titanite, opaques | – – – | – – – |
| $Kiqm_m$ | quartz monzonite | gray to pinkish gray | medium to coarse | porphyritic | – – – | biotite 3–5%<br>muscovite <4% | titanite, apatite, fluorite, garnet, zircon, monazite, rutile, pyrite, epidote | ~65–80* | smoky quartz;<br>locally with K-feldpsar 1.5–5.5 cm |
| $Kiqm_g$ | quartz monzonite | light gray to yellowish gray | fine to coarse | equigranular to slightly porphyritic | Q 20–40<br>A 20–35<br>P 25–35 | biotite 1–5% | epidote (secondary?), hornblende, apatite, zircon, muscovite, titanite, opaques | – – – | cut by abundant aplite dikes;<br>grusy with rare outcrop |
| $Kig_g$ (wall rock) | granite | light to medium gray; pinkish to yellowish | medium to coarse | porphyritic (uncommonly equigranular) | Q 25–40<br>A 16–30<br>P 25–43 | biotite <1–8%<br>hornblende <2%<br>phlogopite <4% | titanite, apatite, zircon, tourmaline, opaques | 101.82 ±0.47<br>103.96 ±0.45 | K-feldspar up to 5 cm in size;<br>cut by abundant dikes and veins;<br>some outcrops |
| $Kig_g$ (veins) | – – – | – – – | – – – | – – – | – – – | – – – | – – – | 88.08 ±0.15<br>99.02 ±0.21 | – – – |
| $Kigd_g$ | granodiorite | light to medium gray | medium | equigranular | Q 22–34<br>A 10–17<br>P 40–58 | biotite 7–10%<br>hornblende <1–3% | titanite, apatite, zircon, epidote, opaques | 100.12 ±0.40<br>100.46 ±0.44<br>103.45 ±0.23 | dikes are rare (?);<br>outcrops abundant and forms ridges |
| Ki | varied | light to dark gray; greenish | fine to pegmatitic | varied; commonly porphyritic | varied | – – – | – – – | 71.64 ±0.13<br>95.07 ±0.18<br>104.28 ±0.64<br>104.38 ±0.20 | – – – |

* Ages from Ludwig and others (1981) and Asmerom and others (1988)

on the new ages, thin sections, and geochemistry (Tables 1 and 2) this unit is likely an interior more-felsic zone of the expansive granodiorite near Fruitland (unit Kigdf).

Kigdf **Granodiorite near Fruitland (Late Cretaceous)**—Light gray to yellowish gray; medium to coarse grained; typically equigranular but locally slightly porphyritic; granodiorite, quartz monzodiorite, and minor diorite (quartz typically 13–22%; K-feldspar ranges from 7–21%; plagioclase is 50–75%); subhedral to euhedral biotite up to 5 percent of the rock is the most common mafic phase; euhedral hornblende is sparse (1–3%); accessory minerals include magnetite, titanite, apatite, and zircon; plagioclase weakly altered to clinozoisite; biotite weakly altered to chlorite; one isolated intrusion east of Adams Mountain has a 2–3-m-wide zone of megacrystic augite (individual crystals up to 3 cm long) at the border with unit Kigf that is gabbroic diorite (station 19); locally contains inclusions of schist and quartz-rich schist 2–15 cm in length near contacts with the Covada Group; near Lake Roosevelt, the contact between this unit and older rocks is a 10–15-m-wide mixing zone; elsewhere the contact does appear to be narrow and sharp, though rarely is it exposed; calc-silicate skarn is typically present near where this unit intrudes carbonate-bearing rock; hornfels are locally common in country rock elsewhere. One very coarse-grained to pegmatitic sample from this unit near a tremolite-bearing skarn classifies as a syenite on Figure 2 (station 85). Description is from my observations, thin sections, and geochemical analyses (Table 2; Fig. 2) supplemented with descriptions from Joseph (1990a).

Four U-Pb zircon ages from rocks of this unit are late Cretaceous: two of the ages (stations 63 and 92) are from granodiorite located just below Eocene volcanic rocks and are very similar (74.0 ±0.2 Ma and 73.7 ±0.3 Ma); a third age from a quartz monzodiorite (station 19) is also similar (73.4 ±0.3 Ma) and is slightly younger than a nearby 74.2 ± 0.3 Ma age from unit Kigf about 70 m farther north (station 18); the fourth age (station 28) is from an isolated intrusion in Proterozoic rocks west of the Turk Mine and is a bit younger than the other three (71.4 ±0.4 Ma).

Kigbf **Gabbro near Fruitland (Late Cretaceous)**—Dark gray gabbro; fine grained; equigranular to slightly porphyritic; primarily composed of actinolite (59%) and plagioclase (30%) with some K-feldspar (5%) and minor titanite and opaques; mapped in two small outcrops, one of which is adjacent to an exposure of unit Kigdf and could represent a more-mafic border phase; geochemistry at two sites (Table 2; Figs. 2 and 3) indicates the rock is gabbro and could be tholeiitic. Though there are no ages from this unit, its association with unit Kigdf suggests it may be of similar age.

## PLUTONIC ROCKS NEAR THE MIDNITE MINE

Kiqmm **Quartz monzonite near the Midnite Mine (Late Cretaceous)**—Gray to pinkish gray; porphyritic; quartz monzonite, monzogranite, and granite; typically deeply weathered; medium- to coarse-grained groundmass with phenocrysts of K-feldspar ranging from 1.5 to 5.5 cm long; locally contains sericitic plagioclase and quartz phenocrysts; quartz is typically anhedral, smoky, and up to 1.5 cm long; contains 3–5 percent biotite, typically altered to chlorite; muscovite typically makes up less than 4 percent of the rock and is found as inclusions in K-feldspar or as an alteration product of biotite; accessory minerals include magnetite, titanite, apatite, fluorite, garnet, zircon, monazite, and rare rutile, pyrite, and epidote. Within about 50 m of the pluton margin, this unit is locally fine grained with sparse biotite-rich schlieren; elsewhere xenoliths are uncommon; intrudes the Togo Formation along a sharp boundary; cut by widely scattered dikes of leucocratic rock. Unit Kiqmm is exposed only in the southeastern corner of the map but is widespread both east and south of here. Description is compiled from Becraft and Weis (1963), Kinart (1980), Joseph (1990a), Waggoner (1990a), Asmerom and others (1988), and Miller (1996).

Near the Midnite Mine, south of the map area, a range of ages have been reported (U-Pb on zircon, Pb-alpha whole rock, and both zircon and apatite fission track) and are generally between about 65 to 80 Ma (Ludwig and others, 1981); a Rb-Sr age of 74.7 ±3 Ma is reported by Asmerom and others (1988). The rock near the mine is enriched in uranium and thorium, with average $U_3O_8$ content of 19 ppm, ranging from 1–46 ppm (Joseph, 1990a).

## PLUTONIC ROCKS NEAR THE GERMANIA MINE

These three units represent zones of a pluton near the Germania mine that grade from an outer equigranular phase of biotite-hornblende granodiorite, through a porphyritic to equigranular granite phase, and into a phase of typically equigranular quartz monzonite; all but the outer phase are cut by abundant aplite-alaskite-pegmatite dikes in this map (shown where thick or extensive as unit Ki; many thin dikes are unmapped); south of this map Becraft and Weis (1963) report that the dikes also cut granodiorite that may correlate with unit Kigdg. The new ages from this effort (Table 1) show that the pluton was emplaced from ~100–105 Ma without any clear age pattern and is substantially older than the granodiorite and granite near Fruitland (units Kigdf and Kigf). For the three units in total, 15 sites have geochemistry and thin sections; five of these sites have U-Pb ages on zircon, and two others have argon ages on muscovite (Tables 1 and 2; Fig. 2).

Kigdg **Granodiorite near the Germania Mine (Middle Cretaceous)**—Very light to medium gray; equigranular; medium grained; granodiorite and minor diorite and granite (quartz from 22–34%, K-feldspar ranges from 10–17%, and plagioclase is 40–58%); biotite is more abundant than in other rocks of this pluton and ranges from 7–10 percent of the rock; hornblende is present, typically at <1–2 percent of the rock; accessory minerals include epidote (at least some of which is from alteration), apatite, zircon, titanite, and opaques. Alteration is ubiquitous and generally presents as plagioclase weakly altering to sericite, smectite, epidote, actinolite, and K-feldspar; hornblende is strongly altered to smectite, chlorite, titanite, epidote, and carbonate; biotite is weakly altered to chlorite and epidote. Geochemical analyses and thin sections (Table 2; Fig. 2) indicate that the rock ranges from monzonite to granite. Description is from my observations supplemented with those from Du (1979).

Three U-Pb ages on zircon from this unit are mid Cretaceous (Table 1); two near the Germania mine yielded ages of 103.5 ±0.2 Ma (station 41), and 100.1 ±0.4 Ma (station 43). The younger age is from near the border with unit Kiqmg and is the youngest U-Pb age from this pluton. The third U-Pb age is from an isolated intrusion north–northeast of the Turk mine (station 21; 100.5 ±0.4 Ma), and due to its similar lithology and age it is included within this unit.

Kigg **Granite near the Germania Mine (Middle Cretaceous)**—Light to medium gray, pinkish gray, or yellowish gray; medium- to coarse-grained; typically moderately to weakly porphyritic; uncommonly equigranular or seriate; granite (25–40% quartz, 16–30% K-feldspar, and 25–43% plagioclase); phenocrysts include quartz (locally brownish) and plagioclase (locally with myrmekite rims) ranging up to 0.6 cm long; phenocrysts of K-feldspar are common, locally abundant, subhedral to euhedral, and range up to 5 cm long; biotite content varies from <1–8 percent, and where biotite is less abundant, phlogopite is up to 4 percent of the rock; typically <2 percent hornblende and locally jacketed by magmatic biotite; apatite, zircon, tourmaline, titanite, magnetite, and other opaques are common accessory minerals. Alteration is ubiquitous; plagioclase is weakly to moderately altered to sericite, smectite, K-feldspar, and tourmaline; biotite is strongly altered to chlorite, leucoxene, phlogopite, and (or) opaques. The unit is typically deeply weathered to soil and grus with abundant fragments of K-feldspar that are distinctive of this unit and allow mapping even where outcrop is sparse. Geochemical analyses and thin sections (Table 2; Fig. 2) indicate that the unaltered and unmineralized portions of this unit are granite and that samples from altered wall rock of the Exodus vein (stations 50 and 51) and mineralized veins within this unit (stations 44, 45, and 47) range widely in composition. Description is from my observations supplemented with those of Becraft and Weis (1963), Du (1979), and Joseph (1990a).

There are two U-Pb ages on zircon from this unit (Table 1), one from a granite porphyry near the unit's border with the granodiorite phase (unit Kigdg) that yielded an age of 104.0 ±0.5 Ma (station 42), and another from the wall rock of the Exodus vein at the Germania mine (station 49) that yielded an age of 101.8 ±0.5 Ma. There are also two Argon ages on muscovite, one from a mica-bearing vein in the pluton along the road to the Germania mine (station 45; 88.1 ±0.1 Ma), and another from a mica-rich zone of the Exodus vein at the Germania mine (station 50; 99.0 ±0.2 Ma); both ages have excess argon and somewhat disturbed age spectra. The similarity between the older muscovite argon age (~99 Ma) and the zircon U-Pb age of the surrounding pluton (~100–104 Ma) suggests they are closely related. The younger argon age (~88 Ma) could be a result of reheating during later pluton emplacement in the late Cretaceous.

Kiqmg **Quartz monzonite near the Germania Mine (Middle Cretaceous)**—Light gray to yellowish gray; grain size varies from fine to coarse but is most commonly medium; typically equigranular, but locally porphyritic as it grades into unit Kigg; finer-grained portions are found adjacent to metasedimentary rock of the Togo Formation; quartz monzonite and granite (typically 20–40% quartz; 20–35% K-feldspar; 25–35% plagioclase); phenocrysts, where present, are mostly quartz and K-feldspar with less abundant plagioclase; quartz is commonly somewhat gray and anhedral to subhedral; K-feldspar is chalky white and perthitic; plagioclase is subhedral and commonly with albite twins and myrmekite along its rim; biotite is 1–5 percent of the rock; accessory minerals include apatite, various types of epidote, hornblende, zircon, muscovite, titanite, and opaques. Alteration is similar to that seen in unit Kigg, with most plagioclase altering to sericite and smectite. This unit is deeply weathered and of all the plutonic units, the most difficult in which to find outcrop. Within the map area, abundant dikes of alaskite, aplite, and (or) pegmatite cut this unit (and unit Kigg) and strike northeast; the dikes are more resistant than the surrounding rock. South of the map area, rock of this unit is also cut by several east-striking pyrite-bearing quartz veins (Becraft and Weis, 1963). Geochemical analyses (Table 2; Fig. 2) indicate that two samples southeast of the Germania mine are granite: one is near the boundary with unit Kigg and another is within the main body of unit Kiqmg; despite these results, other outcrops and previous workers describe the majority of the unit as quartz monzonite. Description is from my observations supplemented with those of Becraft and Weis (1963), Du (1979), and Joseph (1990a).

## Paleozoic Rocks West of the Huckleberry Range Fault

The Huckleberry Range fault divides Paleozoic rocks to the west—correlated with the Roberts Mountains allochthon and accreted during the Antler Orogeny (Smith and Gehrels, 1992b)—from Paleozoic rocks to the east that formed largely in place with respect to western North America after the Neo- to Mesoproterozoic rifting of Rodinia. The Huckleberry Range fault may be correlative to the Golconda thrust of central Nevada (Snook and others, 1981).

Oigb **Intrusive hornblende gabbro (Ordovician?)**—Dark gray to green hornblende gabbro; typically coarse grained; weakly foliated and (or) sheared; found in sill-like lenses intruding rocks of the Covada Group south of Hunters; one geochemical analysis from ~25 km north of the map area indicates that the gabbro is somewhat similar to the greenstone of the Covada Group (Smith, 1991b); despite the lithologic and geochemical similarities, the Ordovician age is queried by Smith (1991a). Description compiled from Smith (1991a).

### BRADEEN HILL ASSEMBLAGE (ORDOVICIAN)

The Bradeen Hill assemblage was described as a series of interbedded chert-rich and slate-rich intervals north of the map area by Smith (1982) and more clearly defined by Smith and Gehrels (1992a) based on detailed mapping by Smith (1991a,b). It lies with apparent conformity on the volcanic rocks of the Butcher Mountain Formation, and locally contains greenstone lenses similar to those in the underlying formation (Smith and Gehrels, 1992a). In the map area it is found only in a small fault-bound block east of Hunters and consists of thin and discontinuous chert within phyllite and slate. Includes:

Omcb **Chert of the Bradeen Hill assemblage**—Dark gray to black chert; bedded; phyllitic partings between beds are common; locally laminated; recrystallized; occurs as thin layers and lenses within the phyllite of unit Ophb. Description is compiled from Smith (1991a) and Campbell and Raup (1964).

Ophb **Phyllite of the Bradeen Hill assemblage**—Dark gray to black phyllite, slate, and minor quartzite; hornfels and spotted phyllite are present to the north of the map area near Twin Lakes (Fullmer, 1986). Description from Smith (1991a).

### COVADA GROUP (ORDOVICIAN)

The Covada Group was first recognized by Pardee (1918) and later mapped extensively by Campbell and Raup (1964), Becraft (1966), Smith (1982), and Snook and others (1990). On the basis of detailed mapping of the group by Smith (1982; 1991a,b), the Butcher Mountain and Daisy Formations were defined by Smith and Gehrels (1992a), correlated with the Lardeau Group of British Columbia, and interpreted as the northern components of the Roberts Mountains Allochthon (Smith and Gehrels, 1992a,b). A limestone unit is included with the Covada Group but was not mapped as part of either the Butcher Mountain or Daisy Formations by Smith (1991a,b).

Ocbc **Limestone and marble of the Covada Group**—Medium to dark gray impure limestone; blue-gray weathering is uncommon; in places sandy with phyllitic partings; typically found as thin lenses and beds within and dividing clastic and volcanic units of the Covada Group; commonly recrystallized. There is a well-exposed outcrop of calc-silicate skarn along Highway 25 just north of Fruitland that is included in this unit. Description compiled from Campbell and Raup (1964), Smith (1991a), and my observations.

### Butcher Mountain Formation of the Covada Group

The Butcher Mountain Formation was defined by Smith and Gehrels (1992) as a sequence of volcanic and minor volcaniclastic units found near the town of Daisy, about 25 km north of this map. Neither the top nor the bottom contacts of the unit are present in the map area, but the top is defined as the depositional contact with overlying chert and argillite of the Bradeen Hill assemblage and the base of the unit is the lowest continuous greenstone (Smith and Gehrels, 1992a). Subdivided into:

Omvb **Greenstone of the Butcher Mountain Formation**—Black, dark gray, or dark green metabasalt (greenstone) with minor basaltic breccia, metatuff, and slate; structureless to well foliated or schistose; locally highly sheared; basalt includes flows and flow breccia and is commonly calcareous; primary textures are generally absent, though pillows are locally present but not abundant; flows are pyroxene porphyritic but most original mineral phases have been altered; groundmass is largely chlorite, albite, actinolite, titanite, epidote, and opaque minerals; two samples of this unit show that it is calc-alkaline basaltic andesite (Figs. 2 and 3) and is composed mostly of plagioclase altered to actinolite (85%) and opaque minerals (8%) with thin veins of actinolite, iron oxides, and quartz; as a whole, the unit has many calcite-filled amygdules; skeletal ilmenite, pleochroism in augite. Geochemical analyses farther north (Smith, 1991b) indicate a high Ti content of the original basalt. Early Ordovician trilobites are found in volcaniclastic rocks interbedded with greenstone about 25 km north of the map area at Butcher Mountain (Snook and others, 1981). Description compiled from Smith (1991a), Joseph (1990a), and my observations.

Omvtb **Meta-tuff of the Butcher Mountain Formation**—Ash tuff to coarse lapilli tuff; finely laminated; predominantly found interbedded with greenstone (unit Omvb), but also sparsely distributed as thin layers throughout unit Omsd. Description from Smith (1991a) and Campbell and Raup (1964).

### Daisy Formation of the Covada Group

The Daisy Formation was defined by Smith and Gehrels (1992a) as a thick sequence of metasedimentary lithologies found near the town of Daisy, about 25 km north of this map. The formation lies below the volcanic rocks of the Butcher Mountain Formation. It is at least 2,500 m thick near its type locality (Smith and Gehrels, 1992a) and its base is not exposed. Includes:

Omsd **Quartzite and minor slate of the Daisy Formation**—Gray, brown, olive, or greenish quartzite and subordinate interbedded gray to black slate; sandstone is typically fine to medium grained, but locally as coarse as granules; thin to very thickly bedded, though difficult to recognize, partly due to a locally developed foliation; slaty intervals laminated to thinly bedded; sandstone ranges from feldspathic wacke to rare quartz arenite, is poorly sorted, angular to subrounded, and coarser beds have large bluish quartz and feldspar grains; graded bedding and small-scale crossbedding are uncommon; Bouma A–E divisions are common; along the shore of

Lake Roosevelt near Cretaceous plutons the unit is a garnet-bearing schist.

On her original map, Smith (1991a) shows a unit southwest of Hunters that is not in her legend or described in her pamphlet, but which I interpret to represent undivided sedimentary units of the Daisy Formation; these rocks are included within unit Omsd on this map. At least 105 m of section was measured along the Hunters–Springdale Road by Smith and Gehrels (1992a); they describe predominantly medium- to thick-bedded medium- to coarse-grained normally graded sandstone beds with subordinate thin to medium interbeds of laminated fine sandstone, siltstone, and shale. Due to faulting, it is not clear where in the unit this section may be but it likely represents a small portion of the true thickness in this map. Description is compiled from Campbell and Raup (1964), Smith (1991a), and my observations.

## Paleozoic Rocks East of the Huckleberry Range Fault

Oarl **Ledbetter Slate (Ordovician)**—Medium to dark gray slate, argillaceous limestone, and calcareous slate; some beds of blue-weathering limestone; light gray to white crystalline dolomite locally present; argillaceous intervals highly fissile; poorly exposed. In rocks of this unit mapped by Smith (1991a) and Campbell and Raup (1964) just north of the map area along the Hunters-Springdale Road, A. G. Harris and J. E. Repetski in Joseph (1990a) report a Middle Cambrian to Early Ordovician conodont from a sequence of proximal turbidites and note that based on alteration, the rock reached at least 300 °C. Middle Ordovician graptolites are also found in the Ledbetter Slate nearby (Snook and others, 1981). Though covered, the base may be conformable with older units; the top is not exposed and a fault is inferred to separate rocks of this unit from those of the assemblage of Bradeen Hill. Description compiled from Campbell and Raup (1964) and Joseph (1990a).

Omc **Chert (Ordovician)**—Dark gray to black chert with minor interlaminated limestone; chert is microcrystalline; limestone is more abundant in the map area compared to farther north; many secondary quartz veins and irregular voids with quartz and limonite; may be partly equivalent to the Ledbetter Slate; unit is poorly exposed. Description is from Campbell and Raup (1964) and Joseph (1990a).

OꞒlm **Metaline Formation (Middle Ordovician to Middle Cambrian)**—Light gray, dark gray, or bluish gray limestone and minor thin interbeds of dark gray slate and medium gray dolomite; limestone is typically fine grained and thin bedded; black chert nodules are common in carbonate rocks; light and dark banding in the dolomite is locally common, especially near the base of the unit south of the Hunters–Springdale Road. The limestone is recrystallized into white to bluish gray coarse-grained marble near intrusive rocks; within a few hundred meters of intrusive rocks calc-silicate skarn is locally well developed, including euhedral garnet up to 3 cm across and multi-centimeter masses of anhedral garnet, diopside, tremolite, and wollastonite; in these locations contorted bedding and small-wavelength (1–2 m) isoclinal folds are locally present. Seven geochemical analyses of this unit—mostly from near and north of the Deer Trail Monitor mine (Table 2)—show that it includes both limestone and dolomite.

This unit was previously mapped by Campbell and Raup (1964) as the Old Dominion Limestone of Weaver (1920), though that name has been replaced by the Metaline Formation as described in Joseph (1990a). Fossil evidence from near Colville in this unit indicates a Middle Cambrian to Middle Ordovician age range (Repetski, 1978; Schuster and others, 1989; Carter, 1989). Based on this map, the unit is at least 480 m thick west of Adams Mountain; the unit is more than 800 m thick to the north of the map area (Smith, 1982). Description compiled from Campbell and Raup (1964), Becraft and Weis (1962), and Joseph (1990a).

## Cambrian to Neoproterozoic Rocks

### ADDY QUARTZITE

The Addy Quartzite was first described by Weaver (1920) and Bennett (1941), defined by Campbell and Loofbourow (1962), and studied in great detail by Lindsey (1988) and Lindsey and others (1990). The unit is 1,100 to 1,400 m thick (Lindsey and others, 1990) and lies along a regional unconformity that omits ~1.1 km of Neo- to Mesoproterozoic strata over 15 km of strike. Regionally the Addy Quartzite is conformably overlain by either the Metaline Formation or the Maitlen Phyllite (Lindsey, 1988). Lindsey (1988) maps four subunits whereas Campbell and Raup (1964) and Becraft and Weis (1963) only map two. Based on past efforts and this mapping, three subunits are mapped: the upper unit from Lindsey (1988), a mostly quartzite unit that combines his other three units, and an argillite subunit.

On the basis of three detrital-zircon samples just north of the map area (Linde and others, 2014) and Early Cambrian trilobites in the upper part of the formation (Okulitch, 1951; Miller and Clark, 1975), the base of the Cambrian was placed in the lower part of the Addy Quartzite by Linde and others (2014); their upper age samples have a few ~560 Ma ages, and their lowest sample has an ~1,100 Ma age peak. Based on this, the upper subunit is Early to Middle (?) Cambrian and the lower two subunits are Early Cambrian through Neoproterozoic, similar to Lindsey (1988) and Miller (1996). Descriptions are compiled from Campbell and Loofbourow (1962), Campbell and Raup (1964), Evans (1987), Lindsey (1988), and Lindsey and others (1990). Subdivided into:

Ꞓpha **Phyllite, argillite, and minor quartzite of the Addy Quartzite (Cambrian)**—Brown, green, and gray phyllite, siltite, and argillite alternating with white to tan quartzite; fine-grained intervals are 10 to 20 m thick and consist of thin to thick beds of planar, wavy, or hummocky strata that are locally mottled; *Planolites* and *Cruziana* trace fossils are present in the map area and other trace and body fossils, including trilobites, are more abundant farther northeast; well-developed cleavage and foliation is common; quartzite intervals are typically 1 to 20 m thick, decrease in abundance and thickness up section, and are fine to medium grained with rare medium beds of pebbly quartzite; bedding ranges from structureless to planar and trough cross bedded with local ripple cross-lamination; medium- to coarser-grained intervals are quartz arenite, whereas fine- to medium-grained intervals are quartz wacke containing up to 20 percent muscovite and chlorite; argillites are mostly muscovite and chlorite and one sample had up to 28 percent iron oxide content; siltites are commonly quartzose; a few thin beds of brown silty limestone are irregularly found near the top of the unit.

Near intrusive rocks the quartzite is vitreous and recrystallized and finer-grained intervals are phyllitic. The lowest >1.5-m-thick argillite with lenticular quartzite defines the base; top defined by the lowest laterally persistent >0.5-m-thick limestone bed. The unit is between 250 and 400 m thick regionally and 285 m thick in the map area. Description is mostly from Lindsey (1988) though the upper interbedded argillite and quartzite of Becraft and Weis (1963) guided mapping in the southern part of the map area. Based on its stratigraphic location and lithology, this unit may correlate with part of the Maitlen Phyllite.

ꞒZara **Argillite of the Addy Quartzite (Cambrian to Neoproterozoic)**—Dark gray to black argillite and siltite; laminated to medium bedded; about 80 m thick just northeast and southwest of the Hunters–Springdale Road and south of O-Ra-Pak-En Creek in the south; in both places it overlies about 50–60 m of basal quartzite (unit ꞒZqa) and is in turn overlain by a thick and continuous package of quartzite of unit ꞒZqa; the two recessional intervals of this unit are bracketed by bold ridges of quartzite and provide an excellent offset marker across minor faults.

ꞒZqa **Quartzite of the Addy Quartzite (Cambrian to Neoproterozoic)**—White, tan, light brown, blue, or lavender quartzite with minor interbeds of argillite; a basal interval is commonly found beneath unit ꞒZara and is fine to medium grained, medium to thick bedded, and contains rare coarse-grained beds and thin discontinuous interbeds and thin partings of purple and brown argillite; sedimentary structures in basal interval are not typically abundant, but where present consist of planar crossbedding with less abundant trough crossbedding; channels are locally abundant. Above unit ꞒZara, and comprising the majority of the entire Addy Quartzite, is a purple-banded quartzite with distinctive 1 mm to 5 cm purple to red banding and layers of heavy minerals (zircon, rutile, and magnetite); thin lenticular beds and partings of argillite are present throughout the basal interval; pebble beds are scarce; planar lamination and bedding is most common; planar cross beds are also common; the purple-banded quartzite is up to 150 m thick near the northern map boundary, but not observed in the southern map area, nor farther south. A coarse-grained quartzite is typically found above the purple-banded quartzite and ranges from medium-grained sand to granule, with pebble conglomerate beds up to 10 cm thick common in some zones; generally thin to medium bedded; planar cross bedding is locally abundant; discontinuous beds of argillite and siltite are scattered throughout; *Scolithos* burrows are found locally near the top of the unit. The main interval of quartzite is 630 to 680 m thick and the basal quartzite (separated by an intervening argillite layer) is 50–60 m thick.

## Neoproterozoic to Mesoproterozoic Rocks

### WINDERMERE GROUP

### Huckleberry Formation

The Huckleberry Formation was defined by Bennett (1941) and Campbell and Loofbourow (1962) and includes a lower conglomeratic unit and an upper greenstone. Both lithologies are present in the northern map area, but neither unit is present south of the map area due to thinning, faulting, and (or) erosion along an unconformity separating rocks of the Windermere Group from the overlying Addy Quartzite. The Huckleberry Formation is concordant with the underlying Buffalo Hump Formation in the map area. Detrital zircon ages (Box and others, 2020) suggest a closer affinity and age between these two formations than previously inferred; however, the Buffalo Hump Formation is not reassigned to the Windermere Group here partly because Campbell and Loofbourow (1962) report an unconformity that juxtaposes the greenstone of the Huckleberry Formation with the Stensgar Dolomite farther north; such a relationship appears to indicate the entire Buffalo Hump Formation was eroded before deposition of the Huckleberry Formation and rules out the two formations being the same age . There are many greenstone dikes and sills in the region that are nearly identical in appearance to the flows of the Huckleberry Formation; earlier workers either did not map them (Campbell and Loofbourow, 1962), or mapped the flows and dikes as separate units (Campbell and Raup, 1964; Evans, 1987). Miller (1996) combined them into a single map unit and that approach is used here, noting that Campbell and Loofbourow (1962) also understood the dikes fed the extrusive flows. Descriptions are compiled from Campbell and Loofbourow (1962), Campbell and Raup (1964), Evans (1987), and Miller (1996).

Zgh **Greenstone of the Huckleberry Formation (Neoproterozoic)**—Dark greenish gray to greenish black or grayish green fine-grained metabasalt (greenstone) and less abundant tuffs and volcaniclastic rocks; metabasalt occurs chiefly as flows, though there are abundant thin, generally poorly outcropping greenstone dikes and sills throughout the map area, many too small to show at map scale; flows are aphyric to porphyritic with up to 10 percent plagioclase; phenocrysts are commonly replaced by epidote, clay, chlorite, pumpellyite, and titanite; groundmass is completely altered to chlorite, titanite, leucoxene, and tremolite; within flows, individual layers are poorly defined; pillow structures are recognized at one locality in the map area and are somewhat abundant, though difficult to identify, east of the map area; vesicles and thin to thick (sometimes up to 10 cm) fractures are filled with calcite and are locally common. Dikes, locally gabbroic, are altered and well cleaved or phyllitic; one dike within the Stensgar Dolomite west of the Deer Trail mine (site 34) is strongly altered, with equal proportions of secondary K-feldspar, biotite, actinolite, and diopside, with less plagioclase and opaques and minor sphene; metabasalt flows are locally schistose; tuffaceous intervals are locally phyllitic. A maximum thickness of about 360 m is calculated from this map; Evans (1987) estimates 750–1,100 m northeast of the map area; overall the unit appears to thin southwestward through the map area and Miller (1996) notes that the unit also appears to thin eastward. Dikes are widespread but absent in younger units; most are thin and poorly exposed and are mapped only where relatively thick and continuous.

Outside of the map area, the upper part of the greenstone has a whole-rock Sm-Nd age of 762 ±44 Ma (Devlin and Bond, 1988). Miller and Clark (1975) describe the greenstone as tholeiitic and Box and others (2020) analyzed whole-rock geochemistry from a dike cutting the Togo Formation, a dike cutting the Stensgar Dolomite, and a flow of the Huckleberry Formation northeast of the map area and conclude that they are all similar, have geochemical traits of enriched mid-ocean ridge basalts, and were likely the result of the continental rifting of western North America. Geochemistry from three dikes and one flow in this report confirm these previously identified geochemical traits (Table 2, Figs. 2 and 3, Data Supplement).

ZYcgh **Metaconglomerate and metadiamictite of the Huckleberry Formation (Neoproterozoic to Mesoproterozoic)**—Pale green, pale gray, buff, or rarely black matrix-supported conglomerate and diamictite; poorly sorted to unsorted; clasts typically pebble size, angular to rounded, and include dolomite, argillite, siltite, quartzite, and milky quartz; matrix mostly sand and silt and much altered to chlorite; bedding poorly developed or obscured by schistosity; well foliated to phyllitic; locally well-developed and closely spaced slaty cleavage; clasts typically at least somewhat flattened and locally stretched; oval cavities are likely dissolved carbonate clasts. In the map area the unit is perhaps 750 m thick but its base is faulted. The unit is absent near the southern map boundary where it is eroded along the unconformity beneath the Addy Quartzite and intruded by Cretaceous plutonic rocks, and in the north it could be duplicated by an unrecognized fault. The unit is between 200 and 500 m thick to the north and east of the map area, and thins to the northeast (Evans, 1987; Miller, 1996). Just north of the map area, the lower Huckleberry Formation has a maximum depositional age of 1,143 ±19 Ma (Box and others, 2020).

## DEER TRAIL GROUP

The Deer Trail Group is a thick sequence of carbonate, quartzite, argillite, slate, and phyllite in northeastern Washington informally called the ‘magnesite belt’ for deposits mined from it in the early 20th century (Campbell and Loofbourow, 1962). Regionally it has long been considered to be unconformably overlain by rocks of the Windermere Group, but recent detrital zircon ages suggest that the upper part of the Deer Trail Group (Buffalo Hump Formation) and the lower Windermere Group (Huckleberry Formation) have similar provenance and age (Box and others, 2020). After revision by Miller (1996), the Deer Trail Group contains, from oldest to youngest, the Togo Formation, Chamokane Creek Formation, Wabash Detroit Formation, McHale Slate, Stensgar Dolomite, and Buffalo Hump Formation. Previous work correlated the Deer Trail Group with the upper part of the Belt-Purcell Supergroup (Miller and Whipple, 1989) based on lithologic and stratigraphic evidence. However, new detrital zircon ages indicate that all of the units, including the Togo Formation, entirely post-date the Belt-Purcell Supergroup (Box and others, 2020).

### Buffalo Hump Formation of the Deer Trail Group

Slate, argillite, and quartzite above the Stensgar Dolomite were identified by Weaver (1920) and Bennett (1941) and named by Campbell and Loofbourow (1962). Box and others (2020) report a 1,112 ±20 Ma U-Pb age from detrital zircons, which is ~200 million years younger than other rocks of the Deer Trail Group. Based on its age and detrital-zircon-age-population similarity with rocks of the Windermere Group, Box and others (2020) suggest that the formation may be part of the Windermere Group.

It is generally difficult to distinguish this unit from older slates and quartzites in the area except that it lacks carbonate-bearing rocks and has some evidence of higher energy deposition. Quartzite forms prominent ridges whereas slaty intervals are recessive, and the previous mapping is refined using these characteristics. Overall, quartzite becomes more prevalent and thicker to the south (Campbell and Loofbourow, 1962) where there appears to be a single thick quartzite bound by two thin argillite intervals; in the north there are three thick argillite intervals and two less-thick quartzite intervals; Evans (1987) estimates a thickness of less than 745 m for this unit; this map is used to estimate a thickness of up to 1,100 m, though faults are common and could have duplicated some of the section; the unit is intruded by Cretaceous plutonic rocks in much of the map area, and seems truncated by the unconformity beneath the Addy Quartzite. Cleavage is pervasive throughout the Formation and varies from very well developed to nearly absent. Descriptions compiled from Campbell and Loofbourow (1962), Campbell and Raup (1964), Evans (1987), and Miller (1996).

ZYarb **Argillite of the Buffalo Hump Formation (Neoproterozoic to Mesoproterozoic)**—Light to medium gray, greenish gray, or olive brown slate, argillite, and minor phyllite; bedding usually absent, but a minor amount is laminated to thinly bedded; in some locations slate grades up into quartzite; thin cleavage is typically well developed, but locally absent; northeast of the map area, the unit consists of mostly quartz and feldspar grains with some chlorite augen, diagenetic reduction spots, pyrite cubes up to 1 cm in size, cleavage-parallel veins of white quartz 4–30-cm thick and sparse porphyroblasts of magnetite (Evans, 1987).

ZYqb **Quartzite of the Buffalo Hump Formation (Neoproterozoic to Mesoproterozoic)**—White, gray, pinkish gray, yellow, brown, or bluish subvitreous to vitreous quartzite; generally fine to medium grained; includes minor thin beds of white, gray, brown, or maroon siltite, argillite, or slate and uncommon stringers and lenses of stretched quartzite-pebble conglomerate; bedding ranges from indistinct to well developed; where visible, bedding is planar to cross bedded and ranges from a few meters up to 300 m thick with substantial variation along strike; sorting increases and the unit is more typically medium grained as the quartzite thickens to the south; jointing and fracturing are abundant.

## Stensgar Dolomite of the Deer Trail Group

Ycbs **Stensgar Dolomite (Mesoproterozoic)**—White, tan, or gray dolomite and dolomitic marble with minor thin interbeds and bedding-plane partings of argillite; dolomite is typically fine grained and becomes coarse where recrystallized; weathers medium gray, which is unique among the Proterozoic carbonates; generally thin bedded to laminated except where recrystallized and bedding is absent; recrystalization is most prevalent south of the Hunters–Springdale Road; some areas have silty or argillaceous interbeds; to the north of the map area an 85-m-thick interval of argillite is present near the middle of the unit (Evans, 1987); nodules of chert and veinlets of secondary chert are locally present but not common.

Thin section analysis to the northeast of the map area (Evans, 1987) indicates the Stensgar Dolomite is 80–99 percent carbonate, mostly dolomite and minor calcite; some beds contain <20 percent silt-size quartz grains that are locally elongate along bedding-plane-parallel cleavage; a wide variety of minerals are present in minor to trace amounts, predominantly along bedding planes. All known occurrences of magnesite in the region are found in this unit; zones up to 100 m wide have been replaced by fine to coarse-grained gray, black, and red magnesite, locally in alternating dark and light layers; magnesite parallels and cuts across bedding.

First named and studied by Weaver (1920) and Bennett (1941); raised to a formation within the Deer Trail Group by Campbell and Loofbourow (1962). The base is the first thick bed of dolomite above which dolomite exceeds argillite; generally a 10–20-m-thick interval. In the northern part of the map area the Stensgar Dolomite is overlain by the Buffalo Hump Formation; the Stensgar Dolomite is not definitively found south of the map area where it appears to be progressively truncated by the sub-Addy Quartzite unconformity. To the north of the map area, Evans (1987) estimates a thickness of >500 m; Campbell and Loofbourow (1962) measure 155–220 m; 175 m is calculated from this map.

## McHale Slate of the Deer Trail Group

Ymmm **McHale Slate (Mesoproterozoic)**—Dark to light gray slate, slaty argillite, argillite, and minor phyllite; weathers brown to olive brown; lower third typically gray with tan to pale gray laminae; upper two thirds typically gray at base grading into alternating intervals of pale green or lavender gray; bedding ranges from thin laminations to fining-upward intervals up to 3 cm thick; typically planar laminated, though wavy beds are also common and some have erosional bases; laminated light and dark gray siltite beds are present locally; thin quartzite beds are rare; in one location north of the map area Evans (1987) found that thin beds of pale-gray dolomite interbedded with silvery slate increase in abundance toward the upper portion of the unit; clasts are mostly quartz, feldspar, and muscovite, with a variety of minor minerals such as chlorite, pyrite, calcite, leucoxene, hematite, magnetite, and tourmaline (Evans, 1987); pyrite and ankerite metacrysts are described by Campbell and Loofbourow (1962) near greenstone dikes.

Slaty cleavage is typical, locally well developed, and ranges from thick to very thin, but in some locations is mostly absent; Becraft and Weis (1963) note that cleavage generally is less steep and more westerly in strike than bedding; Miller (1996) notes that some portions of the unit are better described as phyllite; pencil cleavage is common.

Faults are common within, above, and below the McHale Slate, and it seems likely that repetition of section along these structures explains much of its varied map-pattern thickness: a 150-m thickness is calculated near the southern map boundary and ~350 m near the northern map boundary; Evans (1987) measures a maximum thickness of 1,510 m; Miller (1996) estimates about 370 m; Campbell and Loofbourow (1962) estimate about 330–450 m and note that it is much folded; Becraft and Weis (1963) estimate ~730 m near the south edge of this map, thinning to 230 m farther south where cut by the sub-Cambrian unconformity. The unit was named by Campbell and Loofbourow (1962). Description is compiled from Campbell and Loofbourow (1962), Becraft and Weis (1963), Campbell and Raup (1964), Evans (1987), and Miller (1996).

## Wabash Detroit Formation of the Deer Trail Group (Mesoproterozoic)

Miller (1996) redefined the middle part of the Edna Dolomite of Campbell and Loofbourow (1957) as the Wabash Detroit

Formation, consisting of dolomite, argillite, and minor quartzite below the dark gray McHale Slate and above the carbonate-bearing quartzite of the Chamokane Creek Formation. The upper quartzite, upper dolomite, and middle argillite of the Edna Dolomite from Campbell and Raup (1964) are assigned to this formation. To the south, quartzite and argillite pinch out and dolomite is predominant, with thin quartzite locally near the top (Becraft and Weis, 1963). Based on U-Pb ages from detrital zircons the upper part of the formation is 1,300 ±24 Ma, the lower part is 1,359 ±38 Ma (Box and others, 2020); the base appears conformable (Becraft and Weis, 1963) and is likely gradational with the upper Chamokane Creek Formation.

Excepting quartzite, this formation is poorly exposed and outcrops are sparse; the best exposures are along the Hunters–Springdale Road and along Alder Creek. Miller (1996) reports discontinuous outcrops of greenstone within the Wabash Detroit Formation to the east, though similar outcrops were not found in this effort. A thickness of 390 m is calculated in the middle of the map area near the Turk mine, but sections north and south of there are faulted; Miller (1996) reports a thickness of about 240 m for the formation to the east. Descriptions compiled from Campbell and Loofbourow (1962), Becraft and Weis (1963), Evans (1987), Miller (1996), and my observations.

Yqwd **Quartzite of the Wabash Detroit Formation**—Vitreous light gray, buff, or grayish pink quartzite; poorly defined thick to thin beds; discontinuously present near the top of the formation in the map area and southward; where present, typically about 20–45 m thick. Miller (1996) suggests that the unit may have been continuous but is either faulted out or covered where it appears to be absent.

Ycbwd **Dolomite of the Wabash Detroit Formation**—Impure off-white, buff, pale gray, or rarely dark gray dolomite with minor thin interbeds of pale green to gray argillite or slate; dolomite is fine grained, locally siliceous, ferruginous, or calcareous; ranges from very thin bedded to thick bedded; rare thin beds of limestone are reported just to the northeast (Evans, 1987); chert-bearing beds are present in the map area, and to the east where stromatolites are also reported (Miller, 1996); white quartz veins perpendicular to bedding are up to several cm thick, common, and locally abundant; thick and distinctive brick-red soil in low-lying areas or saddles is commonly the only indication of this unit at the surface. Compared to the Stensgar Dolomite, this unit has consistently higher iron and silica and lower magnesium and was rarely mined for magnesite (Campbell and Loofbourow, 1962). Unit is ~170–190 m thick as calculated from the map.

Yarwd **Argillite and slate of the Wabash Detroit Formation**—Light brown to dark gray slate and argillite with minor siltite; typically appears unbedded with thin bedding preserved only in slightly coarser-grained sections; paper-thin cleavage is common and typically well developed, though not everywhere present; locally siliceous; commonly sheared (Miller, 1996). Unit is ~200–220 m thick as calculated from the map.

## Chamokane Creek Formation of the Deer Trail Group (Mesoproterozoic)

Miller (1996) redefined the lower Edna Dolomite and upper Togo Formation as the Chamokane Creek Formation just to the east of this map. This nomenclature is used here though it appears there are some differences in the proportion and stratigraphic positions of dolomite, quartzite, and argillite intervals from those farther east. In general the lithologic descriptions and mapping of Campbell and Raup (1964) are used and their map units are reassigned to the Chamokane Creek Formation as defined by Miller (1996). Two main lithologic units arise from this: a carbonate-rich interval (unit Ycbcc) composed of the lower dolomite unit of Campbell and Raup (1964), and two quartzite-rich intervals (both labeled unit Yqcc) corresponding to the lower quartzite of the Edna Dolomite and the upper quartzite of the Togo Formation of Campbell and Raup (1964). Following Miller (1996), the base of the Chamokane Creek Formation is the lowest carbonate-bearing clastic rock above the phyllite of the Togo Formation and is gradational. Descriptions of lithologic units compiled from Campbell and Loofbourow (1957, 1962), Becraft and Weis (1963), Campbell and Raup (1964), Evans (1987), and Miller (1996).

Ycbcc **Dolomite and minor argillite of the Chamokane Creek Formation**—Tan, buff, or light gray impure fine-grained dolomite interbedded with carbonate-bearing quartzite, siltite, and slaty argillite to phyllite; dolomite generally thin bedded, but ranges from thick bedded (up to 3 m) to laminated; locally a thin cleavage is developed parallel to bedding; pyrite is ubiquitous but present only in small amounts; dolomite only rarely exposed due to development of thick dark red to reddish-brown soils, locally with chips of green to brown slate; red soils on subtle karst-like topography with thick vegetation or swamps aid identification of this unit in the field.

Yqcc **Quartzite of the Chamokane Creek Formation**—Light gray to white, greenish or bluish gray, or reddish brown fine- to medium-grained quartzite with thin interbeds and partings of dark gray to greenish phyllite, slate, and (or) argillite. The quartzite beds range from quartzitic slate to slaty quartzite, with few beds of pure quartzite; bedding varies from poorly to thinly bedded with even to wavy beds and rare cross beds; many beds have soft-sediment deformation features.

In the Adams Mountain 7.5-minute quadrangle a lower quartzite is common between the carbonate-rich interval of the Chamokane Creek Formation and the Togo Formation; this was previously mapped as quartzite of the Togo Formation (Campbell and Raup, 1964). Quartzite is also found above the carbonate-rich interval, but only in the northern part of the quadrangle; this was previously mapped as quartzite of the Edna Dolomite (Campbell and Raup, 1964). To the east of the Adams Mountain quadrangle, Miller (1996) describes the basal portion of the lower quartzite grading from carbonate-bearing quartzite and argillite to noncarbonate-bearing quartzite over a thickness of 5–10 meters and determines a thickness of 150 m for the lower unit. Regionally, the lower quartzite thickens southward (Campbell and Loofbourow, 1962).

### Togo Formation of the Deer Trail Group (Mesoproterozoic)

The Togo Formation is the oldest unit in the region and was named by Campbell and Loofbourow (1957; 1962) for exposures near the Togo mine. They and others (Campbell and Raup, 1964; Becraft and Weis, 1963; Evans, 1987) described the Togo Formation as containing a lower portion of mostly phyllite and argillite and an upper portion of predominantly quartzite. Later work to the east by Miller (1996) redefined the Togo Formation to include only the carbonate-poor phyllitic rocks, and that definition is used here. The base is not exposed, and is everywhere either faulted or intruded by younger plutonic rocks (Campbell and Loofbourow, 1962; Becraft and Weis, 1963; Miller, 1996). Box and others (2020) report a U-Pb maximum depositional age from detrital zircons of 1,362 ±27 Ma for the Togo Formation.

Pervasive internal deformation and a lack of marker units make determining thickness difficult and seem to exaggerate the map-view width of the unit (Miller, 1996). Estimates of thickness include 6,100 m (Becraft and Weis, 1963), ~1,200 m (Campbell and Loofbourow, 1962), and 600 m (Evans, 1987); Miller (1996) determines a minimum thickness of 800 m. Cleavage and phyllitic foliation are most developed in the Togo Formation compared to all other units in the map area, perhaps in part due to differences in bulk composition, but also likely due to its greater age and depth of burial. Description is mostly compiled from Campbell and Loofbourow (1962), Becraft and Weis (1963), Evans (1987), and Miller (1996), and supplemented with my observations.

Ypht **Phyllite and argillite of the Togo Formation**—Light to dark gray or black phyllite and thinly interbedded slaty argillite to siltite; locally green to dark brown; thinly bedded to laminated, with a prominent and well-developed bedding-plane cleavage; bedding is typically planar but locally wavy; graded bedding locally recognized and soft-sediment deformation is common. Phyllite is composed of quartz, muscovite, biotite, chlorite, feldspar, and lithic fragments; micas are typically parallel or sub-parallel to bedding. Within a few hundred meters of younger plutonic rocks, the phyllite has 5–15-mm ovoid clots of dark fine-grained magnetite and biotite. Campbell and Loofbourow (1962) report dark gray poikilitic andalusite porphyroblasts up to 2.5 cm long and some occurrences of cordierite and tourmaline within a few tens of meters of plutonic boundaries.

This unit contains a few beds of quartzite and, to the south and east, minor amounts of discontinuous dolomite (Becraft and Weis, 1963) and marble (Miller, 1996). Within this quadrangle several exposures of dolomite and marble are mapped ~0.6 km east of the Deer Trail Mine as part of the Chamokane Creek Formation on this map, but were previously mapped as part of the Togo Formation (Campbell and Raup, 1964). Though it is possible that these beds correlate with the discontinuous dolomite and marble seen elsewhere in parts of the Togo Formation, I infer the presence of a throughgoing fault in the area based on irregular bedding orientations that makes the dolomite and marble more likely to be within the Chamokane Creek Formation.

## GEOCHEMISTRY

I use geochemical data from this effort for two main purposes. First, to examine the various igneous rock units in the map area because ore deposits are commonly created by or associated with igneous activity. Second, to assess the occurrence and concentration of various critical and commodity elements in geologic units and at inactive and (or) abandoned mine sites throughout the map area. Because the specific purpose of this publication is to provide framework geologic information for the region, the following sections provide mostly descriptive relationships between mineralization and the associated rock units.

### Petrogenesis of Eocene and Cretaceous Igneous Rocks

Eocene and Cretaceous igneous rocks in the map area share several traits: all are calc-alkaline intermediate to felsic rocks (Figs. 2 and 3) and all appear to have large-ion-lithophile element enrichment and high-field-strength element depletions (Fig. 4). Such characteristics are common in subduction-zone settings. Several other traits also serve to distinguish the different rock units. The rare-earth-element (REE) values of Eocene rocks group closely around their mean compared to all the Cretaceous rocks, which have a much wider distribution (Fig. 4). Eocene rocks and the late Cretaceous Fruitland series (the plutonic rocks near Fruitland) lack a negative Eu anomaly (Fig. 4), and all have geochemical characteristics of adakites (Table 4); both the mid-Cretaceous dikes (unit Ki) and the mid-Cretaceous Germania series (the plutonic rocks near the Germania mine) have notable negative Eu anomalies and are not adakites. Compared to the other rock types, the dikes and Germania series are also notably more depleted in P and Ti (Fig. 4), which could reflect apatite and Fe-Ti oxide fractionation. The Eocene rocks are more enriched in Sr and Ba and more depleted in Rb, Ta, Nb, Y, and Yb, while being less depleted in Ti than other rock types.

Together these data suggest three main geochemical groupings with different implications for petrogenesis. The first group are Eocene adakitic flows and tuffs that appear to be geochemically similar to the Eocene Sanpoil volcanics from the Republic and Toroda Creek grabens northwest of the map area (Morris and others, 2000). Both sets of volcanic rocks formed in structural basins above low-angle normal faults during rapid extension in the late Eocene (Fox and others, 1977; Hansen and Goodge, 1988; Kruckenberg and others, 2008). Morris and others (2000) interpret the unusual geochemistry farther northwest as indicating that magma genesis was entirely a crustal process involving the partial melting of existing continental crust and was not a result of subduction. Tepper and others (2023) use additional geochemistry and geochronology to show that adakitic igneous rocks were widespread in the late Eocene and probably resulted from the combined effects of rollback of the Farallon slab, upwelling hot mantle, and orogenic collapse, similar to the interpretation of Ickert and others (2009) for extrusive volcanics in southern British Columbia.

The second group contains the mid-Cretaceous Fruitland series plutonic rocks. Like the Eocene rocks, these have many characteristics of adakites, but also a much wider variation in major- and trace-element compositions. The third group contains the mid-Cretaceous dikes and mid-Cretaceous Germania series; these were likely subduction-related calc-alkaline plutons. Both sets of rocks were emplaced during mid- to late-Cretaceous arc magmatism associated with terrane accretion (Monger and others, 1982). Their geochemical differences may reflect changes in crustal structure—such as development of an orogenic plateau—between the early phase of the accretion event (group three rocks) and the late phase (group two rocks). Nearby in the

**Table 4**. Average geochemical values for igneous geologic units showing those units which have traits consistent with being an adakite (red text). Threshold values are from Defant and Drummond (1990). (La/Yb)N indicates values normalized to chondrite values from Boynton (1984).

| | $Al_2O_3$ (wt. %) | MgO (wt. %) | Sr (ppm) | Y (ppm) | Yb (ppm) | Sr/Y | (La/Yb)N |
|---|---|---|---|---|---|---|---|
| **Adakite threshold:** | *> 15* | *<4* | *>400* | *<18* | *<1.9* | *>20* | *>10* |
| Eva | 15.2 | 2.9 | 750 | 21.9 | 2.1 | 54.0 | 16.5 |
| Evt | 15.2 | 2.1 | 772 | 15.3 | 1.4 | 52.9 | 18.3 |
| Ki | 14.3 | 0.3 | 92 | 28.7 | 2.5 | 5.1 | 19.5 |
| Kigg | 14.9 | 0.7 | 117 | 26.5 | 3.1 | 4.6 | 7.5 |
| $Kiqm_g$ | 14.2 | 0.4 | 107 | 47.5 | 5.5 | 2.8 | 4.4 |
| $Kigd_g$ | 15.1 | 1.4 | 379 | 23.9 | 2.4 | 15.3 | 9.0 |
| $Kig_f$ | 14.1 | 0.6 | 324 | 14.0 | 1.5 | 45.5 | 15.4 |
| $Kigd_f$ | 16.7 | 1.4 | 658 | 20.2 | 1.9 | 34.5 | 12.6 |
| $Kigb_f$ | 14.6 | 6.5 | 199 | 25.6 | 2.7 | 7.8 | 1.6 |

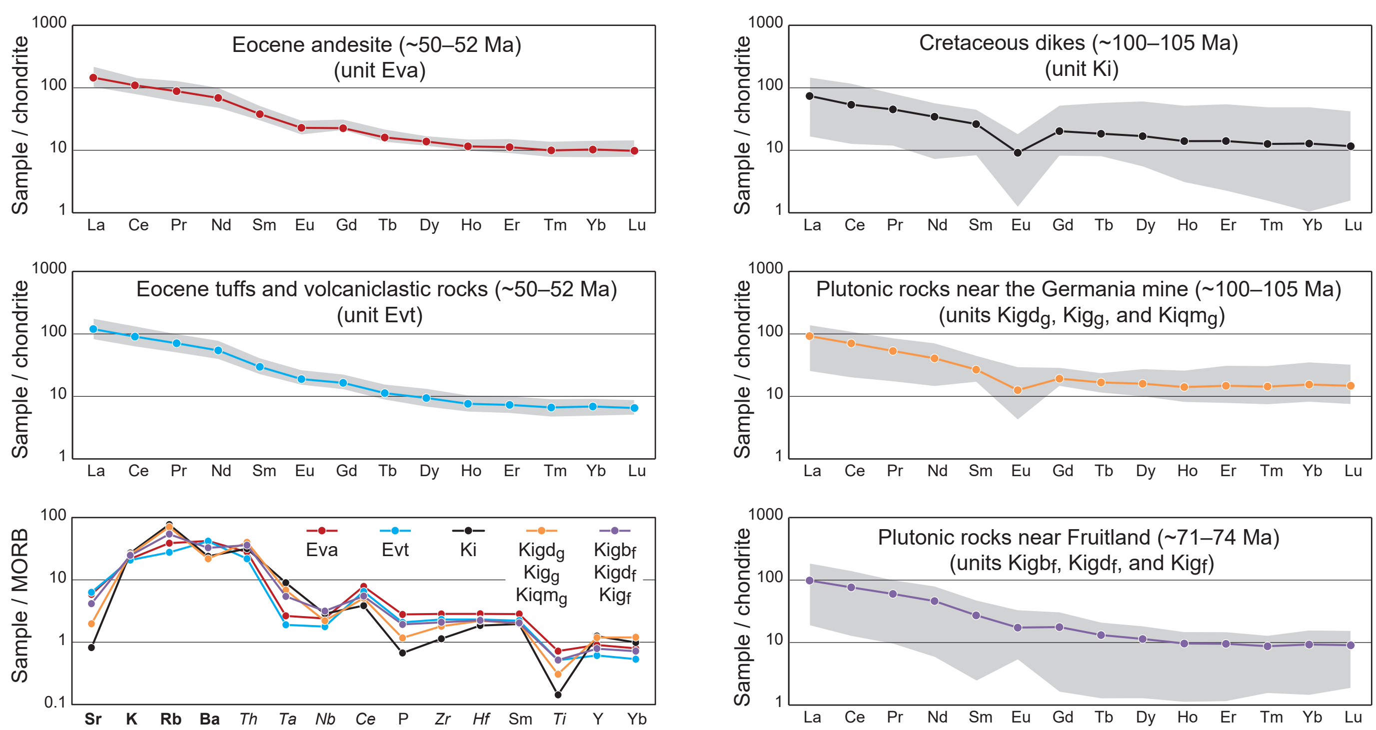


**Figure 4**. Top and right: chondrite-normalized rare-earth-element (REE) values for Eocene to Cretaceous igneous rocks. Solid line indicates average value for the group; gray shading indicates the range of values. Bottom left: mid-ocean-ridge basalt (MORB)-normalized values for Eocene to Cretaceous igneous rocks. Large-ion-lithophile elements are in bold; high-field-strength elements are in italics. Samples identified on Figure 2 as anomalous (stations 35, 44, 45, 47, 50, 51, 67, and 85) are not plotted on either set of diagrams. Chondrite values are from Boynton (1984); MORB values are average of N-MORB and E-MORB from Sun and McDonough (1989).

North Cascades, Miller and others (2009) also document two different phases of plutonism, with the later phase having an age of about 71–78 Ma, and find that the first phase of plutonism significantly altered the geochemical and thermal properties of the crust into which the second phase was emplaced.

## Critical and Commodity Elements

Samples were collected from 20 different geologic units and from seven mine sites throughout the map area to characterize the concentration and distribution of a wide variety of trace elements, including 'critical' elements as defined in Nassar and Fortier (2021). Detailed geochemical data from this effort and the results of Bunning (1985) are in Appendix B and the Data Supplement, though they are difficult to compare because Bunning (1985) only assessed Mo, Sn, and W and did not analyze all three for every reported sample. To summarize these data, Figure 5 shows the maximum concentration of 'critical' elements and other commodity elements (like copper, molybdenum, and others) found in this study. Figure 5 also shows the number of samples that fall within various concentration categories. Table 5 provides a list of elevated-concentration critical and commodity elements by geologic unit.

Across the map area, several elements are present at more than 1 percent concentration: Ba, Mn, W, Zn, Cu, Mo, and B; most, but not all of these are from mine tailings or mine waste rock and exceed the limits of detection (Fig. 5). At slightly lower concentrations (0.1 percent to 1 percent; 1,000 to 10,000 ppm) there is a similar suite of elements (Fig. 5), with the additional appearance of Bi, Rb, Ti, and Pb. The only additions at 500 to 1,000 ppm are As and Zr (Fig. 5). At lower concentrations (100 to 500 ppm) Sb, Ce, Cr, Co, La, Li, Ni, V, Y, Ag, and Cd are present (Fig. 5). Several critical elements were detected at under 50–100 ppm including Ga and Sn. No appreciable amounts of Be, Cs, Dy, Er, Eu, Gd, Ge, Hf, Ho, In, Lu, Pr, Sm, Sc, Ta, Te, or Tb are present in the analyzed samples.

### MINE TAILINGS

Tailings and dump samples from seven inactive and (or) abandoned mine sites or prospects were evaluated in this study; six sites were evaluated in Bunning (1985) and those results are also discussed here. Table 6 shows the various sites, their geologic units, and notable geochemical results. Of the various mines and prospects in the map area, the Deer Trail and Germania are the largest and were focused on Zn-Pb-Ag and W respectively (Fluet, 1986; Du, 1979; Wolff and others, 2006b, 2014). The Cleveland Mine was predominantly Zn-Pb with unusually high values of Sb (Jenkins, 1924; Purdy, 1951; Wolff and others, 2006a). The Turk Mine produced magnesite (Bennett, 1943) and both the Turk and Togo mines produced Cu, Ag, and Au (Huntting, 1956). The Queen Seal Mine produced Ag and is thought to be similar in setting to the Deer Trail Mine (Wolff and others, 2007). There has been no recorded production at the Deer Trail Monitor prospect or Read Mine (from which there are no dump or tailing samples), nor from the unnamed prospect north of the Deer Trail Monitor prospect or the Roselle prospect south of the Germania Mine.

In terms of occurrences of critical minerals, W is notable, with 0.5 to >1 percent values at the Germania Mine and Roselle prospect, both of which are hosted in granite near the Germania Mine (unit Kigg). Concentrations of more than 0.1 percent Bi and Zn are also found in tailings at the Germania Mine. Minor shows (<50 ppm) of W are found at the Cleveland, Turk, and Queen Seal Mines, all of which are hosted in the Stensgar Dolomite (unit Ycbs), typically associated with intrusive rocks (unit Ki), and commonly have minor shows of Sn as well.

Zinc has concentrations from 0.02 to >1 percent at the Deer Trail Mine, with minor to moderate shows (~200–1,300 ppm) at the Togo and Germania mines. The Deer Trail Mine is developed in dolomite of the Chamokane Creek Formation with an unnamed quartz monzonite intrusion at depth (Fluet, 1986; Fluet and others, 1987) and also has elevated concentrations of Ba and Sb. The Togo Mine, located in the Togo Formation (unit Ypht), is associated with mid Cretaceous intrusive rocks (unit Ki) and has elevated concentrations of As and Sn.

The highest concentrations of Ba are found in a tailing sample from the Turk Mine, which has BaO values of nearly 30 percent and likely contained appreciable disseminated barite; this sample also has Sr values of 0.4 percent. Elevated Ba (~770–1,640 ppm) is also found at the Deer Trail Mine. Both mines are developed in dolomite of the Chamokane Creek Formation (unit Ycbcc) at the surface and are associated with nearby mid-Cretaceous dikes (unit Ki) or intrusive rocks.

With regard to commodity minerals, Mo is found at 0.5 to >1 percent at the Deer Trail Monitor Mine and an unnamed prospect to the north of the mine; both are developed near the contact between the bedded lower Metaline Formation (unit OꞒlm) and the phyllitic upper Addy Quartzite (unit Ꞓpha) where it is contact metamorphosed by the granodiorite near Fruitland (unit Kigdf). High values of Mn, La, and Ce are also found at the unnamed prospect. Neither mine has a large volume of material on site. Minor shows of Mo are also found at the Germania Mine (13–119 ppm) and Queen Seal Mine (25 ppm).

The Deer Trail Mine is the largest in the region and, in addition to the high values of Zn noted above, also has >1 percent Cu from a sample of wall rock; a sample of crushed but unprocessed rock also showed 0.7 percent Pb, 326 ppm Cu, and 116 ppm Ag. High values of Cu (1%) are also found at the Turk Mine.

### EOCENE VOLCANIC ROCKS

The Eocene volcanic rocks (units Eva and Evt) have elevated concentrations of Ba, Ce, Cr, V, and Rb compared to many other rocks in the map area, but none of these are found at moderate or high concentrations. Two samples (stations 82 and 84) had notable chalcedony veining and greenish alteration in the field, but do not have anomalous amounts of critical or commodity elements that could be indicative of epithermal deposits. One other site was clearly bleached and silicified adjacent to a fault (station 67) and likewise lacked anomalous values for critical or commodity elements. These results are interesting in light of well-known epithermal deposits hosted by rocks of similar age and setting just to the north and north–northwest in the First Thought and Republic mining districts.

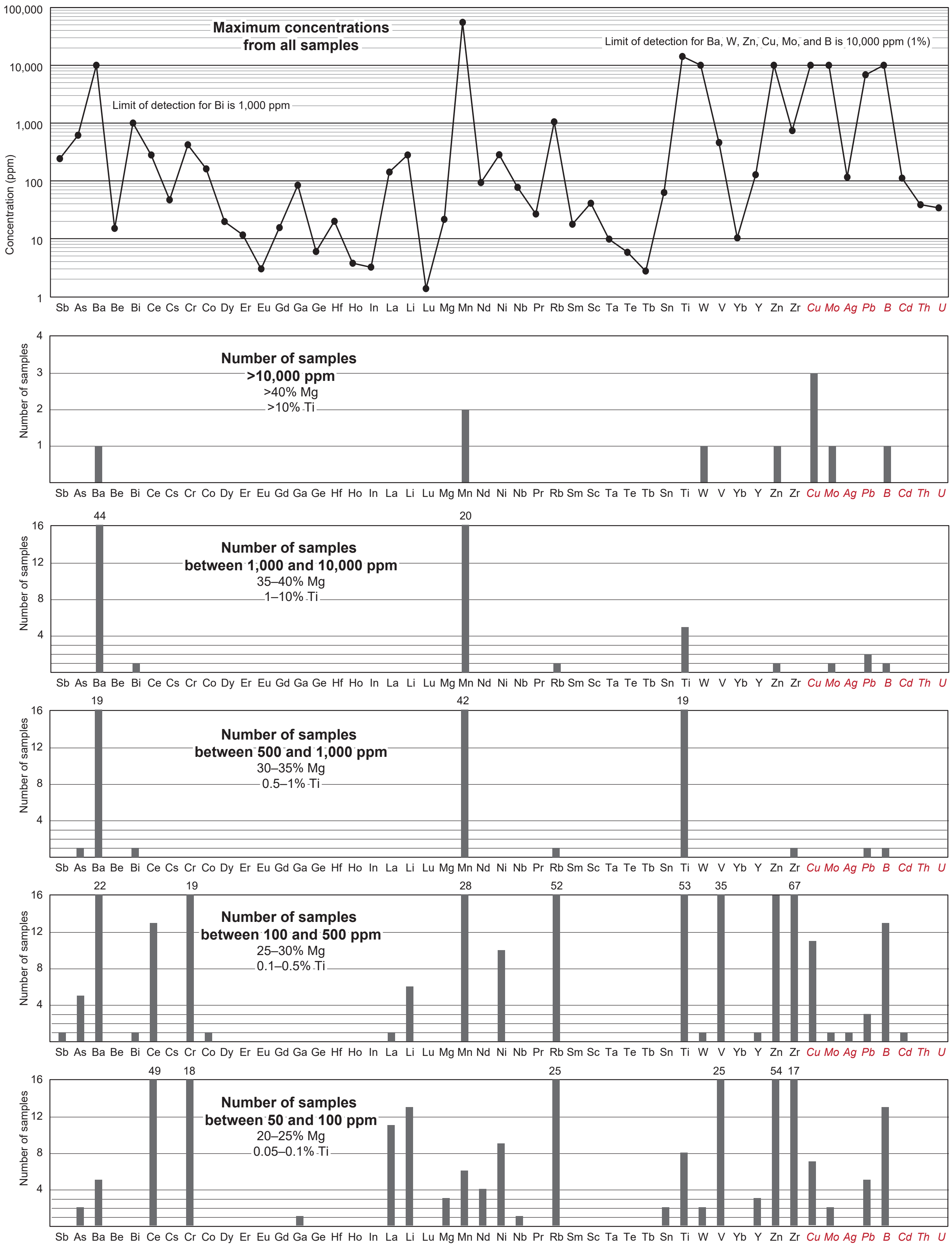


**Figure 5**. Maximum concentrations and number of samples exceeding concentration thresholds for critical elements and other commodities based on new data in this study. Where there are more than 16 samples meeting the cutoff values, the total number of samples is noted above the chart. All concentrations are in parts-per-million (ppm). Samples that have concentrations that exceed limits of detection (LOD) are noted. Commodity elements are in red italics.

**Table 5**. Number of critical element and commodity occurrences above threshold concentration of 100 ppm by geologic unit. Elements are italicized when above five times the threshold concentration and bold where above ten times the threshold concentration. The following elements use a higher threshold: Ba—1,000 ppm, Mn—1,000 ppm; magnesium (Mg), strontium (Sr), titanium (Ti), and zirconium (Zr) are not included in this table. Data from Bunning (1985) is shown in a separate column because only Mo, Sn, and W were measured.

| Map unit | Number of 'elevated' occurences of a critical or commodity element | Samples | Average 'elevated' occurrences per sample | Elements present at >100 ppm in data from this study | Other elements with elevated concentrations | Concentrations >50 ppm from Bunning (1985) |
|---|---|---|---|---|---|---|
| ml (mine tailings) | 38 | 9 | 4.2 | As, **Ba**, **Bi**, Cd, Ce, Co, La, Mn, Ni, Rb, Sb, V, **Zn**, Ag, **B**, **Cu**, **Mo**, **Pb**, **W** | Gd, Pr | **Mo**, Sn, W |
| Eva | 51 | 18 | 2.8 | Ba, Ce, Cr, Rb, V | – – – | – – – |
| Evt | 11 | 7 | 1.6 | Ba, Ce, Cr, V | – – – | – – – |
| $Kig_f$ | 8 | 4 | 2.0 | Ba, Ni, Rb, Zn | | |
| $Kigd_f$ | 22 | 9 | 2.4 | *Ba*, Ce, Mn, Rb, V, Zn | Th | – – – |
| $Kigb_f$ | 10 | 2 | 5.0 | Cr, Mn, Ni, V, Zn, Cu | – – – | – – – |
| Ki | 19 | 10 | 1.9 | Ba, Mn, Rb, Y, B | Be, Dy, Er, Gd | – – – |
| $Kiqm_g$ | 2 | 2 | 1.0 | Rb | | |
| $Kig_g$ (country rock) | 9 | 4 | 2.3 | As, Ba, Li, Rb, Zn, B | W | Mo, **W** |
| $Kig_g$ (veins) | 24 | 4 | 6.0 | *As*, *Bi*, Li, **Mn**, **Rb**, Zn, **B**, Cu, W, **Pb** | Ag, Mo, Sn, U, Y | – – – |
| $Kigd_g$ | 6 | 4 | 1.5 | Ba, Rb, V, Cu | W | – – – |
| $Omv_b$ | 10 | 2 | 5.0 | Ba, Ce, Cr, Mn, Ni, V, Zn | – – – | – – – |
| $Oms_d$ | 1 | 1 | 1.0 | Rb | – – – | – – – |
| $Ocb_c$ | 14 | 2 | 7.0 | Ba, Ce, Cr, Mn, Ni, V, Zn, B, Cu | – – – | – – – |
| $OCl_m$ | 12 | 6 | 2.0 | Ba, Cr, Mn, Rb, V, Zn, **Mo**, Pb | – – – | Sn |
| $Cph_a$ | 6 | 2 | 3.0 | Ba, Ce, Cr, Mn, Rb, V | Gd, Hf, La, Pr, Th, Y | – – – |
| $Zg_h$ | 18 | 4 | 4.5 | Cr, Li, Mn, Ni, V, Zn, Cu | – – – | – – – |
| $ZYcg_h$ | 3 | 2 | 1.5 | Ba, Rb | – – – | – – – |
| $ZYq_b$ | 4 | 1 | 4.0 | Ce, Rb, V, Zn | Nb, Y | – – – |
| $Ycb_s$ | 2 | 3 | 0.7 | Li, Mn | – – – | – – – |
| $Ycb_{wd}$ | 3 | 1 | 3.0 | Li, Rb, V, B | – – – | – – – |
| $Ycb_{cc}$ | 9 | 4 | 2.4 | Ba, Ce, Rb, B | – – – | – – – |

**Table 6**. Geochemical results from samples at mine sites throughout the map area ordered from north to south. Data from Bunning (1985) only include Mo, Sn, and W and not each of these elements were analyzed at each site. Bold text indicates a critical element. Only samples from Bunning (1985) which were described as tailings or mine waste are included here; the remaining samples are included with the analysis by geologic unit in Table 5 and Figs. 5 and 6.

| Station ID | Mine or prospect | Material | Geologic unit(s) involved or associated | Notable results (critical minerals are **bold**) |
|---|---|---|---|---|
| 102* | Cleveland | Dump samples | $Ycb_s$; Ki | 56 ppm **Sn**; 15 ppm **W** |
| 93 | unnamed, north of Deer Trail Monitor | Rubble near adit | $OCl_m$; $Cph_a$?; $Kigd_f$ | >5,000 ppm Mo; 3,245 ppm **Mn**; 2,215 ppm B; 142 ppm **La**; 279 ppm **Ce** |
| 13 | Deer Trail Monitor | Stockpile near addit | $OCl_m$; $Cph_a$?; $Kigd_f$ | >10,000 ppm Mo; 126 ppm **Cr**; 115 ppm **V** |
| 94 | Togo | Tailings (upper adit) | $Yph_t$; Ki | >10,000 ppm Cu; 333 ppm **As**; 183 ppm **Zn**; 161 ppm **Co**; 146 ppm **Ni** |
| 107* | Togo | Dump sample | $Yph_t$; Ki | 38 ppm **Sn** |
| 95 | Turk | Tailings (lower pile) | $Ycb_{cc}$; Ki? | 29.6% **BaO**; >10,000 ppm Cu; 4,000 ppm **Sr** |
| 106* | Turk | Dump and workings | $Ycb_{cc}$; Ki? | 14 ppm **Sn**; 20 ppm **W** |
| 96 | Deer Trail | Spoils and waste rock | $Ycb_{cc}$ | 773 ppm **Ba**; 218 ppm **Zn**; 169 ppm **V**; 166 ppm Cu |
| 97 | Deer Trail | Tailings (Madre adit) | $Ycb_{cc}$ | >10,000 ppm Cu |
| 98 | Deer Trail | Tailings (near crusher) | $Ycb_{cc}$ | >10,000 ppm **Zn**; 6,825 ppm Pb; 1,642 ppm **Ba**; 326 ppm Cu; 241 ppm **Sb**; 116 ppm Ag; 111 ppm Cd; 110 ppm **V** |
| 99 | Queen Seal | Tailings (upper pile) | $Ycb_s$ | ~2,466 ppm B |
| 100 | Queen Seal | Main landing (tailings?) | $Ycb_s$ | None |
| 109* | Queen Seal | Dump sample | $Ycb_s$ | 25 ppm Mo; 25 ppm **W** |
| 101 | Germania | Stockpile (vein talus) | $Kig_g$ | >10,000 ppm **W**; >1,000 ppm **Bi**; 1,370 ppm **Zn**; 348 ppm Rb; 159 ppm Pb; 119 ppm Mo |
| 113* | Germania | Stockpile (vein talus)? | $Kig_g$ | 13 ppm Mo; 16 ppm **Sn**; 40 ppm **W** |
| 114* | Germania | Mill tailings | $Kig_g$ | 385 ppm **W** |
| 116* | Roselle prospect | Dump sample | $Kig_g$ | >5,000 ppm **W** |

* From Bunning (1985); only results from dump or tailing samples are shown here; only Mo, Sn, and W were analyzed, and not for every sample.

## CRETACEOUS INTRUSIVE ROCKS

### Dikes

Rocks from dikes and other small intrusive bodies are scattered throughout the map area; most are porphyritic, many are associated with faults, and those associated with faults are often somewhat bleached and locally silicified. Of the ten dikes evaluated for geochemistry, none had particularly high values of critical or commodity elements. This is somewhat puzzling since they seem to be about the same age and bulk composition as the more-mineralized plutonic rocks near the Germania Mine. One dike has the highest concentration of Be in the map area (station 30; 15 ppm), and another dike intruding the presumably youngest phase of the plutonic rocks near the Germania Mine (unit $Kigd_g$) has 127 ppm Y and elevated (but still <20 ppm) concentrations of Dy, Er, and Gd.

### Plutonic rocks near Fruitland

Rocks from this plutonic suite have few major geochemical anomalies. The two samples of the gabbro from unit $Kigb_f$ have elevated Cr and Cu (~140–200 ppm), some Ni (~100 ppm), V (336 to 360 ppm), and Zn (up to 105 ppm); both samples have relatively high levels of Sc, though still <50 ppm. The remaining five samples from unit $Kig_f$ and ten samples from unit $Kigd_f$ are mostly unremarkable, even where they are close to their intrusive border with rocks that have been altered to calc-silicate skarn or hornfels. Rocks of these two units do have somewhat elevated Th, with values as high as 39 ppm.

### Plutonic rocks near the Germania mine

The granite phase (unit $Kig_g$) is subdivided into samples from veins (and aplite/pegmatite dikes) and those from the country rock and wall rock. As a whole, veins from unit $Kig_g$ have the highest average number of elevated critical and commodity elements compared to any map unit (Table 5), and are much more mineralized than the surrounding country rock or wall rock (Fig. 6). In addition to the elements in Figure 6, veins also have Y up to 56 ppm. Aside from samples taken from mine tailings, stockpiles, and dump rock, vein samples in unit Kig$_g$ are the most enriched in As, Bi, Sb, Sn, W, and Mn of any rock unit in the map area and also have high values of Ag, Cu, Mo, Pb, U, and Zn. The granodiorite phase (unit Kigd$_g$) and quartz-monzonite phase (unit Kiqm$_g$) have relatively fewer geochemical anomalies than the granite phase: one sample in the northern part of the map area has elevated Cu (120 ppm) and V (185 ppm), and one from the high ridge above the Germania Mine has 33 ppm W.

## PALEOZOIC TO PROTEROZOIC METASEDIMENTARY AND METAVOLCANIC ROCKS

### Carbonate units

Several high values of critical and commodity elements are found in skarn of the Metaline Formation (unit OꞒl$_m$) where it has been contact metamorphosed by unit Kigd$_f$ in the north part of the map area. Near the Deer Trail Monitor prospect, Mo is up to 0.5 to >1 percent with less W (up to 150 ppm) and Sn (typically low, but in one sample 42 ppm). Just to the west near the Read Mine, Sn is as high as 64 ppm and W is up to 20 ppm. North of Fruitland, calc-silicate skarn developed in unit Ocb$_c$ near unit Kigd$_f$ is exposed in a highway roadcut and samples yield Cu >200 ppm with elevated Cr, V, Ni, and Zn, which could be due to the close association of the carbonate with greenstone of unit Omv$_b$.

The new data in this report for the Stensgar Formation and Chamokane Creek Formation (units Ycb$_s$ and Ycb$_{cc}$) show few notable anomalies. Data from Bunning (1985) in these same formations was targeted toward mineralized veins, faults, and from within mine workings, and these results show minor enrichments in Mo ranging from 17–28 ppm, Sn from 14–52 ppm, and W from 15–25 ppm.

### Siliciclastic units

Compared to many other rock units, there are few geochemical anomalies within the various siliciclastic units (units Oms$_d$, Ꞓph$_a$, ZYcg$_h$, and ZYq$_b$). Most notable is one sample from the phyllitic upper Addy Quartzite (unit Ꞓph$_a$) which has some of the highest relative values of rare-earth elements, including Gd, Hf, La, Pr, Th, and Y. The concentrations are all quite low (<50 ppm) and they could plausibly result from detrital minerals in the quartzite, such as rutile, monazite, and xenotime. If so, it is possible that there may be other locations with similar or higher-concentration deposits elsewhere within the Addy Quartzite.

### Metavolcanic units

There are only two metavolcanic units in this map area (units Omv$_b$ and Zg$_h$). Both of them are basaltic and tholeiitic (Figs. 2 and 3), and both units show elevated Cr, Ni, V, and some Zn (Table 5). One sample from unit Omv$_b$—which is near the skarn in unit Ocb$_c$ north of Fruitland—has very high Ba and some Ce. Three of four samples from unit Zg$_h$ had elevated Cu (~150–200 ppm) and all are located in the northern part of the map area: one from a large quarry outcrop and two from poorly exposed dikes; the fourth sample lacks Cu but has elevated Li.

## ACKNOWLEDGMENTS

Many thanks go to staff from WGS: Katie Alexander provided summer field assistance with geologic mapping and helped design and implement the field-data collection scheme using Esri FieldMaps; Michael Polenz, Andrew Sadowski, and Trevor Contreras provided initial reviews of the map and writing, and Nikolas Midttun, Daniel Coe, and Susan Schnur provided review, editing, figure production, and layout; data stewardship and quality control were provided by Ashley Cabibbo and Ian Hubert.

## AUTHOR CONTRIBUTIONS

The geologic mapping and compilation were completed by A. Steely, with assistance from K. Alexander. Analysis, cross section development, and all writing were completed by A. Steely.

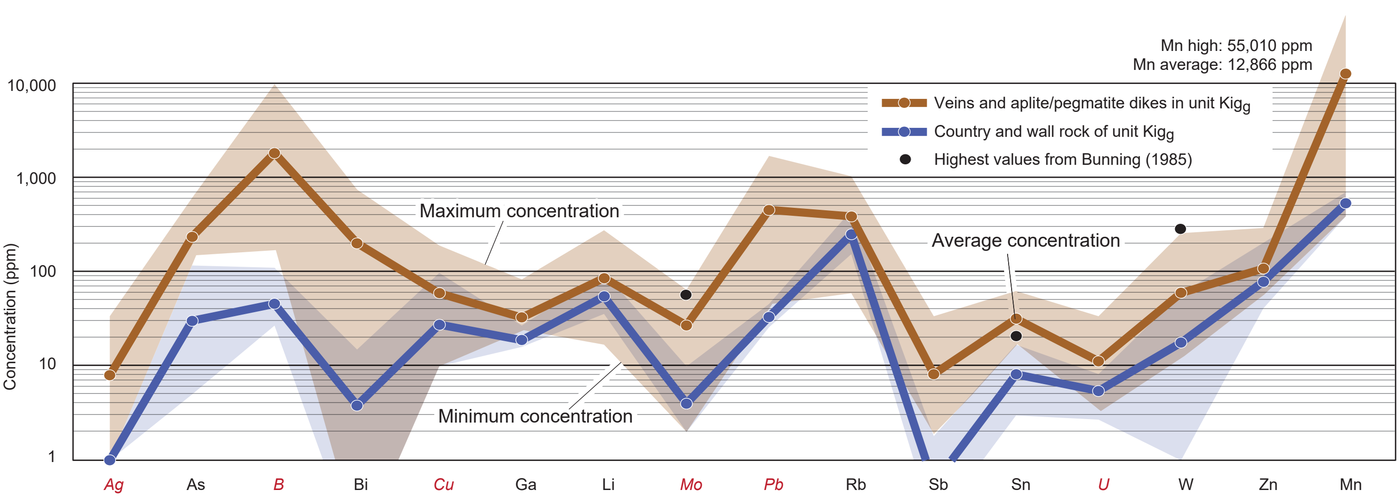


**Figure 6**. Maximum, minimum, and average concentrations for select elements from samples in the granite phase near the Germania mine (unit Kig$_g$) showing differences between mineralized vein samples and less-mineralized country and wall rock samples. Commodity elements are in red italics.

## REFERENCES


Anderson, W. S.; Puffett, W. P., 1954, Final report on the Germania mine, Springdale Mining District, Stevens Co., Washington: U.S. Department of the Interior, Defense Minerals Exploration Administration, docket DMEA-2131X, 18 p. [https://pubs.usgs.gov/ds/1004/scans/wa/dma/2131_DMA.pdf, p. 193–214]

Armstrong, R. L., 1982, Cordilleran metamorphic core complexes—From Arizona to southern Canada: Annual Review of Earth and Planetary Sciences, v. 10, p. 129–154. [https://doi.org/10.1146/annurev.ea.10.050182.001021]

Asmerom, Yemane; Ikramuddin, Mohammed; Kinart, K. P., 1988, Geochemistry of Late Cretaceous granitoids from northeastern Washington: Implication for genesis of two-mica Cordilleran granites: Geology, v. 16, no. 5, p. 431–435. [https://doi.org/10.1130/0091-7613(1988)016%3C0431:GOLCGF%3E2.3.CO;2]

Atwater, B. F., 1986, Pleistocene glacial-lake deposits of the Sanpoil River valley, northeastern Washington: U.S. Geological Survey Bulletin 1661, 39 p., 3 plates. [https://doi.org/10.3133/b1661]

Bancroft, Howland; Lindgren, Waldemar, 1914, The ore deposits of northeastern Washington, including a section on the Republic mining district. U. S. Geological Survey Bulletin 550, 215 p. [https://doi.org/10.3133/b550]

Becraft, G. E., 1966, Geologic map of the Wilmont Creek quadrangle, Ferry and Stevens Counties, Washington: U.S. Geological Survey Geologic Quadrangle Map GQ-538, 1 sheet, scale 1:62,500. [https://doi.org/10.3133/gq538]

Becraft, G. E.; Weis, P. L., 1963, Geology and mineral deposits of the Turtle Lake quadrangle, Washington: U.S. Geological Survey Bulletin 1131, 73 p., 6 plates. [https://doi.org/10.3133/b1131]

Bennett, W. A. G., 1941, Preliminary report on magnesite deposits of Stevens County, Washington: Washington Division of Geology Report of Investigations 5, 25 p., 2 plates. [https://www.dnr.wa.gov/publications/ger_ri5_wdg_prelim_magnesite_dep_stevens_co.pdf]

Bennett, W. A. G., 1943, Character and tonnage of the Turk magnesite deposit: Washington Division of Geology Report of Investigations 7, 22 p., 1 plate. [https://www.dnr.wa.gov/publications/ger_ri7_wdg_turk_magnesite_dep.pdf]

Black, L. P.; Kamo, S. L.; Allen, C. M.; Davis, D. W.; Aleinikoff, J. N.; Valley, J. W.; Mundil, R.; Campbell, I. H.; Korsch, R. J.; Williams, I. S.; Foudoulis, Chris, 2004, Improved $^{206}Pb/^{238}U$ microprobe geochronology by the monitoring of a trace-element-related matrix effect; SHRIMP, ID-TIMS, ELA-ICP-MS and oxygen isotope documentation for a series of zircon standards: Chemical Geology, v. 205, no. 1–2, p. 115–140. [https://doi.org/10.1016/j.chemgeo.2004.01.003]

Box, S. E.; Pritchard, C. J.; Stephens, T. S.; O'Sullivan, P. B., 2020, Between the supercontinents: Mesoproterozoic Deer Trail Group, an intermediate age unit between the Mesoproterozoic Belt–Purcell Supergroup and the Neoproterozoic Windermere Supergroup in northeastern Washington, USA: Canadian Journal of Earth Sciences, v. 57, no. 12, p. 1411–1427. [https://doi.org/10.1139/cjes-2019-0188]

Boynton, W. V., 1984, Cosmochemistry of the rare earth elements; Meteorite studies. *In* Henderson, P., editor, Rare earth element geochemistry: Elsevier, p. 63–114. [https://doi.org/10.1016/B978-0-444-42148-7.50008-3]

Breitsprecher, K.; Thorkelson, D. J.; Groome, W. G.; Dostal, J., 2003, Geochemical confirmation of the Kula-Farallon slab window beneath the Pacific Northwest in Eocene time: Geology, v. 31, no. 4, p. 351–354. [https://doi.org/10.1130/0091-7613(2003)031%3C0351:GCOTKF%3E2.0.CO;2]

Bunning, B. B., 1985, Tin, tungsten, and molybdenum geochemistry of parts of Stevens and Spokane Counties, Washington: Washington Division of Geology and Earth Resources Report of Investigations 28, 57 p. [https://www.dnr.wa.gov/publications/ger_ri28_tin_tung_moly_stevens_spokane_co.pdf]

Campbell, A. B.; Raup, O. B., 1964, Preliminary geologic map of the Hunters quadrangle, Stevens and Ferry Counties, Washington: U.S. Geological Survey Mineral Investigations Field Studies Map MF-276, 1 sheet, scale 1:48,000. [https://doi.org/10.3133/mf276]

Campbell, Ian; Loofbourow, J. S., Jr., 1957, Preliminary geologic map and sections of the magnesite belt, Stevens County, Washington: U.S. Geological Survey Mineral Investigations Field Studies Map MF-117, 1 sheet, scale 1:36,000. [https://doi.org/10.3133/mf117]

Campbell, Ian; Loofbourow, J. S., Jr., 1962, Geology of the magnesite belt of Stevens County, Washington: U.S. Geological Survey Bulletin 1142-F, 53 p., 2 plates. [https://doi.org/10.3133/b1142F]

Carter, Claire, 1989, A Middle Ordovician graptolite fauna from near the contact between the Ledbetter Slate and the Metaline Limestone in the Pend Oreille mine, northeastern Washington State. *In* Sando, W. J., editor, Shorter contributions to paleontology and stratigraphy: U.S. Geological Survey Bulletin 1860, p. A1–A23. [https://doi.org/10.3133/b1860]

Chang, Zhaoshan; Vervoort, J. D.; McClelland, W. C.; Knaack, Charles, 2006, U-Pb dating of zircon by LA-ICP-MS: Geochemistry, Geophysics, Geosystems, v. 7, no. 5, 14 p. [https://doi.org/10.1029/2005GC001100]

Culver, H. E.; Broughton, W. A., 1945, Tungsten resources of Washington: Washington Division of Geology Bulletin 34, 89 p., 23 plates. [https://www.dnr.wa.gov/publications/ger_b34_tungsten_res_wa.pdf]

Defant, M. J.; Drummond, M. S., 1990, Derivation of some modern arc magmas by melting of young subducted lithosphere: Nature, v. 347, p. 662–665. [https://doi.org/10.1038/347662a0]

Derkey, Robert E.; Joseph, Nancy L.; Lasmanis, Raymond, 1990, Metal mines of Washington—Preliminary report: Washington Division of Geology and Earth Resources Open File Report 90-18, 577 p., 1 CD. [http://www.dnr.wa.gov/publications/ger_ofr90-18_metal_mines_pt1.pdf; http://www.dnr.wa.gov/publications/ger_ofr90-18_metal_mines_pt2.pdf]

Devlin, W. J.; Bond, G. C., 1988, The initiation of the early Paleozoic Cordilleran miogeocline – Evidence from the uppermost Proterozoic-Lower Cambrian Hamill Group of southeastern British Columbia: Canadian Journal of Earth Sciences, v. 25, no. 1, p. 1–19. [https://doi.org/10.1139/e88-001]

Du, Ming-Ho, 1979, Geology of the Germania tungsten deposits, Stevens County, Washington: Eastern Washington University Master of Science thesis, 58 p., 1 plate.

Evans, J. G., 1987, Geology of the Stensgar Mountain quadrangle, Stevens County, Washington: U.S. Geological Survey Bulletin 1679, 23 p., 1 plate. [https://doi.org/10.3133/b1679]

Flint, R. F.; Irwin, W. H., 1939, Glacial geology of Grand Coulee Dam, Washington: Geological Society of America Bulletin, v. 50, no. 5, p. 661–680. [https://doi.org/10.1130/GSAB-50-661]

Fluet, D. W., 1986, Genesis of the Deer Trail Zn-Pb-Ag vein deposit, Washington, U.S.A.: University of Alberta Master of Science thesis, 129 p.

Fluet, D. W.; Changkakoti, A.; Morton, R. D.; Gray, J.; Krouse, H. R., 1987, The genesis of the Deer Trail Zn-Pb-Ag vein deposits, northeast Washington, U.S.A.: Evidence from fluid-inclusion and stable-isotope studies: Canadian Journal of Earth Sciences, v. 24, no. 8, p. 1715–1726. [https://doi.org/10.1139/e87-164]

Fox, K. F., Jr.; Rinehart, C. D.; Engels, J. C., 1977, Plutonism and orogeny in north-central Washington—Timing and regional extent: U. S. Geological Survey Professional Paper 989, 27p. [https://doi.org/10.3133/pp989]

Fullmer, C. Y., 1986, Geology of the SE 1/4 of the Twin Lakes quadrangle, Ferry County, Washington: Eastern Washington University Master of Science thesis, 73 p., 1 plate.

Hansen, V. L.; Goodge, J. W., 1988, Metamorphism, structural petrology, and regional evolution of the Okanogan Complex, northeastern Washington. *In* Ernst, W. G., editor, Metamorphism and crustal evolution of the western United States: Prentice-Hall Rubey Volume VII, p. 233–270.

Huntting, M. T., 1956, Inventory of Washington minerals; Part II—Metallic minerals: Washington Division of Mines and Geology Bulletin 37, Part II, 2 v. [https://d92019.eos-intl.net/D92019/OPAC/Details/Record.aspx?BibCode=10313875]

Ickert, R. B.; Thorkelson, D. J.; Marshall, D. D.; Ullrich, T. D., 2009, Eocene adakitic volcanism in southern British Columbia: Remelting of arc basalt above a slab window: Tectonophysics, v. 464, no. 1-4, p. 164–185. [https://doi.org/10.1016/j.tecto.2007.10.007]

Jenkins, O. P., 1924, Lead deposits of Pend Oreille and Stevens Counties, Washington: Washington Division of Geology Bulletin 31, 153 p. [https://www.dnr.wa.gov/Publications/ger_b31_lead_dep_pendoreille_stevens_co.pdf]

Joseph, N. L., compiler, 1990a, Geologic map of the Nespelem 1:100,000 quadrangle, Washington: Washington Division of Geology and Earth Resources Open File Report 90-16, 47 p., 1 plate. [https://www.dnr.wa.gov/Publications/ger_ofr90-16_geol_map_nespelem_100k.zip]

Joseph, N. L., compiler, 1990b, Geologic map of the Spokane 1:100,000 quadrangle, Washington: Washington Division of Geology and Earth Resources Open File Report 90-17, 29 p., 1 plate. [https://www.dnr.wa.gov/Publications/ger_ofr90-17_geol_map_spokane_100k.zip]

Kinart, K. P., 1980, Geochemistry of part of the Loon Lake batholith and its relationship to uranium mineralization at the Midnite mine, northeastern Washington: Eastern Washington University Master of Science thesis, 200 p., 1 plate.

Kiver, E. P.; Stradling, D. F., 1995, Geology of the Franklin D. Roosevelt reservoir shoreline—Glacial geology, terraces, landslides, and lineaments: U.S. Bureau of Reclamation, Pacific Northwest Region, 148 p. [https://ia600502.us.archive.org/11/items/geologyoffrankli00kive/geologyoffrankli00kive.pdf]

Koppers, A. A. P.; Staudigel, Hubert; Wijbrans, J. R., 2000, Dating crystalline groundmass separates of altered Cretaceous seamount basalts by the $^{40}Ar/^{39}Ar$ incremental heating technique: Chemical Geology, v. 166, no. 1–2, p. 139–158. [https://doi.org/10.1016/S0009-2541(99)00188-6]

Koppers, A. A. P., 2002, ArArCALC—Software for $^{40}Ar/^{39}Ar$ age calculations: Computers & Geosciences, v. 28, no. 5, p. 605–619. [https://doi.org/10.1016/S0098-3004(01)00095-4]

Koppers, A. A. P.; Staudigel, Hubert; Pringle, M. S.; Wijbrans, J. R., 2003, Short-lived and discontinuous intraplate volcanism in the South Pacific: Hot spots or extensional volcanism?: Geochemistry, Geophysics, Geosystems, v. 4, no. 10, 49 p. [https://doi.org/10.1029/2003GC000533]

Kruckenberg, S. C.; Whitney, D. L.; Teyssier, Christian; Fanning, C. M.; Dunlap, W. J., 2008, Paleocene-Eocene migmatite crystalization, extension, and exhumation in the hinterland of the northern cordillera: Okanogan dome, Washington, USA: Geological Society of America Bulletin, v. 120, no. 7-8, p. 912–929. [https://doi.org/10.1130/B26153.1]

Kuiper, K. F.; Deino, Alan; Hilgen, F. J.; Krijgsman, Wout; Renne, P. R.; Wijbrans, J. R., 2008, Synchronizing rock clocks of Earth history: Science, v. 320, no. 5875, p. 500–504. [https://doi.org/10.1126/science.1154339]

Lanphere, M A.; Baadsgaard, Halfdan, 2001, Precise K–Ar, $^{40}Ar/^{39}Ar$, Rb–Sr and U/Pb mineral ages from the 27.5 Ma Fish Canyon Tuff reference standard: Chemical Geology, v. 175, no. 3–4, p. 653–671. [ https://doi.org/10.1016/S0009-2541(00)00291-6]

Le Maitre, R. W.; Streckeisen, A.; Zanettin, B; Le Bas, M. J.; Bonin, B.; Bateman, P., 2002, Igneous rocks—A classification and glossary of terms: Cambridge University Press, 236 p. [https://doi.org/10.1017/CBO9780511535581]

Lee, Jee-Yon; Marti, Kurt; Severinghaus, J. P.; Kawamura, Kenji; Yoo, Hee-Soo; Lee, J. B.; Kim, J. S., 2006, A redetermination of the isotopic abundances of atmospheric Ar: Geochimica et Cosmochimica Acta, v. 70, no. 17, p. 4507–4512. [https://doi.org/10.1016/j.gca.2006.06.1563]

Linde, G. M.; Trexler, J. H., Jr.; Cashman, P. H.; Dickinson, W. R., 2014, The provenance of detrital zircons from the Cambrian Addy quartzite, northeast Washington: Connections between British Columbia and central Nevada [abstract]: Geological Society of America Abstracts with Programs, v. 46, no. 5, p. 3. [https://gsa.confex.com/gsa/2014RM/webprogram/Paper238313.html]

Lindsey, K. A., 1988, Geology of parts of the Upper Proterozoic to Lower Cambrian Three Sisters Formation, Gypsy Quartzite, and Addy Quartzite, Stevens and Pend Oreille Counties, northeastern Washington: Washington Division of Geology and Earth Resources Open File Report 88-3, 18 p., 6 plates. [https://www.dnr.wa.gov/publications/ger_ofr88-3_gypsy_addy_quartzite_24k.pdf]

Lindsey, K. A.; Gaylord, D. R.; Groffman, L. H., 1990, Geology of the Upper Proterozoic to Lower Cambrian Three Sisters Formation, Gypsy Quartzite, and Addy Quartzite, Stevens and Pend Oreille Counties, northeastern Washington: Washington Division of Geology and Earth Resources Report of Investigations 30, 37 p. [https://www.dnr.wa.gov/publications/ger_ri30_geology_three_sisters_formation.pdf]

Ludwig, K. R.; Nash, J. T.; Naeser, C. W., 1981, U-Pb isotope systematics and age of uranium mineralization, Midnite Mine, Washington: Economic Geology, v. 76, no. 1, p. 89–110. [https://doi.org/10.2113/gsecongeo.76.1.89]

Miller, F. K., 1996, Geologic map of the Empey Mountain area, Stevens County, Washington: U.S. Geological Survey Miscellaneous Investigations Series Map I-2493, 1 sheet, scale 1:48,000. [https://doi.org/10.3133/i2493]

Miller, F. K.; Clark, L. D., 1975, Geology of the Chewelah-Loon Lake area, Stevens and Spokane Counties, Washington, with a section on potassium-argon ages of the plutonic rocks, by J. C. Engels: U.S. Geological Survey Professional Paper 806, 74 p., 2 plates. [https://doi.org/10.3133/pp806]

Miller, F. K.; Whipple, J. W., 1989, The Deer Trail Group—Is it part of the Belt Supergroup?. *In* Joseph, N. L.; Stoffel, K. L.; Evans, J. G.; Kiilsgaard, T. H.; Korosec, M. A.; Logan, R. L.; Miller, F. K.; Phillips, W. M.; Powell, R. E.; Schasse, H. W.; Schuster, J. E.; Waggoner, S. Z.; Walsh, T. J.; Whipple, J. W., editors, Geologic guidebook for Washington and adjacent areas: Washington Division of Geology and Earth Resources Information Circular 86, p. 1–21. [http://www.dnr.wa.gov/publications/ger_ic86_geol_guide_wa_area.pdf]

Miller, R. B.; Paterson, S. R.; Matzel, J. P., 2009, Plutonism at different crustal levels: Insights from the ~5–40 km (paleodepth) North Cascades crustal section, Washington. *In* Miller, R. B.; Snoke, A. W., editors, Crustal cross sections from the western North American Cordillera and Elsewhere: Implications for Tectonic and Petrologic Processes. Geological Society of America Special Paper 456. [https://doi.org/10.1130/2009.2456(05)]

Min, Kyoungwon; Mundil, Roland; Renne, P. R.; Ludwig, K. R., 2000, A test for systematic errors in $^{40}Ar/^{39}Ar$ geochronology through comparison with U-Pb analysis of a 1.1-Ga rhyolite: Geochimica et Cosmochimica Acta, v. 64, no. 1, p. 73–98. [https://doi.org/10.1016/S0016-7037(99)00204-5]

Monger, J. W. H.; Price, R. A.; Tempelman-Kluit, D. J., 1982, Tectonic accretion and the origin of the two major metamorphic and plutonic welts in the Canadian Cordillera: Geology, v. 10, no. 2, p. 70–75. [https://doi.org/10.1130/0091-7613(1982)10%3C70:TAATOO%3E2.0.CO;2]

Morris, G. A.; Larson, P. B.; Hooper, P. R., 2000, Subduction style magmatism in a non-subduction setting: the Colville Igneous Complex, NE Washington State, USA: Journal of Petrology, v. 41, no. 1, p. 43–67. [https://doi.org/10.1093/petrology/41.1.43]

Muessig, Siegfried Joseph, 1962, Tertiary volcanic and related rocks of the Republic area, Ferry County, Washington. IN Short papers in geology, hydrology, and topography; Articles 120–179; Geological Survey research 1962: U.S. Geological Survey Professional Paper 450-D, article 135, p. 56–58. [https://doi.org/10.3133/10.3133/pp450D]

Nassar, N. T.; Fortier, S. M., 2021, Methodology and technical input for the 2021 review and revision of the U.S. Critical Minerals List: U.S. Geological Survey Open-File Report 2021–1045, 31 p. [https://doi.org/10.3133/ofr20211045]

Okulitch, V. J., 1951, A Lower Cambrian fossil locality near Addy, Washington: Journal of Paleontology, v. 25, no. 3, p. 405–407. [https://www.jstor.org/stable/1299933]

Paces, J. B.; Miller, J. D., Jr., 1993, Precise U-Pb ages of Duluth Complex and related mafic intrusions, northeastern Minnesota: Geochronological insights to physical, petrogene tic, paleomagnetic, and tectonomagmatic processes associated with the 1.1 Ga Midcontinent Rift System: Journal of Geophysical Research, v. 98, no. B8, p. 13,997–14,013. [https://doi.org/10.1029/93JB01159]

Pardee, J. T., 1918, Geology and mineral deposits of the Colville Indian Reservation, Washington: U.S. Geological Survey Bulletin 677, 186 p., 1 plate. [https://doi.org/10.3133/b677]

Paton, Chad; Hellstrom, John; Paul, Bence; Woodhead, Jon; Hergt, Janet, 2011, Iolite: Freeware for the visualization and processing of mass spectrometric data: Journal of Analytical Atomic Spectrometry, v. 26, no. 12, p. 2508–2518. [https://doi.org/10.1039/C1JA10172B]

Pearson, R. C.; Obradovich, J. D., 1977, Eocene rocks in northeast Washington—Radiometric ages and correlation: U.S. Geological Survey Bulletin 1433, 41 p., 1 plate. [https://doi.org/10.3133/b1433]

Purdy, C. P., 1951, Antimony occurrences of Washington: Washington Division of Mines and Geology Bulletin 39, 186 p. [https://www.dnr.wa.gov/Publications/ger_b39_antimony_occurrences_wa.pdf]

Purdy, C. P., 1954, Molybdenum occurrences of Washington: Washington Division of Mines and Geology Report of Investigations 18, 118 p., 7 plates. [https://www.dnr.wa.gov/Publications/ger_ri18_molybdenum_of_wa.pdf]

Repetski, J. E., 1978, Age of the Metaline Limestone or Formation in northeastern Washington. *In* Sohl, N. F.; Wright, W. B., Changes in stratigraphic nomenclature by the U.S. Geological Survey, 1977: U.S. Geological Survey Bulletin 1457-A, p. 107. [https://doi.org/10.3133/b1457A]

Schuster, J. E.; Repetski, J. E.; Carter, Claire; Dutro, J. T., Jr., 1989, Nature of the Metaline Formation-Ledbetter Formation contact and age of the Metaline Formation in the Clugston Creek area, Stevens County, Washington—A reinterpretation: Washington Geologic Newsletter, v. 17, no. 4, p. 13–20. [https://www.dnr.wa.gov/Publications/ger_washington_geology_1989_v17_no4.pdf]

Sláma, Jiří; Košler, Jan; Condon, D. J.; Crowley, J. L.; Gerdes, Alex; Hanchar, J. M.; Horstwood, M. S. A.; Morris, G. A.; Nasdala, Lutz; Norberg, Nicholas; Schaltegger, Urs; Schoene, Blair; Tubrett, M. N.; Whitehouse, M. J., 2008, Plešovice zircon—A new natural reference material for U-Pb and Hf isotopic microanalysis: Chemical Geology, v. 249, no. 1-2, p. 1–35. [https://doi.org/10.1016/j.chemgeo.2007.11.005]

Smith, B. L., 1982, Geology of the southeastern portion of the Inchelium quadrangle, Stevens County, Washington: Eastern Washington University Master of Science thesis, 60 p., 2 plates.

Smith, M T., 1991a, Geologic strip map of the Ninemile Creek-Wilmont Creek-Hunters Creek area, Ferry and Stevens Counties, Washington: Washington Division of Geology and Earth Resources Open File Report 91-4, 9 p., 1 plate. [https://www.dnr.wa.gov/publications/ger_ofr91-4_ninemile_wilmont_hunters_creek_24k.pdf]

Smith, M. T., 1991b, Geologic map of the Old Copper Hill-Butcher Mountain area, Stevens County, Washington: Washington Division of Geology and Earth Resources Open File Report 91-6, 9 p., 1 plate. [https://www.dnr.wa.gov/publications/ger_ofr91-6_old_copper_hill_12k.pdf]

Smith, M. T.; Gehrels, G. E., 1992a, Stratigraphic comparison of the Lardeau and Covada Groups—Implications for revision of stratigraphic relations in the Kootenay Arc: Canadian Journal of Earth Sciences, v. 29, no. 6, p. 1320–1329. [https://doi.org/10.1139/e92-105]

Smith, M. T.; Gehrels, G. E., 1992b, Structural geology of the Lardeau Group near Trout Lake, British Columbia—Implications for the structural evolution of the Kootenay Arc: Canadian Journal of Earth Sciences, v. 29, no. 6, p. 1305–1319. [https://doi.org/10.1139/e92-104]

Snook, J. R.; Campbell, A. B.; Lucas, H. E.; Abrams, M. J.; Janzen, J. H.; Smith, B. L., 1990, Geologic map of the Inchelium quadrangle, Stevens and Ferry Counties, Washington: U.S. Geological Survey Miscellaneous Field Studies Map MF-1752, 1 sheet, scale 1:48,000. [http://pubs.er.usgs.gov/publication/mf1752]

Snook, J. R.; Lucas, H. E.; Abrams, M. J., 1981, A cross section of a Nevada-style thrust in northeast Washington: Washington Division of Geology and Earth Resources Report of Investigations 25, 9 p. [https://www.dnr.wa.gov/publications/ger_ri25_cross_section_trust_ne_wa.pdf]

Steiger, R. H.; Jäger, Emilie, 1977, Subcommission on geochronology: Convention on the use of decay constant in geo- and cosmochronology: Earth and Planetary Science Letters, v. 36, no. 3, p. 359–362. [https://doi.org/10.1016/0012-821X(77)90060-7]

Stosch, Heinz-G., 2022, TAS diagram, $K_2O$-$SiO_2$ diagram and AFM diagram template for Excel (1.0): Zenodo, Microsoft Excel spreadsheet. [https://doi.org/10.5281/zenodo.5977826]

Sun, S. S.; McDonough, W. F., 1989, Chemical and isotopic systematics of oceanic basalts: Implications for mantle composition and processes. *In* Saunders, A. D.; Norry, M. J., editors, Magmatism in the ocean basins: Geological Society, London, Special Publications 42, p. 313–345. [https://doi.org/10.1144/GSL.SP.1989.042.01.19]

Tepper, J. H.; Loewen, M. W.; Caulfield, L. M.; Davidson, P. C.; Ruthenberg, K. L.; Blakely, S. W. F.; Knudsen, D. F. J. F.; Black, D. F.; Nelson, B. K.; Asmerom, Yemane, 2023, Petrology and geochronology of Cretaceous-Eocene plutonic rocks in northeastern Washington, USA: Crustal thickening, slab rollback, and origin of the Challis episode: Geological Society of America Bulletin, 16 p. [https://doi.org/10.1130/B36791.1]

U.S. Geological Survey National Cooperative Geologic Mapping Program, 2020, GeMS (Geologic Map Schema)—A standard format for the digital publication of geologic maps: U.S. Geological Survey Techniques and Methods, book 11, chap. B10, 74 p. [https://doi.org//10.3133/tm11B10]

U.S. Geological Survey, 2021, Geochemical data generated by projects funded by the USGS Earth Mapping Resources Initiative: U.S. Geological Survey data release (ver. 9.0, December 2023). [https://doi.org/10.5066/P9WHRLXH]

Vermeesch, Pieter, 2018, IsoPlotR: A free and open toolbox for geochronology: Geoscience Frontiers, v. 9, no. 5, p. 1479–1493. [https://doi.org/10.1016/j.gsf.2018.04.001]

Waggoner, S. Z., compiler, 1990a, Geologic map of the Coulee Dam 1:100,000 quadrangle, Washington: Washington Division of Geology and Earth Resources Open File Report 90-15, 40 p., 1 plate. [https://www.dnr.wa.gov/Publications/ger_ofr90-15_geol_map_couleedam_100k.zip]

Waggoner, S. Z., compiler, 1990b, Geologic map of the Chewelah 1:100,000 quadrangle, Washington: Washington Division of Geology and Earth Resources Open File Report 90-14, 63 p., 1 plate. [https://www.dnr.wa.gov/Publications/ger_ofr90-14_geol_map_chewelah_100k.zip]

Waitt, R. B., Jr.; Thorson, R. M., 1983, The Cordilleran ice sheet in Washington, Idaho, and Montana. *In* Porter, S. C., editor, The late Pleistocene, Late-Quaternary environments of the United States Volume 1: University of Minnesota Press, p. 53–70.

Washington Geological Survey, 2017, NE Washington Lidar Production, collected between April 7 and Aug. 18, 2016 by GeoTerra, Inc., 3-ft resolution, accessed June 15, 2021 [http://lidarportal.dnr.wa.gov/], metadata available on portal [ger_ne_wa_2016_lidar_report.pdf].

Washington Geological Survey, 2023, Mines and Minerals—GIS data: Washington Geological Survey Digital Data Series 30, version 1.0, January 2023. [https://fortress.wa.gov/dnr/geologydata/publications/data_download/ger_portal_mines_minerals.zip]

Weaver, C. E., 1920, The mineral resources of Stevens County: Washington Geological Survey Bulletin 20, 350 p., 1 plate. [http://www.dnr.wa.gov/Publications/ger_b20_min_resources_stevensco_1.pdf; http://www.dnr.wa.gov/Publications/ger_b20_min_resources_stevensco_2.pdf]

Weis, P. L.; Richmond, G. M., 1965, Maximum extent of late Pleistocene cordilleran glaciation in northeastern Washington and northern Idaho: U.S. Geological Survey Professional Paper 525-C, p. C128-C132. [https://doi.org/10.3133/pp525C]

Wiedenbeck, Michael; Allé, P.; Corfu, Fernando; Griffin, W. L.; Meier, Martin; Oberli, Felix; Von Quadt, Albrecht; Roddick, J. C.; Spiegel, W., 1995, Three natural zircon standards for U-Th-Pb, Lu-Hf, trace element and REE analyses: Geostandards Newsletters, v. 19, no. 1, p. 1–23. [https://doi.org/10.1111/j.1751-908X.1995.tb00147.x]

Williams, I. S., 1998, U-Th-Pb geochronology by ion microprobe. *In* McKibben, M. A.; Shanks III, W. C.; Ridley, W. I., editors, Applications of microanalytical techniques to understanding mineralizing processes: Reviews in Economic Geology, v. 7, p. 1–35. [https://doi.org/10.5382/Rev.07.01]

Wolff, F. E.; Garcia, B. T.; McKay, D. T., Jr.; Norman, D. K., 2014, Inactive and abandoned mine lands—Germania Mine, Cedar Canyon Mining District, Stevens County, Washington: Washington Division of Geology and Earth Resources Information Circular 117, 21 p. [https://www.dnr.wa.gov/Publications/ger_ic117_iaml_germania.pdf]

Wolff, F. E.; McKay, D. K., Jr.; Norman, D. K., 2006a, Inactive and abandoned mine lands—Cleveland mine, Springdale mining district, Stevens County, Washington: Washington Division of Geology and Earth Resources Information Circular 101, 11 p. [https://www.dnr.wa.gov/Publications/ger_ic101_iaml_cleveland.pdf]

Wolff, F. E.; McKay, D. T., Jr.; Norman, D. K., 2006b, Inactive and abandoned mine lands—Deer Trail mine, Cedar Canyon mining district, Stevens County, Washington: Washington Division of Geology and Earth Resources Information Circular 102, 14 p. [https://www.dnr.wa.gov/Publications/ger_ic102_iaml_deertrail.pdf]

Wolff, F. E.; McKay, D. T., Jr.; Norman, D. K., 2007, Inactive and abandoned mine lands—Queen Seal mine, Cedar Canyon mining district, Stevens County, Washington: Washington Division of Geology and Earth Resources Information Circular 104, 10 p. [https://www.dnr.wa.gov/Publications/ger_ic104_iaml_queenseal.pdf]

Yokoyama, R.; Shirasawa, M.; Pike, R. J., 2002, Visualizing topography by openness: A new application of image processing to digital elevation models: Photogrammetric Engineering and Remote Sensing, v. 68, no. 3, p. 251–266. [https://www.asprs.org/wp-content/uploads/pers/2002journal/march/2002_mar_257-265.pdf]

# Appendix A. Geochronology

## $^{40}Ar/^{39}Ar$ DATING

### Overview

Argon dating uses the radioactive decay of $^{40}K$ to $^{40}Ar$ to determine the age of potassium-bearing minerals and materials. In this map area $^{40}Ar/^{39}Ar$ argon dating is used to establish the crystalization age of some intrusive rocks and a number of flows and tuffs in the Eocene volcanic succession. Because previous workers described multiple phases of a single pluton (and multiple plutons), there is concern that later phases may have reheated earlier phases and that argon ages from the older phases might not represent the age of crystalization. Thus, we employ both argon and U-Pb dating (which is not affected by heat in the same way) so that crystalization and cooling ages can be more clearly interpreted.

### Sample Collection and Preparation

Samples for argon dating need to be recovered from in-place rock and should have as little weathering and alteration as possible. Relatively unweathered sites with few fractures were prioritized, though such sites were very difficult to find in this area. Large blocks of the outcrop were removed and broken into smaller pieces in order to remove any weathering rinds on the rock. We placed about 1–3 kg of rock into a cloth or sturdy plastic sample bag. At the conclusion of field work, sites from which samples were collected were ranked based on many factors, including the desire for spatial coverage, stratigraphic location, rock type, and budgetary constraints. Of those samples to be analyzed, the freshest 1–2 kg of material was selected and sent to the lab for irradiation and analysis.

### Analytical Methods

The following section of text is reproduced from an analytical report provided by the Oregon State University Argon Geochronology Laboratory, with minimal modification:

Samples were crushed, sieved, washed, and dried using standard mineral separation techniques. Groundmass splits were obtained for the sample, rinsed with cold water, and then dried in a drying oven at 55 °C. Once the samples were dried, they were sieved to 250–150 µm. Special care was taken to remove any alteration material by using an intensive acid leaching procedure using a combination of HCl and $HNO_3$ at different acid strength (Koppers and others, 2000). A final separate of groundmass was obtained using a binocular microscope. Any visible alteration or adhering crystal phases were carefully removed prior to packaging and irradiation of the sample.

$^{40}Ar/^{39}Ar$ ages were obtained by incremental heating methods using the ThermoFisher Scientific ARGUS-VI mass spectrometer and data collection using internal lab software ArArExperiments version 4.4.0. The samples were irradiated for 6 hours. Samples were irradiated with the Fish Canyon Tuff sanidine (FCT-2-NM sanidine) with an age of 28.201 ±0.023 Ma, 1σ flux monitor (Kuiper and others, 2008). Individual J-values for each sample were calculated by polynomial extrapolation of the measured flux gradient against irradiation height and typically give 0.06–0.12 percent uncertainties (1σ). The $^{40}Ar/^{39}Ar$ incremental heating age determinations were performed on a multi-collector ARGUS-VI mass spectrometer at Oregon State University that has five Faraday collectors fitted, two 1,012 ohm resistors for masses $^{41}Ar$ and $^{40}Ar$ and three 1,013 ohm resistors for argon masses $^{39}Ar$, $^{38}Ar$, and $^{37}Ar$ and one ion-counting CuBe electron multiplier (located in a position next to the lowest mass Faraday collector). This allows us to measure simultaneously all argon isotopes, with mass 36 on the multiplier and masses 37 through 40 on the four adjacent Faradays. This configuration provides the advantages of running in a full multi-collector mode while measuring the lowest peak (on mass 36) on the highly sensitive electron multiplier (which has an extremely low dark-noise and a very high peak/noise ratio). Irradiated samples were loaded into Cu-planchettes in an ultra-high vacuum sample chamber and incrementally heated by scanning a Synrad Firestar 20-watt defocused $CO_2$ laser beam in pre-set patterns across the sample, in order to release the argon evenly. Each heating step is 62 seconds. After heating, reactive gasses were cleaned up using four SAES Zr-Al AP-10 getters for 3 minutes; two operated at 450 °C and two operated at room temperature (21 °C). All ages were calculated using the corrected Steiger and Jäger (1977) decay constant of $5.530 \pm 0.097 \times 10^{-10}$ $yr^{-1}$ (2σ) as reported by Min and others (2000). For all other constants used in the age calculations we refer to table 2 in Koppers and others (2003). Incremental heating plateau ages and isochron ages were calculated as weighted means with 1/σ2 as weighting factor and as YORK2 least-square fits with correlated errors using the ArArCALC v2.6.2 software from Koppers (2002) available from the website at http://earthref.org/ArArCALC/.

Argon isotopic results are corrected for system blanks, radioactive decay, mass discrimination, reactor-induced interference reactions, and atmospheric argon contamination. Decay constants reported by Min and others (2000) are utilized for age calculation. Isotope interference corrections as determined using the ARGUS VI are: $(^{36}Ar/^{37}Ar)Ca$=0.0002703 ±0.000005; $(^{39}Ar/^{37}Ar)Ca$=0.0006425 ±0.0000059; $(^{40}Ar/^{39}Ar)K$= 0.000607 ±0.000059; $(^{38}Ar/^{39}Ar)K$=0.012077 ±0.000011. Ages were calculated assuming an atmospheric $^{40}Ar/^{36}Ar$ ratio of 298.56 ±0.113 (Lee and others, 2006). Data reduction and age calculation were processed using ArAr Calc 2.7.0 (Koppers, 2002). Plateau ages are defined as including >50% of the total $^{39}Ar$ released with at least three consecutive steps, where the $^{40}Ar/^{39}Ar$ ratio for each step is in agreement with the mean at the 95% confidence level. In many cases only a mini-plateau age is given, where a mini-plateau is <50% of the $^{39}Ar$ released.

## Results

In total, 11 samples were analyzed: three are from tuffs, four are from intermediate to felsic flows, two are from porphyritic felsic dikes, and two are from muscovite-bearing dikes within the interior granitic phase of the pluton near the Germania mine. Summary data are in Table 1 and Table A1; analytical data are in the Data Supplement.

**Table A1**. Argon geochronology sample information and results. Uncertainties are provided at 2-sigma unless otherwise noted. Ages are reported with internal uncertainty, followed by full external uncertainty in parentheses. Detailed results are in the Data Supplement. NA stands for 'not applicable.'

| **Station ID** | Station 33 | **Age (Ma) ±2σ*** | **Age type** | **Material** | **% total $^{39}Ar$ included in age** | **Heating steps included in age** | **MSWD** |
|---|---|---|---|---|---|---|---|
| **Sample ID** | 14A22-5 | 95.07 ±0.18 (4.88) | plateau | biotite | 74% | 17 (of 41) | 2.24 |
| **Lab ID** | 23G09966 | From roadcut; blocks of porphyritic (plagioclase) fine-grained intrusive rock within dark gray slate. | | | | | |
| **Geochemical classification** | dacite | | | | | | |
| **Map unit** | Ki | | | | | | |
| **TRS location** | sec. 6, T29N R38E | | | | | | |
| **Latitude (degrees)** | 48.04276 | | | | | | |
| **Longitude (degrees)** | -118.06603 | | | | | | |
| **Elevation (ft)** | 4,345 | | | | | | |

| **Station ID** | Station 38 | **Age (Ma) ±2σ*** | **Age type** | **Material** | **% total $^{39}Ar$ included in age** | **Heating steps included in age** | **MSWD** |
|---|---|---|---|---|---|---|---|
| **Sample ID** | 14A22-2 | 71.64 ±0.13 (3.69) | plateau | muscovite | 60% | 24 (of 42) | 0.85 |
| **Lab ID** | 23G09891 | From roadcut on abandoned road east of Deer Trail mine; large outcrop of white to pale yellow felsic intrusive rock with abundant yellow brown red staining, probably due to oxidized pyrite; faint banding or foliation; abundant slickensided surfaces. | | | | | |
| **Geochemical classification** | rhyolite | | | | | | |
| **Map unit** | Ki | | | | | | |
| **TRS location** | sec. 6, T29N R38E | | | | | | |
| **Latitude (degrees)** | 48.03485 | | | | | | |
| **Longitude (degrees)** | -118.08575 | | | | | | |
| **Elevation (ft)** | 4,084 | | | | | | |

| **Station ID** | Station 45 | **Age (Ma) ±2σ*** | **Age type** | **Material** | **% total $^{39}Ar$ included in age** | **Heating steps included in age** | **MSWD** |
|---|---|---|---|---|---|---|---|
| **Sample ID** | 12A22-3 | 88.08 ±0.15 (4.53) | total fusion | muscovite | 100% | 36 (of 36) | NA |
| **Lab ID** | 23G10091 | From roadcut and nearby natural exposure on road to Germania mine; equigranular medium-grained granitic rock hosting northeast-striking pegmatite or vein up to 8 cm thick consisting of coarse-grained white mica and quartz that is locally stained red; sampled the pegmatite/dike. | | | | | |
| **Geochemical classification** | granite | | | | | | |
| **Map unit** | Kig$_{g}$ | | | | | | |
| **TRS location** | sec. 14, T29N R37E | | | | | | |
| **Latitude (degrees)** | 48.01743 | | | | | | |
| **Longitude (degrees)** | -118.10727 | | | | | | |
| **Elevation (ft)** | 4,219 | | | | | | |

* First uncertainty is internal; second (larger) uncertainty in parentheses is the full external.

**Table A1**. Continued.

| Station ID | Station 50 | Age (Ma) ±2σ* | Age type | Material | % total $^{39}$Ar included in age | Heating steps included in age | MSWD |
|---|---|---|---|---|---|---|---|
| **Sample ID** | 13A22-2 | 99.02 ±0.21 (5.08) | plateau | muscovite | 99% | 29 (of 36) | 8.15 |
| **Lab ID** | 23G10040 | From wallrock of Exodus vein at Germania mine; wall rock of mined-out Exodus vein is punky and appears hydrothermally altered for several cem away from exposed edge; sampled quartz and white-mica rich block detached from side of vein. | | | | | |
| **Geochemical classification** | monzonite | | | | | | |
| **Map unit** | Kig$_g$ | | | | | | |
| **TRS location** | sec. 13, T29N R37E | | | | | | |
| **Latitude (degrees)** | 48.00712 | | | | | | |
| **Longitude (degrees)** | -118.10276 | | | | | | |
| **Elevation (ft)** | 3,659 | | | | | | |

| Station ID | Station 62 | Age (Ma) ±2σ* | Age type | Material | % total $^{39}$Ar included in age | Heating steps included in age | MSWD |
|---|---|---|---|---|---|---|---|
| **Sample ID** | 9J22-3 | 51.55 ±0.10 (2.66) | plateau | hornblende plagioclase | 99% | 22 (of 30) | 0.95 |
| **Lab ID** | 23G09525 | From base of natural cliff exposure just uphill from station 63; gray to dark gray and blocky flow rock. | | | | | |
| **Geochemical classification** | dacite | | | | | | |
| **Map unit** | Eva | | | | | | |
| **TRS location** | sec. 25, T30N R36E | | | | | | |
| **Latitude (degrees)** | 48.06705 | | | | | | |
| **Longitude (degrees)** | -118.22142 | | | | | | |
| **Elevation (ft)** | 2,131 | | | | | | |

| Station ID | Station 66 | Age (Ma) ±2σ* | Age type | Material | % total $^{39}$Ar included in age | Heating steps included in age | MSWD |
|---|---|---|---|---|---|---|---|
| **Sample ID** | 6A22-6 | 52.12 ±0.14 (2.69) | plateau | plagioclase | 30% | 18 (of 30) | 1.33 |
| **Lab ID** | 23G09677 | From natural exposure on a small knoll; light-colored tuff; blocky to platy. | | | | | |
| **Geochemical classification** | rhyolite | | | | | | |
| **Map unit** | Evt | | | | | | |
| **TRS location** | sec. 31, T30N R37E | | | | | | |
| **Latitude (degrees)** | 48.05759 | | | | | | |
| **Longitude (degrees)** | -118.20656 | | | | | | |
| **Elevation (ft)** | 2,260 | | | | | | |

| Station ID | Station 73 | Age (Ma) ±2σ* | Age type | Material | % total $^{39}$Ar included in age | Heating steps included in age | MSWD |
|---|---|---|---|---|---|---|---|
| **Sample ID** | 4A22-3 | | | | | | |
| **Lab ID A** | 23G09459 | 51.59 ±0.10 (2.68) | plateau | hornblende | 70% | 10 (of 28) | 1.21 |
| **Lab ID B** | 23G09786 | 51.61 ±0.11 (2.67) | mini plateau | groundmass | 24% | 10 (of 31) | 0.60 |
| **Lab ID C** | 23G11199 | 52.06 ±0.10 (2.69) | plateau | biotite | 77% | 16 (of 42) | 3.64 |
| **Geochemical classification** | trachy-andesite | From natural cliff exposure on east side of incised gorge; only 20 m from contact with granitic rock; gray cryptocrystalline groundmass with aligned hornblende up to 1 cm in size and sparse stubby pyroxene. | | | | | |
| **Map unit** | Eva | | | | | | |
| **TRS location** | sec. 5, T29N R37E | | | | | | |
| **Latitude (degrees)** | 48.04107 | | | | | | |
| **Longitude (degrees)** | -118.18447 | | | | | | |
| **Elevation (ft)** | 2,333 | | | | | | |

* First uncertainty is internal; second (larger) uncertainty in parentheses is the full external.

**Table A1**. Continued.

| Station ID | Station 74 | Age (Ma) ±2σ* | Age type | Material | % total $^{39}$Ar included in age | Heating steps included in age | MSWD |
|---:|---|---|---|---|---|---|---|
| **Sample ID** | 15A22-1 | | | | | | |
| **Lab ID A** | 23G09632 | 51.94 ±0.09 (2.68) | plateau | hornblende | 83% | 12 (of 30) | 1.44 |
| **Lab ID B** | 23G11278 | 50.10 ±0.10 (2.59) | mini plateau | groundmass | 7% | 7 (of 27) | 1.94 |
| **Geochemical classification** | andesite | From base of natural cliff; monolithologic pyroclastic breccia consisting of angular boulder to pebble-sized clasts; light gray trachytic hornblende-phyric rock; little matrix between clasts. | | | | | |
| **Map unit** | Evt | | | | | | |
| **TRS location** | sec. 6, T29N R37E | | | | | | |
| **Latitude (degrees)** | 48.03723 | | | | | | |
| **Longitude (degrees)** | -118.19518 | | | | | | |
| **Elevation (ft)** | 2,303 | | | | | | |

| Station ID | Station 77 | Age (Ma) ±2σ* | Age type | Material | % total $^{39}$Ar included in age | Heating steps included in age | MSWD |
|---:|---|---|---|---|---|---|---|
| **Sample ID** | 4A22-9 | 51.50 ±0.10 (2.66) | plateau | hornblende | 95% | 22 (of 30) | 1.18 |
| **Lab ID** | 23G09570 | From natural low exposures just west of Mudgett Road. Maroon flow or flow breccia with abundant phenocrysts of 1–5 mm hornblende. | | | | | |
| **Geochemical classification** | trachy-andesite | | | | | | |
| **Map unit** | Eva | | | | | | |
| **TRS location** | sec. 12, T29N R36E | | | | | | |
| **Latitude (degrees)** | 48.02908 | | | | | | |
| **Longitude (degrees)** | -118.21786 | | | | | | |
| **Elevation (ft)** | 2,075 | | | | | | |

| Station ID | Station 88 | Age (Ma) ±2σ* | Age type | Material | % total $^{39}$Ar included in age | Heating steps included in age | MSWD |
|---:|---|---|---|---|---|---|---|
| **Sample ID** | 3A22-7 | | | | | | |
| **Lab ID A** | 23G09740 | 52.01 ±0.11 (2.69) | mini plateau | plagioclase | 37% | 19 (of 30) | 0.99 |
| **Lab ID B** | 23G11120 | 51.63 ±0.10 (2.67) | plateau | biotite | 69% | 14 (of 42) | 1.28 |
| **Geochemical classification** | dacite | From 2–4-m-tall cliff exposure above gravel road; white to salmon-colored to gray crystal-vitric lapilli tuff with abundant pumice clasts; phenocrysts of hornblende, plagioclase, and quartz. | | | | | |
| **Map unit** | Evt | | | | | | |
| **TRS location** | sec. 20, T29N R37E | | | | | | |
| **Latitude (degrees)** | 48.00516 | | | | | | |
| **Longitude (degrees)** | -118.18656 | | | | | | |
| **Elevation (ft)** | 2,185 | | | | | | |

| Station ID | Station 90 | Age (Ma) ±2σ* | Age type | Material | % total $^{39}$Ar included in age | Heating steps included in age | MSWD |
|---:|---|---|---|---|---|---|---|
| **Sample ID** | 3A22-8 | 52.19 ±0.09 (2.70) | mini plateau | groundmass | 39% | 15 (of 27) | 0.82 |
| **Lab ID** | 23G09850 | From natural slope and 1–3-m-tall cliff exposures above gravel road; brown to dark gray aphanitic flow rock with slightly trachytic euhedral hornblende to 1.5 cm; uniformly tabular with 2–4-cm-thick plates. | | | | | |
| **Geochemical classification** | andesite | | | | | | |
| **Map unit** | Eva | | | | | | |
| **TRS location** | sec. 19, T29N R37E | | | | | | |
| **Latitude (degrees)** | 48.00087 | | | | | | |
| **Longitude (degrees)** | -118.19286 | | | | | | |
| **Elevation (ft)** | 2,133 | | | | | | |

* First uncertainty is internal; second (larger) uncertainty in parentheses is the full external.

# U-PB ZIRCON DATING

## Overview

Zircons are common accessory minerals in most rocks because they are hard, chemically inert, and can survive through many rock cycles. Decay of trace uranium to lead within zircon can be used to establish an individual age for each grain. Analyzing many grains within a sample can do several things: (1) establish a crystalization age for igneous samples; (2) establish a maximum depositional age for sedimentary rocks based on the idea that the deposit must be younger than the youngest grain it contains; (3) the variety of ages in a single sample can provide insight into the provenance of the sample.

In this map, zircon dating is used to establish the crystalization ages of the widespread plutonic rocks that have largely been assumed to be late Cretaceous in age based on similarity with other late-Cretaceous plutons. Because these plutons are often zoned, there is concern that re-heating from subsequent phases would reset argon ages, so zircon dating (which is not affected in the same way) is a better approach.

## Sample Collection and Preparation

In general, 2–4 kg of fresh rock is retrieved for each sample, making sure to minimize any contact with soil or other surface deposits that could introduce anomalous zircons. The packaged samples are sent to ZirChron, LLC for mineral separation using the following procedure: Samples are pressure washed with water and then disaggregated using an Electro Pulse Disaggregator (EPD, Marx generator) at 1 Hz with discharges of ~250 kV for 15 minutes. Any clasts >500 µm are crushed in a crusher or pulverizer. Using stainless steel sieves, the fraction between 350 µm and 25 µm is retained and then processed using the Wilfley water table, Frantz paramagnetic separator, and a two-step (3.00 g/cm$^3$ and 3.32 g/cm$^3$) heavy liquid methylene iodide separation. Zircon grains from each sample are hand selected and mounted in epoxy, then polished to expose the grain centers. Regions suitable for analysis are identified from optical imaging.

## Analytical Methods

The following text is reproduced from a technical write-up by the Washington State University Radiogenic Isotope and Geochronology Laboratory with minimal modification:

Zircon U-Pb ages are measured at the Radiogenic Isotope and Geochronology Lab (RIGL) at Washington State University using an Analyte G2 193 excimer laser ablation system coupled with a Thermo-Finnigan Element 2 single-collector inductively coupled plasma mass spectrometer. The laser parameters are 25-µm-diameter spot size, 10 Hz repetition rate, and fluence of ~5.0 J/cm$^2$. For the U-Pb measurement, we mostly followed the method of Chang and others (2006), except for the use of a 193-nm laser system. A 10-second blank measurement of the He and Ar carrier gasses (laser off) before each analysis is followed by 250 scans across masses $^{202}$Hg, $^{204}$Pb+Hg, $^{206}$Pb, $^{207}$Pb, $^{208}$Pb, $^{232}$Th, $^{235}$U, and $^{238}$U during ~30-second laser ablation periods. Analyses of zircon unknowns, standards, and quality control zircon grains are interspersed with analyses of external calibration standards, typically with 10–12 unknowns bracketed by multiple analyses of two different zircon standards (Plešovice and FC-1). The Plešovice standard (337 Ma; Sláma and others, 2008) is used to calibrate the $^{206}$Pb/$^{238}$U and $^{207}$Pb/$^{235}$U ages, and the FC-1 standard (1,099 Ma; Paces and Miller, 1993) is used for calibration of $^{207}$Pb/$^{206}$Pb ages owing to its high-count rate for $^{207}$Pb (~2–4 times higher than that of Plešovice). Zircon 91500 (1,065 Ma; Wiedenbeck and others, 1995), Fish Canyon Tuff (~27.5 Ma; Lanphere and others, 2001) and Temora 2 (417 Ma; Black and others, 2004) are used as quality control standards. Data are processed offline using the Iolite software (Paton and others, 2011). Common Pb correction is performed using the $^{207}$Pb method (Williams, 1998).

## Results

In total 13 samples were analyzed: two from felsic dikes, five from the plutonic rocks near Fruitland, and four from the plutonic rocks near the Germania mine. A discordance filter (-5% to +10%) is used and weighted-mean concordia ages are computed using IsoPlotR (Vermeesch, 2018) with a random-effects model applied that accounts for overdispersion of ages; external uncertainties (from decay constants) are propagated into our age statements. Summary data are in Table 1 and Table A2; individual zircon ages and analytical data are in the Data Supplement.

**Table A2**. U-Pb geochronology sample information and results. Uncertainties are provided at 2-sigma unless otherwise noted. Detailed results are in the Data Supplement.

| Sample ID (Station ID) | | Age ±2σ (Ma) | Age type |
|---|---|---|---|
| **10J22-3 (Station 15)** | | 104.28 ±0.64 | Weighted mean (n=25) |
| **TRS** | sec. 21, T30N R38E | From ~30-m-wide roadcut on north side of Springdale–Hunters Road; tan to light gray felsic intrusive rock that is locally porphyritic with 2-mm laths or acicular hornblende and tabular altered plagioclase. Fractures and small faults are abundant throughout the outcrop and most is stained yellow or brown; rock is punky to brecciated near larger fault strands. | Overdispersion 1.49 ±0.47 Ma; two Archean grains and several Jurassic–Triassic and Paleozoic grains |
| **Latitude Longitude (degrees)** | 48.08388 -118.03319 | | |
| **Elevation (ft)** | 3,114 | | |
| **Number of grains analyzed** | 41 | | |
| **Geologic unit** | Ki | | |
| **Geochemical classification** | rhyolite | | |
| **14A22-9 (Station 18)** | | 74.17 ±0.34 | Weighted mean (n=37) |
| **TRS** | sec. 31, T30N R38E | From ridge on north side of dirt road near small saddle; leucocratic fine- to medium-grained equigranular granitic rock; sparse biotite and hornblende; red staining is prevalent and the rock is uniformly platy subparallel to the ground surface with 4–10-cm-thick plates. Appears more altered than intrusive rock just to south (station 19). | Overdispersion 0.92 ±0.26 Ma; four mid-Cretaceous grains |
| **Latitude Longitude (degrees)** | 48.06269 -118.07460 | | |
| **Elevation (ft)** | 4,266 | | |
| **Number of grains analyzed** | 46 | | |
| **Geologic unit** | Kig$_f$ | | |
| **Geochemical classification** | granite | | |
| **14A22-10 (Station 19)** | | 73.35 ±0.28 | Weighted mean (n=38) |
| **TRS** | sec. 31, T30N R38E | From just south of dirt road near small saddle; equigranular fine- to medium-grained granodiorite, locally with banded aggregates of megacrystic pyroxene up to 1–3 cm in size; notably fresher than intrusive rock to north (station 18). | Overdispersion 0.57 ±0.26 Ma |
| **Latitude Longitude (degrees)** | 48.06214 -118.07510 | | |
| **Elevation (ft)** | 4,261 | | |
| **Number of grains analyzed** | 43 | | |
| **Geologic unit** | Kigd$_f$ | | |
| **Geochemical classification** | gabbroic diorite | | |
| **14A22-12 (Station 21)** | | 100.46 ±0.44 | Weighted mean (n=38) |
| **TRS** | sec. 31, T30N R38E | From small roadcut on west side of road; gray plagioclase-phyric medium-grained granite; magnetic; intruded by thin aplite dikes. | Overdispersion 1.15 ±0.35 Ma |
| **Latitude Longitude (degrees)** | 48.05982 -118.07268 | | |
| **Elevation (ft)** | 4,249 | | |
| **Number of grains analyzed** | 41 | | |
| **Geologic unit** | Kigd$_g$ | | |
| **Geochemical classification** | monzonite | | |
| **7J22-1 (Station 23)** | | 104.38 ±0.20 | Weighted mean (n=34) |
| **TRS** | sec. 31, T30N R38E | From roadcut uphill (northeast) of Turk mine; gray medium-grained porphyritic dike with plagioclase and biotite phenocrysts in a gray groundmass; dike 1–2 m wide. | Overdispersion 0.19 ±0.28 Ma; one Archean grain |
| **Latitude Longitude (degrees)** | 48.05314 -118.07901 | | |
| **Elevation (ft)** | 3,769 | | |
| **Number of grains analyzed** | 45 | | |
| **Geologic unit** | Ki | | |
| **Geochemical classification** | dacite | | |
| **16A22-3 (Station 28)** | | 71.44 ±0.35 | Weighted mean (n=39) |
| **TRS** | sec. 1, T29N R37E | From large roadcut along Alder Creek heading uphill toward Deer Trail mine; light gray medium-grained equigranular biotite granodiorite. | Overdispersion 0.90 ±0.28 Ma; five mid-Cretaceous grains |
| **Latitude Longitude (degrees)** | 48.04800 -118.09592 | | |
| **Elevation (ft)** | 2,944 | | |
| **Number of grains analyzed** | 47 | | |
| **Geologic unit** | Kigdf | | |
| **Geochemical classification** | granodiorite | | |

**Table A2**. Continued.

| Sample ID (Station ID) | | Age ±2σ (Ma) | Age type |
|---|---|---|---|
| **12A22-9 (Station 41)** | | 103.45 ±0.23 | Weighted mean (n=38) |
| **TRS** | sec. 12, T29N R37E | From roadcut just downhill toward Germania mine from major road intersection on ridgeline; fresh medium- to coarse-grained biotite granodiorite, sparse hornblende, and possible tourmaline. | Overdispersion 0.33 ±0.23 Ma |
| **Latitude Longitude (degrees)** | 48.02659<br>-118.09657 | | |
| **Elevation (ft)** | 4,310 | | |
| **Number of grains analyzed** | 46 | | |
| **Geologic unit** | $\mathrm{Kigd_g}$ | | |
| **Geochemical classification** | granodiorite | | |

| Sample ID (Station ID) | | Age ±2σ (Ma) | Age type |
|---|---|---|---|
| **12A22-1 (Station 42)** | | 103.96 ±0.45 | Weighted mean (n=36) |
| **TRS** | sec. 11, T29N R37E | From roadcut and natural exposure on road to Germania mine; porphyritic granitic rock with very abundant megacrystic K-feldspar up to 2-cm across in medium-grained groundmass that includes some biotite and smoky quartz. | Overdispersion 1.21 ±0.34 Ma |
| **Latitude Longitude (degrees)** | 48.02032<br>-118.10695 | | |
| **Elevation (ft)** | 4,340 | | |
| **Number of grains analyzed** | 38 | | |
| **Geologic unit** | $\mathrm{Kig_g}$ | | |
| **Geochemical classification** | granite | | |

| Sample ID (Station ID) | | Age ±2σ (Ma) | Age type |
|---|---|---|---|
| **13A22-5 (Station 43)** | | 100.12 ±0.40 | Weighted mean (n=36) |
| **TRS** | sec. 18, T29N R38E | From natural slab exposure below road; light gray coarse- to medium-grained equigranular quartz monzonite, rarely with outsize phenocrysts of K-feldspar; identical to rock found just uphill of road. | Overdispersion 0.99 ±0.31 Ma; one Archean grain |
| **Latitude Longitude (degrees)** | 48.01948<br>-118.08426 | | |
| **Elevation (ft)** | 3,675 | | |
| **Number of grains analyzed** | 43 | | |
| **Geologic unit** | $\mathrm{Kigd_g}$ | | |
| **Geochemical classification** | granite | | |

| Sample ID (Station ID) | | Age ±2σ (Ma) | Age type |
|---|---|---|---|
| **13A22-1 (Station 49)** | | 101.82 ±0.47 | Weighted mean (n=40) |
| **TRS** | sec. 13, T29N R37E | From wallrock of Exodus vein at Germania mine; light to medium gray equigranular medium-grained quartz monzonite or granite with relatively abundant biotite. | Overdispersion 1.29 ±0.36; two Archean grains |
| **Latitude Longitude (degrees)** | 48.00771<br>-118.10233 | | |
| **Elevation (ft)** | 3,628 | | |
| **Number of grains analyzed** | 44 | | |
| **Geologic unit** | $\mathrm{Kig_g}$ | | |
| **Geochemical classification** | granite | | |

| Sample ID (Station ID) | | Age ±2σ (Ma) | Age type |
|---|---|---|---|
| **9J22-2 (Station 63)** | | 74.04 ±0.24 | Weighted mean (n=42) |
| **TRS** | sec. 25, T30N R36E | From natural exposure just downhill from station 62; light gray medium-grained biotite granodiorite with sparse blocky K-feldpsar and sparse euhedral hornblende; rock much altered to grus. | Overdispersion 0.61 ±0.19 Ma; one Archean grain and several mid-Cretaceous grains |
| **Latitude Longitude (degrees)** | 48.06646<br>-118.22116 | | |
| **Elevation (ft)** | 2,038 | | |
| **Number of grains analyzed** | 47 | | |
| **Geologic unit** | $\mathrm{Kigd_f}$ | | |
| **Geochemical classification** | granodiorite | | |

| Sample ID (Station ID) | | Age ±2σ (Ma) | Age type |
|---|---|---|---|
| **5A22-7 (Station 64)** | | 73.34 ±0.34 | Weighted mean (n=35) |
| **TRS** | sec. 33, T30N R37E | From natural cliff exposure just above kame terrace; light gray slightly porphyritic granodiorite or granite with sparse biotite. | Overdispersion 0.89 ±0.25 Ma; one Archean grain |
| **Latitude Longitude (degrees)** | 48.06139<br>-118.16357 | | |
| **Elevation (ft)** | 2,373 | | |
| **Number of grains analyzed** | 41 | | |
| **Geologic unit** | $\mathrm{Kig_f}$ | | |
| **Geochemical classification** | granite | | |

**Table A2**. Continued.

<table>
<tr><th colspan="2">Sample ID (Station ID)</th><th>Age ±2σ (Ma)</th><th>Age type</th></tr>
<tr><td colspan="2">3A22-6 (Station 92)</td><td>73.69 ±0.33</td><td>Weighted mean (n=42)</td></tr>
<tr><td>TRS</td><td>sec. 17, T29N R37E</td><td rowspan="6">From natural cliff exposure within incised bedrock gorge; medium-grained equigranular biotite granodiorite; a few possible hornblende noted in hand sample.</td><td rowspan="6">Overdispersion 0.97 ±0.25 Ma; one Archean grain; two mid-Cretaceous grains</td></tr>
<tr><td>Latitude Longitude (degrees)</td><td>48.00892<br>-118.18131</td></tr>
<tr><td>Elevation (ft)</td><td>2,248</td></tr>
<tr><td>Number of grains analyzed</td><td>45</td></tr>
<tr><td>Geologic unit</td><td>Kigd$_{f}$</td></tr>
<tr><td>Geochemical classification</td><td>diorite</td></tr>
</table>

# Appendix B. Geochemistry

## OVERVIEW

Major- and trace-element analyses are used in this report in a variety of ways: (1) to classify igneous rocks in the map area and aid in their identification and correlation; (2) to characterize the composition and critical mineral abundance of a wide variety of host rocks throughout the area; and (3) to assess the quantity of critical minerals in mine tailings from the area. In total, 100 samples were analyzed: 9 are from mine tailings and lack associated thin sections; 24 are from sites that also have geochronology (and a thin section); the remainder are from various rock types throughout the map area and nearly all also have a thin section.

## SAMPLE COLLECTION AND PREPARATION

Large samples are collected in the field and a small sledge hammer is used to break off the freshest pieces, which are then placed into a small plastic bag. A minimum of ~120 g of fresh material is packaged and shipped to USGS Sample Control who catalog the shipment, add quality-control samples, and forward all the samples to a third-party contractor for preparation using standard crushing and separation techniques.

## ANALYTICAL METHODS

Geochemical data for this project were required to be processed by the USGS, who contract with a laboratory for analysis of the material. Upon completion and final quality assurance, the data are then published by the USGS in a quarterly data release. For this project, major-element oxides are determined by wavelength dispersive X-Ray fluorescence (WDXRF). Each sample is fused with lithium metaborate/lithium tetraborate flux and the resultant glass disk is introduced into the WDXRF and irradiated by an x-ray tube. The method also provides a gravimetric loss-on-ignition (LOI). Data are deemed acceptable if recovery of each major oxide is ±5 percent at five times the lower limit of determination (LOD) and the calculated relative standard deviation (RSD) of duplicate samples is no greater than 5 percent. In addition to major-element oxides, sixty elements are determined using inductively coupled plasma mass spectroscopy (ICP-MS) and inductively coupled plasma optical emission spectroscopy (ICP-OES). Samples are fused at 750 °C with sodium peroxide and the fusion cake is dissolved in a dilute nitric acid. The resulting solution is analyzed by ICP-OES and ICP-MS. Data are deemed acceptable if recovery of each element is ±15 percent at five times the LOD and the calculated RSD of duplicate samples is no greater than 15 percent.

The laboratory inserted a reagent blank and an internal geologic reference material (GRM) with every batch of 20 samples. Within every job of samples submitted to the laboratory, the USGS inserted a set of USGS in-house GRMs at a rate of 10 percent that were blind to the laboratory. Specific GRMs were chosen based on the sample media and requested analytical methods since GRMs often lack expected values for certain elements or constituents and may not be useful for every analytical method. In addition to the GRMs, at least one randomly chosen sample per job was split and submitted blind to the laboratory as an analytical duplicate. All USGS GRMs, as well as the original and duplicate analytical split samples are included and identified in the USGS data release. A full description of the QA/QC process is provided in the metadata file within the USGS data release.

## RESULTS

The full USGS data release (U.S. Geological Survey, 2021) was updated in 2023 to include the geochemical analyses from this publication, and is available online at https://doi.org/10.5066/P9WHRLXH. A summary geochemical classification for samples with associated geochronology is in Table 1; location data are in Table B1; analytical data are reproduced from the official USGS publication (REF) in the Data Supplement. Sample duplicates are provided in the Data Supplement and labeled 'duplicate' but are not shown on figures in this pamphlet. Major-element oxides are from WDXRF and provided as weight-percent (wt. %); trace-element data and major-element data are from ICP-OES and ICP-MS and are provided in parts-per-million concentration (ppm) or weight-percent (wt. %).

**Table B1**. Geochemistry sample information and summary classification based on the Total-Alkali-Silica diagram of Le Maitre and others (2002). Detailed results are in the Data Supplement.

| Sample ID (Station ID) | | Geochemical Classification | Co-located analyses (* indicates petrographic analysis for thin section) |
|---|---|---|---|
| **29A22-4 (Station 1)** | | rhyolite | TS1* |
| **TRS** | sec. 9<br>T30N R38E | From abandoned dirt road; abundant liesegang banding; very altered white to yellow and tan felsic material; poorly exposed | |
| **Latitude Longitude (degrees)** | 48.11890<br>-118.02930 | | |
| **Elevation (ft)** | 3,241 | | |
| **Geologic unit** | Ki | | |
| **29A22-5 (Station 2)** | | – – – | TS2 |
| **TRS** | sec. 9<br>T30N R38E | From roadcut on abandoned road; light gray to tan with gritty phyllite; abundant pock-marks on surface may be dissolved dolomite grains | |
| **Latitude Longitude (degrees)** | 48.11852<br>-118.03724 | | |
| **Elevation (ft)** | 3,085 | | |
| **Geologic unit** | $ZYcg_h$ | | |
| **29A22-2 (Station 3)** | | potassic trachybasalt | TS3 |
| **TRS** | sec. 9<br>T30N R38E | From abundant float along slope and road to Cleveland mine; dark greenish gray dense rock | |
| **Latitude Longitude (degrees)** | 48.11732<br>-118.02872 | | |
| **Elevation (ft)** | 3,233 | | |
| **Geologic unit** | $Zg_h$ | | |
| **29A22-1 (Station 4)** | | – – – | TS4 |
| **TRS** | sec. 9<br>T30N R38E | From roadcut on road above (east) Cleveland mine; dolomite | |
| **Latitude Longitude (degrees)** | 48.11389<br>-118.02185 | | |
| **Elevation (ft)** | 3,649 | | |
| **Geologic unit** | $Ycb_s$ | | |
| **28S22-2 (Station 5)** | | – – – | TS5 |
| **TRS** | sec. 12<br>T30N R37E | From roadcut; off white crystalline dolomite interbedded with gray dolomite or limestone | |
| **Latitude Longitude (degrees)** | 48.11711<br>-118.10100 | | |
| **Elevation (ft)** | 2,446 | | |
| **Geologic unit** | $OCl_m$ | | |
| **28S22-4 (Station 6)** | | – – – | TS6 |
| **TRS** | sec. 12<br>T30N R37E | From roadcut; thinly bedded dark bluish limestone | |
| **Latitude Longitude (degrees)** | 48.11506<br>-118.10188 | | |
| **Elevation (ft)** | 2,494 | | |
| **Geologic unit** | $OCl_m$ | | |
| **28S22-13 (Station 7)** | | rhyolite | TS7 |
| **TRS** | sec. 12<br>T30N R37E | From natural exposure above kame terrace of medium gray porphyritic dike intruded parallel to bedding in limestone | |
| **Latitude Longitude (degrees)** | 48.11440<br>-118.08775 | | |
| **Elevation (ft)** | 2,814 | | |
| **Geologic unit** | Ki | | |

**Table B1**. Continued.

| Sample ID (Station ID) | | Geochemical Classification | Co-located analyses (* indicates petrographic analysis for thin section) |
|---|---|---|---|
| **28S22-11 (Station 8)** | | andesite | TS8 |
| **TRS** | sec. 12<br>T30N R37E | From natural outcrop; porphyritic dike about 3–4-m-thick intruding limestone; dike bleached near contacts | |
| **Latitude Longitude (degrees)** | 48.10977<br>-118.10075 | | |
| **Elevation (ft)** | 2,826 | | |
| **Geologic unit** | Eva | | |
| **28S22-10 (Station 9)** | | – – – | TS9 |
| **TRS** | sec. 12<br>T30N R37E | From natural exposure; black to very dark gray faintly laminated hackly argillite with abundant disseminated and concentrated pyrite | |
| **Latitude Longitude (degrees)** | 48.10891<br>-118.09876 | | |
| **Elevation (ft)** | 3,026 | | |
| **Geologic unit** | OCl$_m$ | | |
| **28S22-8 (Station 10)** | | – – – | TS10 |
| **TRS** | sec. 12<br>T30N R37E | From natural cliff outcrop; thin bedded greenish gray to tan quartzite, gritty quartzite, and siltite | |
| **Latitude Longitude (degrees)** | 48.10644<br>-118.09816 | | |
| **Elevation (ft)** | 3,099 | | |
| **Geologic unit** | Cph$_a$ | | |
| **28S22-5 (Station 11)** | | – – – | TS11* |
| **TRS** | sec. 13<br>T30N R37E | From near top of small hill; calc-silicate skarn, locally with original (?) bedding preserved and contorted; euhedral garnets studded in white marble, locally banded brown where garnet is massive | |
| **Latitude Longitude (degrees)** | 48.10551<br>-118.10207 | | |
| **Elevation (ft)** | 2,846 | | |
| **Geologic unit** | OCl$_m$ | | |
| **15S22-13 (Station 12)** | | basalt | TS12 |
| **TRS** | sec. 18<br>T30N R38E | From large abandoned quarry; west side of quarry mostly unfoliated greenstone (sampled); east side to center is green phyllite to foliated very fine quartzite; abundant calcite veins to few cm thick with clots of dark green actinolite | |
| **Latitude Longitude (degrees)** | 48.10598<br>-118.06557 | | |
| **Elevation (ft)** | 2,780 | | |
| **Geologic unit** | Zg$_h$ | | |
| **15S22-2 (Station 13)** | | – – – | TS13 |
| **TRS** | sec. 24<br>T30N R37E | From pile of mine rock at mouth of adit for Deer Trail Monitor mine; calc-silicate skarn developed in dark blue and white thinly bedded to laminated limestone and siltstone; thoroughly rextal, with voluminous green, tan, brown coarse-grained skarn; thin stringers of molybdenite abundant on many surfaces | |
| **Latitude Longitude (degrees)** | 48.09124<br>-118.10544 | | |
| **Elevation (ft)** | 3,459 | | |
| **Geologic unit** | OCl$_m$ | | |
| **15S22-1 (Station 14)** | | granodiorite | TS14* |
| **TRS** | sec. 24<br>T30N R37E | From natural outcrop of medium-grained equigranular granodiorite with sparse hornblende; relatively fresh; abundant pods of mafic rock (schlieren?); a few thin quartz veins or dikes; one thin green vein of epidote (?) | |
| **Latitude Longitude (degrees)** | 48.09045<br>-118.10586 | | |
| **Elevation (ft)** | 3,436 | | |
| **Geologic unit** | Kigd$_f$ | | |

**Table B1**. Continued.

| Sample ID (Station ID) | | Geochemical Classification | Co-located analyses (* indicates petrographic analysis for thin section) |
|---|---|---|---|
| **10J22-3 (Station 15)** | | rhyolite | TS15*; GD15 |
| **TRS** | sec. 21 T30N R38E | From ~3-m-wide roadcut on north side of Springdale–Hunters Road; tan to light gray felsic intrusive rock that is locally porphyritic with 2-mm laths or acicular hornblende and tabular altered plagioclase. Fractures and small faults are abundant throughout the outcrop and most is stained yellow or brown; rock is punky to brecciated near larger fault strands. | |
| **Latitude Longitude (degrees)** | 48.08388 -118.03319 | | |
| **Elevation (ft)** | 3,114 | | |
| **Geologic unit** | Ki | | |
| **15S22-4 (Station 16)** | | – – – | TS16 |
| **TRS** | sec. 24 T30N R37E | From small borrow pit along road at ridge crest; coarsely recrystalized quartzite and interbedded phyllite and impure quartzite; darker fine-grained layers are spotted and locally micaceous | |
| **Latitude Longitude (degrees)** | 48.07872 -118.10568 | | |
| **Elevation (ft)** | 3,558 | | |
| **Geologic unit** | $Cph_a$ | | |
| **15S22-5 (Station 17)** | | – – – | TS17 |
| **TRS** | sec. 25 T30N R37E | From roadcut; hornfelsed dark blue foliated rock with clots of metamorphic biotite | |
| **Latitude Longitude (degrees)** | 48.07647 -118.09718 | | |
| **Elevation (ft)** | 3,466 | | |
| **Geologic unit** | $ZYcg_h$ | | |
| **14A22-9 (Station 18)** | | granite | TS18*; GD18 |
| **TRS** | sec. 31 T30N R38E | From ridge on north side of dirt road near small saddle; leucocratic fine- to medium-grained equigranular granitic rock; sparse biotite and hornblende; red staining is prevalent and the rock is uniformly platy subparallel to the ground surface with 4–1-cm-thick plates. Appears more altered than intrusive rock just to south (station 19). | |
| **Latitude Longitude (degrees)** | 48.06269 -118.07460 | | |
| **Elevation (ft)** | 4,266 | | |
| **Geologic unit** | $Kig_f$ | | |
| **14A22-10 (Station 19)** | | gabbroic diorite | TS19*; GD19 |
| **TRS** | sec. 31 T30N R38E | From just south of dirt road near small saddle; equigranular fine- to medium-grained granodiorite, locally with banded aggregates of megacrystic pyroxene up to 1–3 cm across; notably fresher than intrusive rock to north (station 18) | |
| **Latitude Longitude (degrees)** | 48.06214 -118.07510 | | |
| **Elevation (ft)** | 4,261 | | |
| **Geologic unit** | $Kigd_f$ | | |
| **14A22-13 (Station 20)** | | dacite | TS20* |
| **TRS** | sec. 31 T30N R38E | From abundant float along north side of medium-grained intrusive rock; dike (?) of gray hornblende-phyric rock identical to unit Eva elsewhere | |
| **Latitude Longitude (degrees)** | 48.06006 -118.07280 | | |
| **Elevation (ft)** | 4,249 | | |
| **Geologic unit** | Eva | | |
| **14A22-12 (Station 21)** | | monzonite | TS21*; GD21 |
| **TRS** | sec. 31 T30N R38E | From small roadcut on west side of road; gray plagioclase-phyric medium-grained granite; magnetic; intruded by thin aplite dikes | |
| **Latitude Longitude (degrees)** | 48.05982 -118.07268 | | |
| **Elevation (ft)** | 4,249 | | |
| **Geologic unit** | $Kigd_g$ | | |

**Table B1**. Continued.

| Sample ID (Station ID) | | Geochemical Classification | Co-located analyses (* indicates petrographic analysis for thin section) |
|---|---|---|---|
| **14A22-11 (Station 22)** | | gabbro | TS22 |
| **TRS** | sec. 31 T30N R38E | From float of dark gray microcrystalline rock | |
| **Latitude Longitude (degrees)** | 48.05957 -118.07345 | | |
| **Elevation (ft)** | 4,315 | | |
| **Geologic unit** | $Zg_h$ | | |

| Sample ID (Station ID) | | Geochemical Classification | Co-located analyses |
|---|---|---|---|
| **7J22-1 (Station 23)** | | dacite | TS23*; GD23 |
| **TRS** | sec. 31 T30N R38E | From roadcut uphill (northeast) of Turk mine; gray medium-grained porphyritic dike with plagioclase and biotite phenocrysts in a gray groundmass; dike 1–2 m wide | |
| **Latitude Longitude (degrees)** | 48.05314 -118.07901 | | |
| **Elevation (ft)** | 3,769 | | |
| **Geologic unit** | Ki | | |

| Sample ID (Station ID) | | Geochemical Classification | Co-located analyses |
|---|---|---|---|
| **14S22-1 (Station 24)** | | – – – | TS24 |
| **TRS** | sec. 36 T30N R37E | From roadcut along main road up Alder Creek to Turk mine; tan weathering; dark blue to green where fresh; banded quartzite (?) and dolomite with small blebs of gray to iridescent green-blue metallic mineral | |
| **Latitude Longitude (degrees)** | 48.05136 -118.09704 | | |
| **Elevation (ft)** | 2,893 | | |
| **Geologic unit** | $Ycb_s$ | | |

| Sample ID (Station ID) | | Geochemical Classification | Co-located analyses |
|---|---|---|---|
| **14S22-2 (Station 25)** | | – – – | TS25 |
| **TRS** | sec. 36 T30N R37E | From roadcut along main road up Alder Creek to Turk mine; white to tan to light bluish gray recrystallized coarse-grained dolomite, locally with 1–2 mm biotite books | |
| **Latitude Longitude (degrees)** | 48.05111 -118.09647 | | |
| **Elevation (ft)** | 2,915 | | |
| **Geologic unit** | $Ycb_s$ | | |

| Sample ID (Station ID) | | Geochemical Classification | Co-located analyses |
|---|---|---|---|
| **14A22-8 (Station 26)** | | rhyolite | TS26* |
| **TRS** | sec. 31 T30N R38E | From small roadcut; white to tannish yellow with rusty fractures; sparse quartz eyes in fine-grained felsic groundmass | |
| **Latitude Longitude (degrees)** | 48.04972 -118.06839 | | |
| **Elevation (ft)** | 4,191 | | |
| **Geologic unit** | Ki | | |

| Sample ID (Station ID) | | Geochemical Classification | Co-located analyses |
|---|---|---|---|
| **14S22-4 (Station 27)** | | – – – | TS27 |
| **TRS** | sec. 1 T29N R37E | From main road to Turk mine along Alder Creek; dark gray to blueish gray phyllite and argillite; laminated to thickly bedded; interbedded with gray-green quartzite and tan dolomite | |
| **Latitude Longitude (degrees)** | 48.04850 -118.09446 | | |
| **Elevation (ft)** | 3,034 | | |
| **Geologic unit** | $Ycb_{wd}$ | | |

| Sample ID (Station ID) | | Geochemical Classification | Co-located analyses |
|---|---|---|---|
| **16A22-3 (Station 28)** | | granodiorite | TS28*; GD28 |
| **TRS** | sec. 1 T29N R37E | From large roadcut along Alder Creek heading uphill toward Deer Trail mine; light gray medium-grained equigranular biotite granodiorite | |
| **Latitude Longitude (degrees)** | 48.04800 -118.09592 | | |
| **Elevation (ft)** | 2,944 | | |
| **Geologic unit** | $Kigd_f$ | | |

**Table B1**. Continued.

| Sample ID (Station ID) | | Geochemical Classification | Co-located analyses (* indicates petrographic analysis for thin section) |
|---|---|---|---|
| **14S22-5 (Station 29)** | | | TS29 |
| **TRS** | sec. 6<br>T29N R38E | From roadcut west of road intersection; thin- to thick-bedded white, green, and dark brown quartzite, argillite, and minor dolomite | |
| **Latitude Longitude (degrees)** | 48.04717<br>-118.08441 | | |
| **Elevation (ft)** | 3,308 | | |
| **Geologic unit** | $Ycb_{cc}$ | | |
| **14A22-6 (Station 30)** | | rhyolite | TS30* |
| **TRS** | sec. 4<br>T29N R38E | From roadcut and nearby natural exposures; leucocratic fine-grained dike with rusty pyrite and sparse quartz eyes; within phyllite and slate | |
| **Latitude Longitude (degrees)** | 48.04496<br>-118.03523 | | |
| **Elevation (ft)** | 3,886 | | |
| **Geologic unit** | Ki | | |
| **13A22-6 (Station 31)** | | gabbro | TS31* |
| **TRS** | sec. 1<br>T29N R37E | From roadcut near ridge crest; fine-grained gabbro or diorite, with 75% mafics and the remainder plagioclase | |
| **Latitude Longitude (degrees)** | 48.04541<br>-118.09785 | | |
| **Elevation (ft)** | 3,346 | | |
| **Geologic unit** | $Kigb_{f}$ | | |
| **14S22-10 (Station 32)** | | – – – | TS32* |
| **TRS** | sec. 1<br>T29N R37E | From roadcut; tan dolomite | |
| **Latitude Longitude (degrees)** | 48.04399<br>-118.09075 | | |
| **Elevation (ft)** | 3,347 | | |
| **Geologic unit** | $Ycb_{cc}$ | | |
| **14A22-5 (Station 33)** | | dacite | TS33; GD33 |
| **TRS** | sec. 6<br>T29N R38E | From roadcut; blocks of porphyritic (plagioclase) fine-grained intrusive rock within dark gray slate | |
| **Latitude Longitude (degrees)** | 48.04276<br>-118.06603 | | |
| **Elevation (ft)** | 4,345 | | |
| **Geologic unit** | Ki | | |
| **14S22-18 (Station 34)** | | basalt | TS34* |
| **TRS** | sec. 2<br>T29N R37E | From roadcut and nearby float; foliated greenstone; locally sheared | |
| **Latitude Longitude (degrees)** | 48.03754<br>-118.11034 | | |
| **Elevation (ft)** | 3,815 | | |
| **Geologic unit** | $Zg_{h}$ | | |
| **10J22-1A (Station 35)** | | granite | TS35 |
| **TRS** | sec. 2<br>T29N R37E | From cliff and roadcut; pegmatite (this sample) intruding blueish quartzite (sample 10J22-1A; station 35); pegmatite is mostly quartz and K-feldpsar with biotite, muscovite, and tourmaline | |
| **Latitude Longitude (degrees)** | 48.03770<br>-118.12007 | | |
| **Elevation (ft)** | 3,590 | | |
| **Geologic unit** | Ki | | |

**Table B1**. Continued.

| Sample ID (Station ID) | | Geochemical Classification | Co-located analyses (* indicates petrographic analysis for thin section) |
|---|---|---|---|
| **10J22-1B (Station 36)** | | | TS36 |
| **TRS** | sec. 2 T29N R37E | From cliff and roadcut; pegmatite (sample 10J22-1B; station 36) intruding blueish bedded quartzite (this sample) | |
| **Latitude Longitude (degrees)** | 48.03770 -118.12007 | | |
| **Elevation (ft)** | 3,590 | | |
| **Geologic unit** | $ZYq_b$ | | |
| **14S22-12 (Station 37)** | | – – – | TS37 |
| **TRS** | sec. 1 T29N R37E | From wall rock of adit at Deer Trail mine; banded dolomite | |
| **Latitude Longitude (degrees)** | 48.03557 -118.09787 | | |
| **Elevation (ft)** | 3,615 | | |
| **Geologic unit** | $Ycb_{cc}$ | | |
| **14A22-2 (Station 38)** | | rhyolite | TS38; GD38 |
| **TRS** | sec. 6 T29N R38E | From roadcut on abandoned road east of Deer Trail mine; large outcrop of white to pale yellow felsic intrusive rock with abundant yellow brown red staining, probably due to oxidized pyrite; faint banding or foliation; abundant slickensided surfaces | |
| **Latitude Longitude (degrees)** | 48.03485 -118.08575 | | |
| **Elevation (ft)** | 4,084 | | |
| **Geologic unit** | Ki | | |
| **14A22-4 (Station 39)** | | – – – | TS39 |
| **TRS** | sec. 12 T29N R37E | From roadcut of abandoned road; dark gray spotted quartzite or siltite; locally micaceous; thick beds of spotted rock with sparse discontinuous intervals of thinly bedded dark to tan dolomite (?) | |
| **Latitude Longitude (degrees)** | 48.03417 -118.08902 | | |
| **Elevation (ft)** | 4,118 | | |
| **Geologic unit** | $Ycb_{cc}$ | | |
| **13S22-14 (Station 40)** | | gabbro | TS40 |
| **TRS** | sec. 11 T29N R37E | From roadcut; fine-grained mafic-rich gabbro or diorite similar to that at G31 | |
| **Latitude Longitude (degrees)** | 48.03054 -118.11707 | | |
| **Elevation (ft)** | 4,189 | | |
| **Geologic unit** | $Kigb_f$ | | |
| **12A22-9 (Station 41)** | | granodiorite | TS41*; GD41 |
| **TRS** | sec. 12 T29N R37E | From roadcut just downhill toward Germania mine from major road intersection on ridgeline; fresh medium to coarse-grained biotite granodiorite, sparse hornblende, and possible tourmaline | |
| **Latitude Longitude (degrees)** | 48.02659 -118.09657 | | |
| **Elevation (ft)** | 4,310 | | |
| **Geologic unit** | $Kigd_g$ | | |
| **12A22-1 (Station 42)** | | granite | TS42*; GD42 |
| **TRS** | sec. 11, T29N R37E | From roadcut and natural exposure on road to Germania mine; porphyritic granitic rock with very abundant megacrystic K-feldspar up to 2-cm across in medium-grained groundmass that includes some biotite and smoky quartz | |
| **Latitude Longitude (degrees)** | 48.02032 -118.10695 | | |
| **Elevation (ft)** | 4,340 | | |
| **Geologic unit** | $Kig_g$ | | |

**Table B1**. Continued.

| Sample ID (Station ID) | | Geochemical Classification | Co-located analyses (* indicates petrographic analysis for thin section) |
|---|---|---|---|
| **13A22-5 (Station 43)** | | granite | TS43*; GD43 |
| **TRS** | sec. 18<br>T29N R38E | From natural slab exposure below road; light gray coarse- to medium-grained equigranular quartz monzonite, rarely with outsize phenocrysts of K-feldspar; identical to rock found just uphill of road | |
| **Latitude Longitude (degrees)** | 48.01948<br>-118.08426 | | |
| **Elevation (ft)** | 3,675 | | |
| **Geologic unit** | $Kigd_g$ | | |

| 12A22-2 (Station 44) | | granodiorite | TS44 |
|---|---|---|---|
| TRS | sec. 14<br>T29N R37E | From roadcut and nearby natural exposure on road to Germania mine; several-cm-thick veins of quartz and bladed to radiating accicular black mineral that ranges from massive agglomerations to dispersed acicular minerals (sampled rock) within country rock of equigranular to slightly porphyritic granitic rock, with up to 1 cm quartz phenocrysts, some biotite, and less K-feldspar than just uphill | |
| Latitude Longitude (degrees) | 48.01782<br>-118.10719 | | |
| Elevation (ft) | 4,233 | | |
| Geologic unit | $Kig_g$ | | |

| 12A22-3 (Station 45) | | granite | TS45; GD45 |
|---|---|---|---|
| **TRS** | sec. 14<br>T29N R37E | From roadcut and nearby natural exposure on road to Germania mine; equigranular medium-grained granitic rock hosting NE-striking pegmatite or vein to 8 cm thick consisting of coarse-grained white mica and quartz that is locally stained red; sampled the pegmatite/dike | |
| **Latitude Longitude (degrees)** | 48.01743<br>-118.10727 | | |
| **Elevation (ft)** | 4,219 | | |
| **Geologic unit** | $Kig_g$ | | |

| 12A22-7A (Station 46) | | granite | TS46* |
|---|---|---|---|
| **TRS** | sec. 14<br>T29N R37E | From roadcut near Owl Creek; two samples from same location: country rock (this sample) of porphyritic granitic rock with phenocrysts of quartz and K-feldspar in a fine-grained groundmass; contains veins of dark gray to black accicular, bladed, or massive minerals and quartz (sample 12A22-7B) | |
| **Latitude Longitude (degrees)** | 48.01667<br>-118.11166 | | |
| **Elevation (ft)** | 3,769 | | |
| **Geologic unit** | $Kig_g$ | | |


| 12A22-7A (Station 46) | | granite | TS46* |
|---|---|---|---|
| **TRS** | sec. 14<br>T29N R37E | From roadcut near Owl Creek; two samples from same location: country rock (this sample) of porphyritic granitic rock with phenocrysts of quartz and K-feldspar in a fine-grained groundmass; contains veins of dark gray to black accicular, bladed, or massive minerals and quartz (sample 12A22-7B) | |
| **Latitude Longitude (degrees)** | 48.01667<br>-118.11166 | | |
| **Elevation (ft)** | 3,769 | | |
| **Geologic unit** | $Kig_g$ | | |


| 12A22-5 (Station 48) | | andesite | TS48 |
|---|---|---|---|
| **TRS** | sec. 14<br>T29N R37E | From poor exposure in roadcut; silvery gray soil with blocks of light gray hornblende-phyric volcanic rock with sparse plagioclase and biotite (?); surrounded by porphyritic granitic rock; abundant float of slickensided surfaces could be faults or dike edges; looks identical to unit Eva elsewhere. | |
| **Latitude Longitude (degrees)** | 48.01147 -118.11172 | | |
| **Elevation (ft)** | 3,863 | | |
| **Geologic unit** | Eva | | |

| 13A22-1 (Station 49) | | granite | TS49*; GD49 |
|---|---|---|---|
| **TRS** | sec. 13<br>T29N R37E | From wallrock of Exodus vein at Germania mine; light to medium gray equigranular medium-grained quartz monzonite or granite with relatively abundant biotite | |
| **Latitude Longitude (degrees)** | 48.00771<br>-118.10233 | | |
| **Elevation (ft)** | 3,628 | | |
| **Geologic unit** | $Kig_g$ | | |

**Table B1**. Continued.

| Sample ID (Station ID) | | Geochemical Classification | Co-located analyses (* indicates petrographic analysis for thin section) |
|---|---|---|---|
| **13A22-2 (Station 50)** | | monzonite | TS50; GD50 |
| **TRS** | sec. 13 T29N R37E | From wallrock of Exodus vein at Germania mine; wall rock of mined-out Exodus vein is punky and appears hydrothermally altered for several cm away from exposed edge; sampled quartz and muscovite-rich block detached from side of vein | |
| **Latitude Longitude (degrees)** | 48.00712 -118.10276 | | |
| **Elevation (ft)** | 3,659 | | |
| **Geologic unit** | Kig$_g$ | | |
| **13A22-4 (Station 51)** | | granite | TS51 |
| **TRS** | sec. 13 T29N R37E | From in-situ north side of Exodus vein near ground surface; altered granitic rock with notable thin quartz and mica-rich vein containing sulfides | |
| **Latitude Longitude (degrees)** | 48.00673 -118.10318 | | |
| **Elevation (ft)** | 3,720 | | |
| **Geologic unit** | Kig$_g$ | | |
| **14S22-15 (Station 52)** | | granite | TS52 |
| **TRS** | sec. 24 T29N R37E | From small adit (?) or cliff; medium- to coarse-grained equant quartz monzonite; locally porphyritic | |
| **Latitude Longitude (degrees)** | 48.00358 -118.09135 | | |
| **Elevation (ft)** | 3,140 | | |
| **Geologic unit** | Kiqm$_g$ | | |
| **14S22-17 (Station 53)** | | granite | TS53 |
| **TRS** | sec. 24 T29N R37E | From ditch cut across abandoned road; fine-grained equigranular quartz monzonite; locally has thin 1-3-mm-wide black veinlets | |
| **Latitude Longitude (degrees)** | 48.00269 -118.08611 | | |
| **Elevation (ft)** | 3,131 | | |
| **Geologic unit** | Kiqm$_g$ | | |
| **14S22-16 (Station 54)** | | granite | TS54 |
| **TRS** | sec. 24 T29N R37E | From roadcut; leucocratic fine-grained equigranular granitic rock with quartz, K-feldspar, and sparse muscovite | |
| **Latitude Longitude (degrees)** | 48.00246 -118.08732 | | |
| **Elevation (ft)** | 3,146 | | |
| **Geologic unit** | Ki | | |
| **27S22-3 (Station 55)** | | trachy-dacite | TS55 |
| **TRS** | sec. 12 T30N R36E | From tall cliff adjacent to road; multiple pyroclastic breccia deposits; some intervals of tuff and lapilli tuff; all contain similar clasts of hornblende-phyric volcanic rock | |
| **Latitude Longitude (degrees)** | 48.11657 -118.21966 | | |
| **Elevation (ft)** | 1,560 | | |
| **Geologic unit** | Evt | | |
| **15S22-11 (Station 56)** | | basaltic andesite | TS56* |
| **TRS** | sec. 18 T30N R37E | From natural outcrop on south side of incised canyon; blueish-green dark gray fine-grained greenstone | |
| **Latitude Longitude (degrees)** | 48.10370 -118.20061 | | |
| **Elevation (ft)** | 2,027 | | |
| **Geologic unit** | Omv$_b$ | | |

**Table B1**. Continued.

| Sample ID (Station ID) | | Geochemical Classification | Co-located analyses (* indicates petrographic analysis for thin section) |
|---|---|---|---|
| **15S22-8 (Station 57)** | | – – – | TS57 |
| **TRS** | sec. 19 T30N R37E | From natural outcrop; laminated to medium-bedded quartzite | |
| **Latitude Longitude (degrees)** | 48.09097 -118.20165 | | |
| **Elevation (ft)** | 1,886 | | |
| **Geologic unit** | $Oms_d$ | | |
| **15S22-7 (Station 58)** | | – – – | TS58 |
| **TRS** | sec. 19 T30N R37E | From top of small hill; top and most of side to west is fine-grained greenstone with seams and pods of calcite | |
| **Latitude Longitude (degrees)** | 48.08946 -118.20144 | | |
| **Elevation (ft)** | 1,996 | | |
| **Geologic unit** | $Omv_b$ | | |
| **15S22-9B (Station 59)** | | – – – | TS59 |
| **TRS** | sec. 19 T30N R37E | – – – | |
| **Latitude Longitude (degrees)** | 48.08825 -118.20461 | | |
| **Elevation (ft)** | 1,788 | | |
| **Geologic unit** | $Ocb_c$ | | |
| **15S22-9A (Station 60)** | | – – – | TS60 |
| **TRS** | sec. 19 T30N R37E | From roadcut along Highway 25; belt of multihued calc-silicate skarn; actinolite, garnet, epidote, calcite are all abundant; protolith is unclear | |
| **Latitude Longitude (degrees)** | 48.08825 -118.20461 | | |
| **Elevation (ft)** | 1,788 | | |
| **Geologic unit** | $Ocb_c$ | | |
| **27S22-2 (Station 61)** | | granodiorite | TS61 |
| **TRS** | sec. 19 T30N R37E | From natural outcrop; medium-grained equant biotite-hornblende granodiorite | |
| **Latitude Longitude (degrees)** | 48.08310 -118.19672 | | |
| **Elevation (ft)** | 1,887 | | |
| **Geologic unit** | $Kigd_f$ | | |
| **9J22-3 (Station 62)** | | dacite | TS62; GD62 |
| **TRS** | sec. 25 T30N R36E | From base of natural cliff exposure just uphill from age site station 63; gray to dark gray and blocky flow rock | |
| **Latitude Longitude (degrees)** | 48.06705 -118.22142 | | |
| **Elevation (ft)** | 2,131 | | |
| **Geologic unit** | Eva | | |
| **9J22-2 (Station 63)** | | granodiorite | TS63*; GD63 |
| **TRS** | sec. 25 T30N R36E | From natural exposure just downhill from station 62; light gray medium-grained biotite granodiorite with sparse blocky K-feldpsar and sparse euhedral hornblende; rock much altered to grus | |
| **Latitude Longitude (degrees)** | 48.06646 -118.22116 | | |
| **Elevation (ft)** | 2,038 | | |
| **Geologic unit** | $Kigd_f$ | | |

**Table B1**. Continued.

| Sample ID (Station ID) | | Geochemical Classification | Co-located analyses (* indicates petrographic analysis for thin section) |
|---|---|---|---|
| **5A22-7 (Station 64)** | | granite | TS64*; GD64 |
| **TRS** | sec. 33<br>T30N R37E | From natural cliff exposure just above kame terrace; light gray slightly porphyritic granodiorite or granite with sparse biotite | |
| **Latitude Longitude (degrees)** | 48.06139<br>-118.16357 | | |
| **Elevation (ft)** | 2,373 | | |
| **Geologic unit** | $Kig_f$ | | |
| **6A22-8 (Station 65)** | | granodiorite | TS65* |
| **TRS** | sec. 31<br>T30N R37E | From natural outcrop; medium-grained equigranular granitic rock; notable but sparse phenocrysts of K-feldpsar; occasional clots of mafic minerals (hornblende?) altered green; biotite typically fresh; rock is far less altered than volcanic rocks just to south | |
| **Latitude Longitude (degrees)** | 48.06190<br>-118.20301 | | |
| **Elevation (ft)** | 1,924 | | |
| **Geologic unit** | $Kig_f$ | | |
| **6A22-6 (Station 66)** | | rhyolite | TS66; GD66 |
| **TRS** | sec. 31<br>T30N R37E | From natural exposure on a small knoll; light-colored tuff; blocky to platy | |
| **Latitude Longitude (degrees)** | 48.05759<br>-118.20656 | | |
| **Elevation (ft)** | 2,260 | | |
| **Geologic unit** | Evt | | |
| **6A22-4 (Station 67)** | | rhyolite | TS67 |
| **TRS** | sec. 31<br>T30N R37E | From cliff outcrop; white, red, purple, and tan; locally silicified and very hard; some brecciated; nearby float has red and purple and brown liesegang banding, some pieces with slickenlined fault surfaces; protolith uncertain but may be flow rock | |
| **Latitude Longitude (degrees)** | 48.05706<br>-118.19926 | | |
| **Elevation (ft)** | 2,520 | | |
| **Geologic unit** | Eva | | |
| **6A22-3B (Station 68)** | | rhyolite | TS68 |
| **TRS** | sec. 31<br>T30N R37E | From natural outcrop; light-colored thin-bedded vitric-crystal tuff with clear quartz eyes | |
| **Latitude Longitude (degrees)** | 48.05097<br>-118.21277 | | |
| **Elevation (ft)** | 2,247 | | |
| **Geologic unit** | Evt | | |
| **13S22-1 (Station 69)** | | trachy-andesite | TS69 |
| **TRS** | sec. 36<br>T30N R36E | From talus pile shed from nearby cliff; dark gray hornblende-phyric platy flow | |
| **Latitude Longitude (degrees)** | 48.05016<br>-118.22041 | | |
| **Elevation (ft)** | 1,907 | | |
| **Geologic unit** | Eva | | |
| **15A22-5 (Station 70)** | | andesite | TS70 |
| **TRS** | sec. 5<br>T29N R37E | From top of large cliff; platy to blocky or rubbly; pale gray hornblende-phyric flow rock with stubby sparse plagioclase | |
| **Latitude Longitude (degrees)** | 48.04761<br>-118.18544 | | |
| **Elevation (ft)** | 2,615 | | |
| **Geologic unit** | Eva | | |

**Table B1**. Continued.

| Sample ID (Station ID) | | Geochemical Classification | Co-located analyses (* indicates petrographic analysis for thin section) |
|---|---|---|---|
| **27S22-1 (Station 71)** | | granodiorite | TS71* |
| **TRS** | sec. 2 T29N R37E | From natural outcrop near road; medium-grained biotite-hornblende granodiorite; fresh | |
| **Latitude Longitude (degrees)** | 48.04488 -118.12553 | | |
| **Elevation (ft)** | 2,815 | | |
| **Geologic unit** | $Kigd_f$ | | |

| Sample ID (Station ID) | | Geochemical Classification | Co-located analyses |
|---|---|---|---|
| **15A22-3 (Station 72)** | | dacite | TS72 |
| **TRS** | sec. 6 T29N R37E | From natural outcrop; white to light mauve to gray tuff with euhedral hornblende and clear quartz eyes; strong mineral alignment; there are a few irregular-shaped altered green and white blobs which may be pumice fragments | |
| **Latitude Longitude (degrees)** | 48.04196 -118.19765 | | |
| **Elevation (ft)** | 2,585 | | |
| **Geologic unit** | Evt | | |

| Sample ID (Station ID) | | Geochemical Classification | Co-located analyses |
|---|---|---|---|
| **4A22-3 (Station 73)** | | trachy-andesite | TS73; GD73 |
| **TRS** | sec. 5 T29N R37E | From natural cliff exposure on east side of incised gorge; only 2 m from contact with granitic rock; gray cryptocrystalline groundmass with aligned hornblende up to 1 cm in size and sparse stubby pyroxene | |
| **Latitude Longitude (degrees)** | 48.04107 -118.18447 | | |
| **Elevation (ft)** | 2,333 | | |
| **Geologic unit** | Eva | | |

| Sample ID (Station ID) | | Geochemical Classification | Co-located analyses |
|---|---|---|---|
| **15A22-1 (Station 74)** | | andesite | TS74; GD74 |
| **TRS** | sec. 6 T29N R37E | From base of natural cliff; monolithologic pyroclastic breccia consisting of angular boulder to pebble sized clasts; light gray trachytic hornblende-phyric rock; little matrix between clasts | |
| **Latitude Longitude (degrees)** | 48.03723 -118.19518 | | |
| **Elevation (ft)** | 2,303 | | |
| **Geologic unit** | Evt | | |

| Sample ID (Station ID) | | Geochemical Classification | Co-located analyses |
|---|---|---|---|
| **8J22-4 (Station 75)** | | trachy-andesite | TS75 |
| **TRS** | sec. 12 T29N R36E | From natural outcrop; medium gray, lavender gray, olive gray, or brown; rubbly, often broken into chaotic 1–2 cm blocky pieces; hornblende is prominent and fresh up to 1 cm in size; typically trachytic in dull groundmass | |
| **Latitude Longitude (degrees)** | 48.03110 -118.23345 | | |
| **Elevation (ft)** | 1,564 | | |
| **Geologic unit** | Eva | | |

| Sample ID (Station ID) | | Geochemical Classification | Co-located analyses |
|---|---|---|---|
| **13S22-6 (Station 76)** | | dacite | TS76* |
| **TRS** | sec. 7 T29N R37E | From recent roadcut; medium gray fine-grained plagioclase-phyric volcanic rock | |
| **Latitude Longitude (degrees)** | 48.02886 -118.19724 | | |
| **Elevation (ft)** | 1,896 | | |
| **Geologic unit** | Eva | | |

| Sample ID (Station ID) | | Geochemical Classification | Co-located analyses |
|---|---|---|---|
| **4A22-8 (Station 77)** | | trachy-andesite | TS77; GD77 |
| **TRS** | sec. 12 T29N R36E | From natural low exposures just west of Mudgett Road. Maroon flow or flow breccia with abundant phenocrysts of 1–5 mm hornblende | |
| **Latitude Longitude (degrees)** | 48.02908 -118.21786 | | |
| **Elevation (ft)** | 2,075 | | |
| **Geologic unit** | Eva | | |

**Table B1**. Continued.

| Sample ID (Station ID) | | Geochemical Classification | Co-located analyses (* indicates petrographic analysis for thin section) |
|---|---|---|---|
| **5A22-2 (Station 78)** | | andesite | TS78 |
| **TRS** | sec. 12 T29N R36E | From natural exposure; gray cryptocrystalline groundmass with fresh appearing hornblende | |
| **Latitude Longitude (degrees)** | 48.02895 -118.22359 | | |
| **Elevation (ft)** | 2,130 | | |
| **Geologic unit** | Eva | | |
| **13S22-5 (Station 79)** | | dacite | TS79 |
| **TRS** | sec. 7 T29N R37E | From natural outcrop; flattened (partially welded?) pumice lapilli tuff | |
| **Latitude Longitude (degrees)** | 48.02847 -118.20087 | | |
| **Elevation (ft)** | 1,964 | | |
| **Geologic unit** | Evt | | |
| **13S22-4 (Station 80)** | | andesite | TS80 |
| **TRS** | sec. 7 T29N R37E | From natural outcrop; mauve flow; at least one 1-m-wide dike nearby of identical lithology | |
| **Latitude Longitude (degrees)** | 48.02309 -118.20599 | | |
| **Elevation (ft)** | 2,021 | | |
| **Geologic unit** | Eva | | |
| **13S22-11 (Station 81)** | | granite | TS81 |
| **TRS** | sec. 14 T29N R37E | From in-situ rock at mouth of adit for Aichan Bee mine; gray equigranular biotite granodiorite; mostly fresh looking | |
| **Latitude Longitude (degrees)** | 48.01664 -118.12720 | | |
| **Elevation (ft)** | 3,249 | | |
| **Geologic unit** | Kigd$_{g}$ | | |
| **4A22-6 (Station 82)** | | trachy-andesite | TS82 |
| **TRS** | sec. 18 T29N R37E | From cliff exposure; gray cryptocrystalline groundmass with quartz eyes and sparse tabular mafic minerals; somewhat altered green | |
| **Latitude Longitude (degrees)** | 48.01800 -118.21210 | | |
| **Elevation (ft)** | 1,988 | | |
| **Geologic unit** | Eva | | |
| **13S22-2 (Station 83)** | | dacite | TS83 |
| **TRS** | sec. 18 T29N R37E | From natural exposure; mauve flow | |
| **Latitude Longitude (degrees)** | 48.01402 -118.20018 | | |
| **Elevation (ft)** | 2,358 | | |
| **Geologic unit** | Eva | | |
| **4A22-7 (Station 84)** | | trachy-andesite | TS84 |
| **TRS** | sec. 13 T29N R36E | From natural cliff exposure; varied color, gray to green and red or purple flow rock of gray groundmass with biotite, stubby hornblende, and rare quartz; all rock is altered to various shades of green with abundant veins of quartz, locally well formed to several cm thick and with dull chalcedony | |
| **Latitude Longitude (degrees)** | 48.01227 -118.21619 | | |
| **Elevation (ft)** | 1,947 | | |
| **Geologic unit** | Eva | | |

**Table B1**. Continued.

| Sample ID (Station ID) | | Geochemical Classification | Co-located analyses (* indicates petrographic analysis for thin section) |
|---|---|---|---|
| **4A22-2 (Station 85)** | | syenite | TS85* |
| **TRS** | sec. 16<br>T29N R37E | From tailing and cut-bank exploration pit; altered pegmatite (quartz and K-feldspar) in medium-grained granodiorite | |
| **Latitude Longitude (degrees)** | 48.01060<br>-118.15672 | | |
| **Elevation (ft)** | 2,883 | | |
| **Geologic unit** | $Kigd_f$ | | |
| **4A22-1 (Station 86)** | | – – – | TS86 |
| **TRS** | sec. 16<br>T29N R37E | From small exploration pit; coarse-grained white to blueish white marble with notable tremolite | |
| **Latitude Longitude (degrees)** | 48.01038<br>-118.15661 | | |
| **Elevation (ft)** | 2,887 | | |
| **Geologic unit** | $OCl_m$ | | |
| **12A22-8 (Station 87)** | | granite | TS87 |
| **TRS** | sec. 22<br>T29N R37E | From roadcut below mine; equigranular medium-grained granitic rock to K-feldspar porphyritic; somewhat altered | |
| **Latitude Longitude (degrees)** | 48.00481<br>-118.14104 | | |
| **Elevation (ft)** | 3,612 | | |
| **Geologic unit** | $Kigd_f$ | | |
| **3A22-7 (Station 88)** | | dacite | TS88; GD88 |
| **TRS** | sec. 20<br>T29N R37E | From 2–4-m-tall cliff exposure above gravel road; white to salmon-colored to gray crystal-vitric lapilli tuff with abundant pumice clasts; phenocrysts of hornblende, plagioclase, and quartz | |
| **Latitude Longitude (degrees)** | 48.00516<br>-118.18656 | | |
| **Elevation (ft)** | 2,185 | | |
| **Geologic unit** | Evt | | |
| **3A22-4 (Station 89)** | | granite | TS89* |
| **TRS** | sec. 21<br>T29N R37E | From small knoll outcrop; varied plutonic rocks in this location; analyzed sample is medium-grained granitic rock that hosts: 1) a coarse-grained K-feldpsar and quartz pegmatite with black to green tourmaline up to 3 cm long and some biotite, and 2) thin 1–3 cm white fine- to medium-grained aplite dikes | |
| **Latitude Longitude (degrees)** | 48.00302<br>-118.17097 | | |
| **Elevation (ft)** | 2,579 | | |
| **Geologic unit** | $Kig_f$ | | |
| **3A22-8 (Station 90)** | | andesite | TS90; GD90 |
| **TRS** | sec. 19<br>T29N R37E | From natural slope and 1–3-m-tall cliff exposures above gravel road; brown to dark gray aphanitic flow rock with slightly trachytic euhedral hornblende up to 1.5 cm in size; uniformly tabular with 2–4-cm-thick plates | |
| **Latitude Longitude (degrees)** | 48.00087<br>-118.19286 | | |
| **Elevation (ft)** | 2,133 | | |
| **Geologic unit** | Eva | | |
| **3A22-6 (Station 92)** | | diorite | GD92 |
| **TRS** | sec. 17<br>T29N R37E | From natural cliff exposure within incised bedrock gorge; medium-grained equigranular biotite granodiorite; a few possible hornblende noted in hand sample | |
| **Latitude Longitude (degrees)** | 48.00892<br>-118.18131 | | |
| **Elevation (ft)** | 2,248 | | |
| **Geologic unit** | $Kigd_f$ | | |

**Table B1**. Continued.

| Sample ID (Station ID) | | Geochemical Classification | Co-located analyses (* indicates petrographic analysis for thin section) |
|---|---|---|---|
| **28S22-9 (Station 93)** | | – – – | – – – |
| **TRS** | sec. 12<br>T30N R37E | Tailings or waste rock from near collapsed mine adit north of Deer Trail Monitor mine and east of Read mine; bedded grayish marble much altered to brown; abundant thin stringers of molybdenite; dark to pistachio green calc-silicate skarn with alternating bands of pink to brown colored rock | |
| **Latitude Longitude (degrees)** | 48.10698<br>-118.09815 | | |
| **Elevation (ft)** | 3,075 | | |
| **Geologic unit** | ml | | |
| **14S22-8 (Station 94)** | | – – – | – – – |
| **TRS** | sec. 6<br>T29N R38E | Tailings from upper adit of Togo mine; punky altered rock with quartz veins, copper sulfide minerals, and some tremolite (?); nearby float of milky quartz up to 1 cm wide | |
| **Latitude Longitude (degrees)** | 48.04859<br>-118.07216 | | |
| **Elevation (ft)** | 3,913 | | |
| **Geologic unit** | ml | | |
| **14S22-9 (Station 95)** | | – – – | – – – |
| **TRS** | sec. 6<br>T29N R38E | Tailings from lower pile of Turk mine | |
| **Latitude Longitude (degrees)** | 48.04831<br>-118.08389 | | |
| **Elevation (ft)** | 3,364 | | |
| **Geologic unit** | ml | | |
| **14S22-11 (Station 96)** | | – – – | – – – |
| **TRS** | sec. 1<br>T29N R37E | Tailings/waste rock from Deer Trail mine site; grab bag of major lithologies | |
| **Latitude Longitude (degrees)** | 48.03627<br>-118.09666 | | |
| **Elevation (ft)** | 3,566 | | |
| **Geologic unit** | ml | | |
| **14A22-3 (Station 97)** | | – – – | – – – |
| **TRS** | sec. 1<br>T29N R37E | Tailings from small adit/working east of Deer Trail mine; mostly thin- to medium-bedded pale green to brownish green to white dolomite? and skarn with chalcopyrite | |
| **Latitude Longitude (degrees)** | 48.03598<br>-118.08649 | | |
| **Elevation (ft)** | 4,061 | | |
| **Geologic unit** | ml | | |
| **14S22-13 (Station 98)** | | – – – | – – – |
| **TRS** | sec. 1<br>T29N R37E | Tailings from near mill of Deer Trail mine | |
| **Latitude Longitude (degrees)** | 48.03545<br>-118.09696 | | |
| **Elevation (ft)** | 3,564 | | |
| **Geologic unit** | ml | | |
| **13S22-13 (Station 99)** | | – – – | – – – |
| **TRS** | sec. 11<br>T29N R37E | Tailings from top of Queen Seal mine | |
| **Latitude Longitude (degrees)** | 48.02602<br>-118.12196 | | |
| **Elevation (ft)** | 3,983 | | |
| **Geologic unit** | ml | | |

**Table B1**. Continued.

| Sample ID (Station ID) | | Geochemical Classification | Co-located analyses (* indicates petrographic analysis for thin section) |
|---|---|---|---|
| **13S22-12 (Station 100)** | | – – – | – – – |
| **TRS** | sec. 11<br>T29N R37E | Tailings from main landing/tailings pile at Queen Seal mine | |
| **Latitude Longitude (degrees)** | 48.02521<br>-118.12095 | | |
| **Elevation (ft)** | 3,891 | | |
| **Geologic unit** | ml | | |

| Sample ID (Station ID) | | Geochemical Classification | Co-located analyses |
|---|---|---|---|
| **27A22-1 (Station 101)** | | – – – | – – – |
| **TRS** | sec. 13<br>T29N R37E | Waste rock pile from Germania mine; predominantly medium-grained equigranular to slightly porphyritic granitic rock; contains quartz veins and greisen veins, typically associated with sulfides, molybdenite, and rarely large tabular wolframite | |
| **Latitude Longitude (degrees)** | 48.00772<br>-118.10020 | | |
| **Elevation (ft)** | 3,515 | | |
| **Geologic unit** | ml | | |

| Sample ID (Station ID) | | Geochemical Classification | Co-located analyses |
|---|---|---|---|
| **81-85(a); 83-28B; 83-29B; 83-30B (Station 102)** | | – – – | – – – |
| **TRS** | sec. 9<br>T30N R38E | From Bunning (1985); Cleveland mine; samples 81-85(a), 83-28B, 83-29B, and 83-30B.<br>81-85(a): ore sample of galena, sphalerite, and pyrite in siderite and quartz.<br>83-28B: dump sample; high grade; predominantly galena.<br>83-29B: dump sample; high grade; predominantly sphalerite.<br>83-30B: dump sample; high grade; predominantly pyrite, chalcopyrite, arsenopyrite. | |
| **Latitude Longitude (degrees)** | 48.11574<br>-118.02546 | | |
| **Elevation (ft)** | 3,363 | | |
| **Geologic unit** | ml | | |

| Sample ID (Station ID) | | Geochemical Classification | Co-located analyses |
|---|---|---|---|
| **81-98B; 83-15B; 83-16B; 83-17B; 83-18B (Station 103)** | | – – – | – – – |
| **TRS** | sec. 11<br>T30N R37E | From Bunning (1985); Read prospect; samples 81-98B, 83-15B, 83-16B, 83-17B, and 83-18B.<br>81-98B: magnetite ore with minor pyrite or arsenopyrite in calcium-rich granite at dolomite contact; granite is composed of chlorite, quartz, euhedral feldspar, garnet, and pyrite with minor magnetite veinlets; minor malachite staining.<br>83-15B: same decline sampled in 1981 (81-98B); granodiorite footwall is silicified; actinolite, minor garnet, 0.5% pyrite with some chalcopyrite on fracture surfaces; sample is from granodiorite footwall.<br>83-16B: dolomite hanging wall from same locality as 83-15B.<br>83-17B: above decline; sample for garnet at dolomite-granodiorite contact; garnet is massive, flesh-colored, with feldspar and diopside(?).<br>83-18B: magnetite and serpentine(?) above shaft. | |
| **Latitude Longitude (degrees)** | 48.10924<br>-118.11355 | | |
| **Elevation (ft)** | 2,764 | | |
| **Geologic unit** | $OCl_m$ | | |

| Sample ID (Station ID) | | Geochemical Classification | Co-located analyses |
|---|---|---|---|
| **83-12B; 83-13B; 83-14B (Station 104)** | | – – – | – – – |
| **TRS** | sec. 14<br>T30N R37E | From Bunning (1985); Read prospect; samples 83-12B, 83-13B, and 83-14B.<br>83-12B: massive magnetite within recrystallized limestone.<br>83-13B: garnet-diopside skarn; near dolomite outcrop.<br>83-14B: magnetite from prospect in limestone near old rotary drill holes. | |
| **Latitude Longitude (degrees)** | 48.10614<br>-118.12461 | | |
| **Elevation (ft)** | 2,817 | | |
| **Geologic unit** | $OCl_m$ | | |

| Sample ID (Station ID) | | Geochemical Classification | Co-located analyses |
|---|---|---|---|
| **81-102B; 83-51B; 83-52B (Station 105)** | | – – – | – – – |
| **TRS** | sec. 24<br>T30N R37E | From Bunning (1985); Deer Trail Monitor mine; samples 81-102B, 83-51B, and 83-52B.<br>81-102B: calc-silicate hornfels near granite contact carries sphalerite, galena, molybdenite, pyrite, magnetite, chalcopyrite, epidote, actinolite, and calcite; molybdenite in greenish carbonate with garnet was not closely associated with galena and sphalerite.<br>83-51B: andradite garnet.<br>83-52B: high-grade molybdenite ore. | |
| **Latitude Longitude (degrees)** | 48.09118<br>-118.10580 | | |
| **Elevation (ft)** | 3,456 | | |
| **Geologic unit** | ml | | |

**Table B1**. Continued.

| Sample ID (Station ID) | | Geochemical Classification | Co-located analyses (* indicates petrographic analysis for thin section) |
|---|---|---|---|
| **81-71B; 83-24B; 83-25B; 83-26B; 83-27B (Station 106)** | | – – – | – – – |
| **TRS** | sec. 6 T29N R38E | From Bunning (1985); Turk mine; samples 81-71B, 83-24B, 83-25B, 83-26B, 83-27B<br>81-71B: High-grade sample of chalcopyrite, pyrite, malachite, quartz, and barite from dump<br>83-24B: Actinolite, epidote, manganese oxide adjacent to quartz vein in fault zone from workings on west side of hill<br>83-25B: Silicified, brecciated quartz vein in fault; dominant fractures trend N84E and dip 85N<br>83-26B: Footwall side of quartz vein and fault zone is yellow-brown altered limestone with tremolite; abundant manganese oxide and malachite<br>83-27B: Silicified red and green dolomitic argillite with pyrite, chalcopyrite, and actinolite | |
| **Latitude Longitude (degrees)** | 48.04838 -118.08458 | | |
| **Elevation (ft)** | 3,454 | | |
| **Geologic unit** | $Ycb_{cc}$ | | |

| Sample ID (Station ID) | | Geochemical Classification | Co-located analyses (* indicates petrographic analysis for thin section) |
|---|---|---|---|
| **81-84B (Station 107)** | | – – – | – – – |
| **TRS** | sec. 6 T29E R37E | From Bunning (1985); Togo mine; sample 81-84B. Dump sample; tremolite with chalcopyrite and pyrite | |
| **Latitude Longitude (degrees)** | 48.04795 -118.07338 | | |
| **Elevation (ft)** | 3,787 | | |
| **Geologic unit** | $Yph_t$ | | |

| Sample ID (Station ID) | | Geochemical Classification | Co-located analyses (* indicates petrographic analysis for thin section) |
|---|---|---|---|
| **81-72B; 83-35B; 83-36B; 83-37B; 83-38B; 83-39B; 83-40B; 83-41B (Station 108)** | | – – – | – – – |
| **TRS** | sec. 1 T29N R37E | From Bunning (1985); Deer Trail mine; samples 81-72B, 83-35B, 83-36B, 83-37B, 83-38B, 83-39B, 83-40B, 83-41B<br><br>81-72B: Sample of quartz monzonite-limestone intrusion breccia; some rhodochrosite, abundant manganese oxide; garnet, sphalerite, galena, and pyrite<br>83-35B: Pod of garnet in chloritized schist with calcite veinlets, pyrite, and epidote in 5029 raise, left sub, Madre adit<br>83-36B: Vein material from muck in slope; above Madre adit<br>83-37B: Pyritized wall rock; Madre adit 5028<br>83-38B: Vein with galena, sphalerite, pyrite<br>83-39B: DDH L-5; 75′ to 80′; pyrite in argillite<br>83-40B: DDH L-4; 294.8′ to 295.8′; galena, sphalerite vein<br>83-41B: DDH L-5; 276′ to 277′; galena-sphalerite vein | |
| **Latitude Longitude (degrees)** | 48.03511 -118.09778 | | |
| **Elevation (ft)** | 3,605 | | |
| **Geologic unit** | ml | | |

| Sample ID (Station ID) | | Geochemical Classification | Co-located analyses (* indicates petrographic analysis for thin section) |
|---|---|---|---|
| **81-86B (Station 109)** | | – – – | – – – |
| **TRS** | sec. 11 T29N R37E | From Bunning (1985); Queen and Seal mine; sample 81-86B. Dump sample with argenite, pyrite, galena, chalcopyrite, copper oxides in quartz with tremolite | |
| **Latitude Longitude (degrees)** | 48.02602 -118.12196 | | |
| **Elevation (ft)** | 3,983 | | |
| **Geologic unit** | $Ycb_s$ | | |

| Sample ID (Station ID) | | Geochemical Classification | Co-located analyses (* indicates petrographic analysis for thin section) |
|---|---|---|---|
| **81-87B (Station 110)** | | – – – | – – – |
| **TRS** | sec. 15 T29N R37E | From Bunning (1985); Aichan Bee prospect; 81-87B. Pyrite and galena in vitreous black quartz vein, and disseminated in clear, vitreous quartzite of Buffalo Hump Formation (?) | |
| **Latitude Longitude (degrees)** | 48.01588 -118.13364 | | |
| **Elevation (ft)** | 3,045 | | |
| **Geologic unit** | $Ycb_s$ | | |

| Sample ID (Station ID) | | Geochemical Classification | Co-located analyses (* indicates petrographic analysis for thin section) |
|---|---|---|---|
| **81-83B (Station 111)** | | – – – | – – – |
| **TRS** | sec. 13 T29N R37E | From Bunning (1985); “outcrops along road”; sample 81-83B. Apatite with quartz phenocrysts; quartz-feldspar porphyry with biotite; quartz-feldpsar porphyry with euhedral quartz crystals and greenish feldspar. | |
| **Latitude Longitude (degrees)** | 48.01379 -118.10729 | | |
| **Elevation (ft)** | 4,115 | | |
| **Geologic unit** | $Kig_g$ | | |

**Table B1**. Continued.

| Sample ID (Station ID) | | Geochemical Classification | Co-located analyses (* indicates petrographic analysis for thin section) |
|---|---|---|---|
| **81-77B (Station 112)** | | – – – | – – – |
| **TRS** | sec. 13 T29N R37E | From Bunning (1985); Germania mine; sample 81-77B. Ore minerals in quartz vein; high-grade sample; wolframite, molybdenite, pyrite. | |
| **Latitude Longitude (degrees)** | 48.00877 -118.09961 | | |
| **Elevation (ft)** | 3,513 | | |
| **Geologic unit** | $Kig_g$ | | |
| **81-78B (Station 113)** | | – – – | – – – |
| **TRS** | sec. 13 T29N R37E | From Bunning (1985); Germania mine; sample 81-78B. Greisen assemblage with quartz and pyrite. | |
| **Latitude Longitude (degrees)** | 48.00771 -118.10065 | | |
| **Elevation (ft)** | 3,521 | | |
| **Geologic unit** | ml | | |
| **81-79B (Station 114)** | | – – – | – – – |
| **TRS** | sec. 13 T29N R37E | From Bunning (1985); Germania mine; sample 81-79B. Mill tailings from Germania mine. | |
| **Latitude Longitude (degrees)** | 48.00769 -118.09888 | | |
| **Elevation (ft)** | 3,442 | | |
| **Geologic unit** | ml | | |
| **81-82B (Station 115)** | | – – – | – – – |
| **TRS** | sec. 14 T29N, R37E | From Bunning (1985); “prospect on the ridge (no name);” sample 81-82B. Quartz-feldspar porphyry with large feldspar phenocrysts and clear to lavendar, shattered, rounded quartz phenocrysts; chloritized biotite; strong jarosite-goethite staining | |
| **Latitude Longitude (degrees)** | 48.00626 -118.10630 | | |
| **Elevation (ft)** | 3,927 | | |
| **Geologic unit** | $Kig_g$ | | |
| **81-80B (Station 116)** | | – – – | – – – |
| **TRS** | sec. 24 T29N R37E | From Bunning (1985); Roselle prospect; sample 81-80B. Dump sample of slightly altered biotite granite; granite with quartz veinlets, and greisenized granite with wolframite-quartz veins; possible molybdenite in greisen | |
| **Latitude Longitude (degrees)** | 48.00222 -118.10387 | | |
| **Elevation (ft)** | 3,683 | | |
| **Geologic unit** | $Kig_g$ | | |
| **81-81B (Station 117)** | | – – – | – – – |
| **TRS** | sec. 23 T29N R37E | From Bunning (1985); Green prospect; sample 81-81B. Trench float is greisenized (quartz and muscovite) granite with manganese oxide; wall rock adjacent to quartz veins is silicified | |
| **Latitude Longitude (degrees)** | 48.00088 -118.10487 | | |
| **Elevation (ft)** | 3,784 | | |
| **Geologic unit** | $Kig_g$ | | |